Dissertation zur Erlangung des Doktorgrades
der Fakultät für Chemie und Pharmazie der
Ludwig-Maximilians-Universität München

Proteomic studies on testicular aging using the non-human primate Callithrix jacchus as a model

Jan Bernd Stöckl

aus

Augsburg

2021

Erklärung

Diese Dissertation wurde im Sinne von § 7 der Promotionsordnung vom 28. November 2011 von Herrn Prof. Dr. Eckhard Wolf betreut und von Herrn Prof. Dr. Ernst Wagner von der Fakultät für Chemie und Pharmazie vertreten.

Eidesstattliche Versicherung

Diese Dissertation wurde eigenständig und ohne unerlaubte Hilfe erarbeitet.

München, den 25.08.2021

.....

Jan Bernd Stöckl

Dissertation eingereicht am 26.08.2021

1. Gutachter: Prof. Dr. Ernst Wagner

2. Gutachter: Prof. Dr. Eckhard Wolf

Mündliche Prüfung am 13.10.2021

Meiner Familie

Table of Contents

1. Introduction

1.1. Aging and its Hallmarks

Aging can be defined as the changes that happen during an organism's life span (Kirkwood, 2005), typically leading to a progressive functional decline (Lopez-Otin et al., 2013). Another definition describes aging as a breakdown of self-organizing systems concurrent with a reduced adaptability to the environment (Vasto et al., 2010). In humans, this typically manifests in reduced integrity of physiological and anatomical structures, which impacts bodily functions such as blood pressure, stride, vision, and respiratory cycle, eventually leading to an increased risk of mortality (da Costa et al., 2016). What exactly causes aging has yet to be resolved, but a common theory is that accumulated damage overcomes the capabilities of the repair mechanisms (Lopez-Otin et al., 2013, Ferrucci et al., 2020). Other theories argue for a genetically programmed nature of aging, or for a combination of both (Jin, 2010, da Costa et al., 2016). Due to the high complexity of aging as a process with numerous interdependent mechanisms, it is hard to decipher. Nevertheless, there are various hallmarks which are characteristic for aging (Figure 1) (Lopez-Otin et al., 2013, Sierra, 2016, Ferrucci et al., 2020).

One of these hallmarks is genomic instability caused by the accumulation of genetic damage (Kubben and Misteli, 2017, Li et al., 2021). The source of DNA damage can be intrinsic e.g., by replicative stress or reactive oxygen species (ROS) or extrinsic e.g., by ionizing radiation or environmental chemicals (Tiwari and Wilson, 2019). While there are a wide range of complex mechanisms in place to repair damaged DNA, with increasing age, the capability to maintain the genome declines (Chen et al., 2020). Unrepaired DNA damage leads to the DNA damage response (DDR), which causes cells to go into apoptosis or senescence (Ou and Schumacher, 2018). Overall, there is increasing evidence that DNA damage and the DDR contribute to the development of aging (Burtner and Kennedy, 2010, Kubben and Misteli, 2017).

With increasing age, continued cell division affects different aspects of the cell and can also give rise to hallmarks of aging. For instance, the telomeres, which are repetitive regions (in mammals: TTAGGG) at the end of chromosomal DNA, shorten with each

cell division due to the nature of the DNA replication process (Zhu et al., 2019). Germ cells and stem cells express the enzyme telomerase, which resynthesizes these lost repeats (Morin, 1989, Kim et al., 1994). However, most cells do not possess telomerase, therefore, their telomeres gradually shorten, which leads to telomere attrition (Mensà et al., 2019). Telomere attrition triggers the DDR, limiting how often a cell can divide and is therefore considered a hallmark of aging (Hayflick and Moorhead, 1961, Olovnikov, 1973, Blackburn et al., 2006).

Stem cell exhaustion is another hallmark of aging associated with constant cell division. It is associated with reduced regenerative capability in tissues due to age-related increase of somatic mutations, altered metabolic regulation and epigenetic drift in stem cells (Goodell and Rando, 2015, Ren et al., 2017). This can be observed for instance in human hematopoietic stem cells (de Haan and Lazare, 2018). However, overall data on stem cell exhaustion in human aging is still limited and more research is needed to investigate to what extent stem cell exhaustion influences the aging process (Ferrucci et al., 2020).

Increased age is further associated with increased epigenetic alterations (Talens et al., 2012). Most prominent is a general loss of histones leading to transcriptional deregulation (Sen et al., 2016). Another age-related epigenetic alteration is the epigenetic drift, which is an accumulation of errors in DNA methylation patterns due to imperfect transfer from parental to daughter strands during DNA replication (Yu et al., 2020). These age-related epigenetic alterations affect aging and drive the development of age-related diseases such as cardiovascular and neurodegenerative diseases (Brunet and Berger, 2014).

A recently introduced hallmark of aging is dysfunctional alternative splicing, which arises due to the age-induced impairment in proteostasis, telomere attrition and genomic instability (Bhadra et al., 2020). However, the role of splicing factors and targets in aging are not yet well understood.

Hallmarks of aging are not limited to the genome and epigenome level but also impact post-translational processes. For instance, increased age impacts the proteostasis network, which ensures a functional proteome by finely controlling protein synthesis,

folding, conformation and degradation (Kaushik and Cuervo, 2015, Klaips et al., 2017). Across species there is an age-dependent functional decline in this system, which contributes to the aging process in general but is also associated with neurodegenerative diseases such as Alzheimer's and Parkinson's disease (Labbadia and Morimoto, 2015, Klaips et al., 2017).

Aging is further associated with mitochondrial dysfunction due to the accumulation of mutations in mitochondrial DNA, which majorly stem from replication errors (Kauppila et al., 2017). This alters mitochondrial morphology, leads to impairment of cellular energy conversion and increased levels of ROS. Elevated ROS levels were originally assumed to be the earliest triggers of aging, but increasing evidence highlights a more complex and less direct role of ROS in aging (Hekimi et al., 2011, Davalli et al., 2016b). For instance, depending on the circumstances, high ROS levels in the brain can either extend longevity or drive aging (Stefanatos and Sanz, 2018). Oxidative damage can occur if there is an imbalance between mitochondrial oxidative metabolism and antioxidative enzymes (Nguyen-Powanda and Robaire, 2020), but ROS are also part of a complex redox system influencing signal transduction, gene expression and cell proliferation with distinct functional profiles for different ROS molecules (Schieber and Chandel, 2014, Sies and Jones, 2020). Overall, mitochondrial dysfunction and altered ROS signaling are far from being completely understood but are nevertheless a key component of the aging process (Davalli et al., 2016b).

Increasing age also leads to alterations in intercellular communication (Fafián-Labora and O'Loghlen, 2020). For instance, endocrine functions undergo changes, such as alterations in hormonal networks and hormonal imbalances (Kauppila et al., 2017). Additionally, there is a progressive increase in the proinflammatory status, a process commonly referred to as inflamm-aging (Franceschi et al., 2000). Inflamm-aging is characterized by a low intensity inflammatory phenotype, which due to altered intercellular communication cannot be resolved and becomes chronic (Xia et al., 2016).

The sensing of nutrients such as sugars, amino acids and lipids is essential for the regulation of cellular metabolism (Efeyan et al., 2015). During aging, this ability deteriorates, which might accelerate aging and could explain the higher susceptibility to diabetes and cardiovascular diseases (Santos et al., 2016).

Furthermore, aged organisms often display an accumulation of senescent cells. Therefore, cellular senescence is considered a hallmark of aging (Lopez-Otin et al., 2013, Di Micco et al., 2021) and will be discussed in detail in the following chapter.

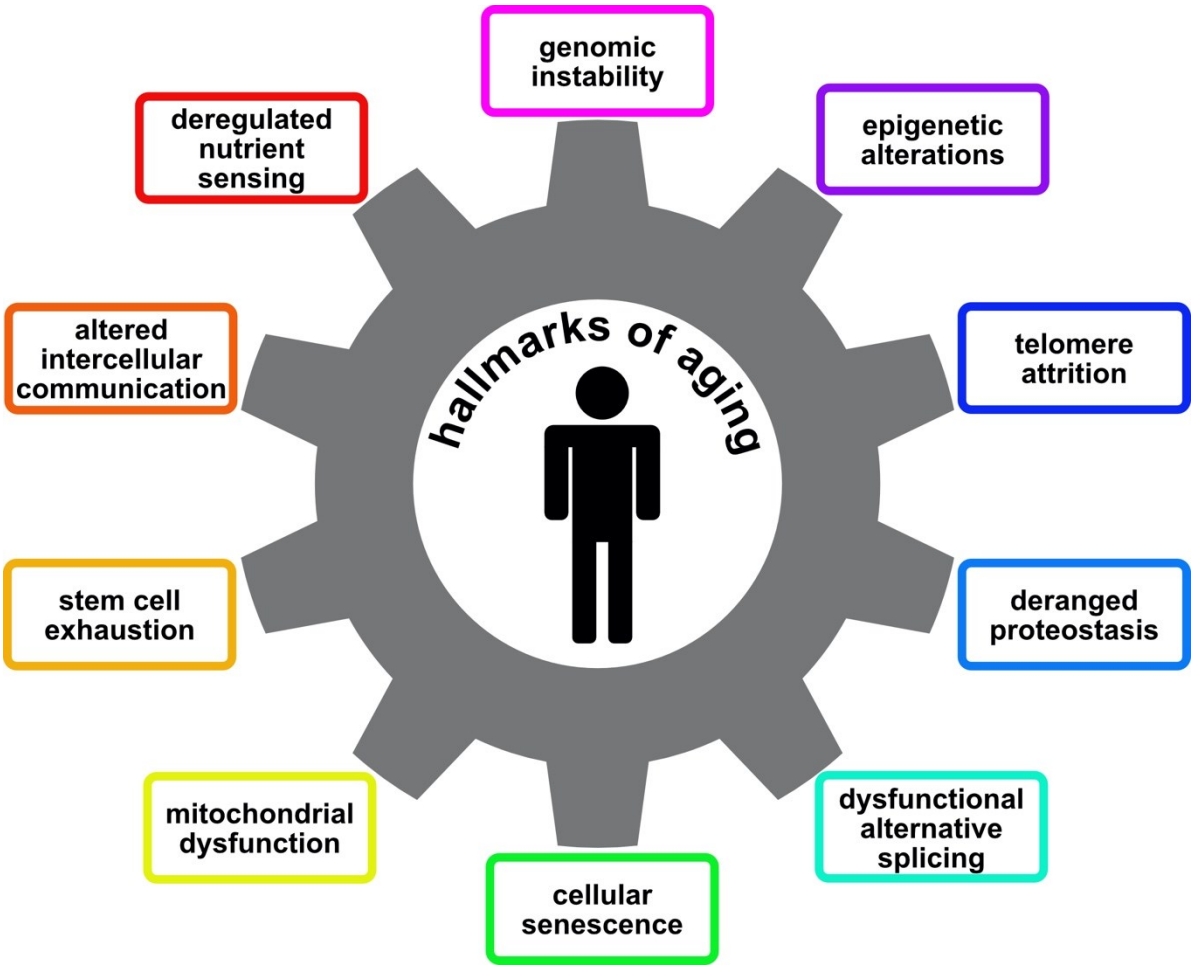

Figure 1: Hallmarks of aging

1.2. Cellular Senescence

Cellular senescence was first described several decades ago in fibroblasts culture, where a gradual loss of the ability to proliferate and to divide was observed (Hayflick and Moorhead, 1961). Cellular senescence can be triggered by various stressors often involving the DDR (de Magalhaes and Passos, 2018, Hernandez-Segura et al., 2018, Gorgoulis et al., 2019). For instance, telomere attrition (Harley et al., 1990, Fagagna et al., 2003, Narita and Lowe, 2005), excessive oxidative stress (Davalli et al., 2016b) and mitochondrial dysfunction (Wiley et al., 2016) all lead to cellular senescence. Therefore, cellular senescence, by preventing the proliferation of damaged cells, is an important tumor-suppressor mechanism (Campisi, 2001). Additionally, cellular

senescence plays regulatory roles in wound healing and embryogenesis (Adams, 2009, Storer et al., 2013, Demaria et al., 2014). However, accumulation of senescent cells in tissues is a driver for aging (Gil, 2019), contributes towards “inflamm-aging” (Franceschi et al., 2000), promotes age-associated disease (Baker et al., 2011), and shortens the healthy life-span (Baker et al., 2016).

Senescence associated growth cycle arrest depends on the activation of the p53/$p21^{CIP1}$ and the $p16^{INK4a}$/Rb tumor suppressor pathways (Salama et al., 2014, Herranz and Gil, 2018). Cellular tumor antigen p53 activation induces the transcription of cyclin-dependent kinase inhibitor 1 (CDKN1A; also known as $p21^{CIP1}$) which in turn results in a cell cycle arrest by inhibiting cyclin-dependent kinase 2 (d'Adda di Fagagna, 2008). CDKN1A is particularly important for the initiation of cellular senescence but its expression is not persistent (Sharpless and Sherr, 2015). Therefore, for establishing a permanent growth cycle arrest in a senescent cell, the $p16^{INK4a}$/Rb pathway is essential (Beauséjour et al., 2003). Cyclin-dependent kinase inhibitor 2A (CDKN2A, also known as $p16^{INK4a}$) inhibits the two cyclin-dependent kinases 4 and 6, which stops the transition of the cell from G1 phase to S1 phase (Rayess et al., 2012). CDKN2A expression is normally absent in healthy tissues but highly expressed in aged and stressed cells, which qualifies it as a potential biomarker for cellular senescence and for aging (Krishnamurthy et al., 2004, Ressler et al., 2006, Burd et al., 2013, Sharpless and Sherr, 2015). However, its usability as a marker is to some extent limited as not all senescent cells express CDNK2A (Herbig et al., 2004).

The most commonly employed assay to detect senescence is measuring the activity of the senescence-associated β-galactosidase at a pH of 6 (Dimri et al., 1995, Kurz et al., 2000, Hall et al., 2016a). β-galactosidase activity is increased in senescent cells due to increased lysosomal content and activity (Lee et al., 2006, Cho and Hwang, 2012). Senescent cells typically also display substantial morphological alterations such as increased cell size (Biran et al., 2017, Neurohr et al., 2019), changes in cell shape (Hwang et al., 2009, Druelle et al., 2016) and an accumulation of dysfunctional mitochondria (Korolchuk et al., 2017, Tai et al., 2017). Furthermore, senescent cells display a depletion of the nuclear lamina protein Lamin-B1 which results in the destabilization of the nucleus, altered chromatin architecture, and altered gene

expression (Sadaie et al., 2013, Shah et al., 2013, Hernandez-Segura et al., 2017, Lukášová et al., 2018).

Interestingly, senescent cells develop a so called “senescent-associated secretory phenotype” (SASP) which is characterized by the secretion of various factors such as interleukins and chemokines but also proteases and extracellular matrix (ECM) components (Coppé et al., 2008, Coppé et al., 2010). SASP composition varies depending on cell type and tissue, but there is a core set comprising three proinflammatory proteins: interleukin-6 (IL6), interleukin-8 (CXCL8) and C-C motif chemokine 2 (CCL2) (Coppé et al., 2008, Di Micco et al., 2021). The SASP is regulated by Nuclear factor NF-kappa-B (NFKB1) and CCAAT/enhancer-binding protein beta (CEBPB) (Acosta et al., 2008, Ohanna et al., 2011, Hoare et al., 2016) and has several roles: for instance, through an autocrine activity it reinforces the senescent state in the senescent cell itself and also has an inflammatory effect on both adaptive and innate immune system (Hoare and Narita, 2013, Acosta et al., 2013, Salama et al., 2014). Additionally, the SASP has contradictory roles in tumorigenesis. While it drives senescence in neighboring cells, thereby preventing tumorigenesis, in specific circumstances it can also create an immunosuppressive environment which promotes tumorigenesis (Acosta et al., 2013, Hoare and Narita, 2013, Rao and Jackson, 2016).

1.3. Testicular Function: Structure and Spermatogenesis

The testis is encapsulated by the tunica albuginea, a layer of connective fibers and smooth muscle cells (Fig. 2A). It is structurally separated into the seminiferous tubules and the interstitial compartment, the sites of sperm production and steroidogenesis, respectively, which represent the two main functions of the testis. These functions are regulated by the hypothalamus-pituitary-testicular (HPT) axis: the hypothalamus periodically releases gonadotrophin-releasing hormone, which in return stimulates the release of luteinizing hormone (LH) and follicle stimulating hormone (FSH) from the pituitary gland (Araujo and Wittert, 2011, Santiago et al., 2019).

The interstitial compartment (Fig. 2B) contains the steroid hormone producing Leydig cells and immune cells together with blood and lymph vessels. The steroid hormone production of the Leydig cells is regulated by LH stimulation of the LH receptor (LHR), a G-protein coupled receptor. The signaling of LHR follows a cAMP-dependent

pathway which, through protein kinase A, leads to the translocation of cholesterol into mitochondria, facilitating the production of steroid hormones (Zirkin and Papadopoulos, 2018). The main androgen testosterone, often termed the male sex hormone, influences various tissues and is essential for spermatogenesis and well-being (Mooradian et al., 1987).

The seminiferous tubule compartment is organized into around 270 testicular lobules separated by fibrous testicular septa, each containing one or several seminiferous tubules (Countouris and Holstein, 1985). The seminiferous tubules are loops with both ends connected to the rete testis which in turn is connected via the efferent ducts to the epididymis, allowing the constant transport of spermatids from the testis to epididymis (Dym, 1974). The tubules are surrounded by the lamina propria containing extracellular matrix and the contractile testicular peritubular cells (TPCs) organized in several concentrical layers. The tubules are lined by the germinal epithelium that constantly produces spermatids which are released into the tubule lumen.

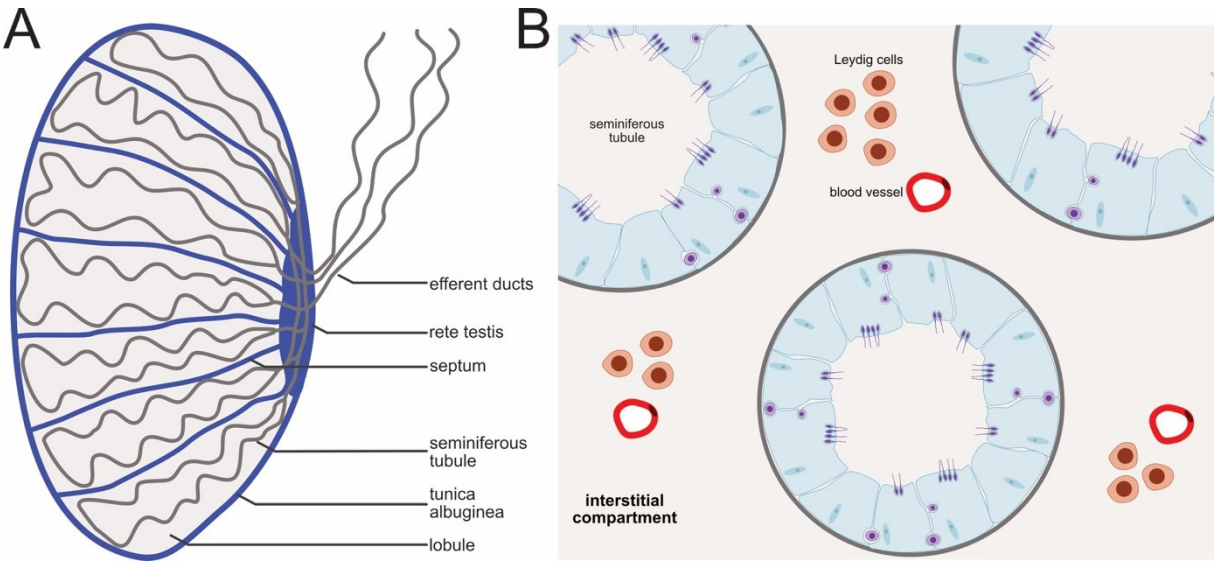

Figure 2: (A) Schematic overview of the testicular structure; (B) Cross section of seminiferous tubule and interstitial compartment

The germinal epithelium consists of Sertoli cells and germ cells sitting on a basal lamina (Figure 3). The Sertoli cells are anchored to the basal lamina and are connected to each other by tight junctions which separate the tubules into an adluminal and a basal compartment. This ensures the structural integrity of the seminiferous tubules and forms an anatomical barrier, the so-called blood-testis barrier (BTB) (Rato et al., 2012, Mazaud-Guittot et al., 2010). Sertoli cells modulate the immune system, which

together with the BTB shields the differentiating germ cells from the immune system (Su et al., 2011, Kaur et al., 2014). Sertoli cells are in direct contact with the germ cells and support them structurally as well as metabolically, and are therefore commonly referred to as “nurse cells” (Rato et al., 2012). Sertoli cells also release paracrine factors which promote meiosis of spermatocytes, regulated by FSH stimulation (Chen and Liu, 2015).

Spermatogenesis starts with the spermatogonia, which are situated on or close to the basal lamina and can be divided into type A and type B. Type A spermatogonia are the spermatogonial stem cells (SSCs), defined by the potential to self-renew, and differentiate in spermatogonia type B, which further differentiate in spermatocytes (Fayomi and Orwig, 2018). SSCs can be morphologically distinguished between the rarely dividing A_{dark} and mitotically active A_{pale} classes (Sharma et al., 2019). One subpopulation of A_{dark} spermatogonia acts as reserve SSCs (Caldeira-Brant et al., 2020). Spermatogonia function is regulated by a highly complex microenvironment called SSC niche. Various testicular cells types contribute to the maintenance of the SSC niche, guaranteeing the continuous self-renewal and differentiation of the stem cells (Oatley and Brinster, 2012). After emerging from spermatogonia type A, type B spermatogonia enter a pre-meiosis state (preleptotene spermatocyte) before relocating through the BTB into the adluminal compartment and completing their differentiation into primary spermatocytes. Primary spermatocytes undergo meiosis I, becoming secondary spermatocytes, which rapidly undergo meiosis II and give rise to the round spermatids (Griswold, 2016). Subsequently, spermatids differentiate into spermatozoa before they are released into the lumen in a process called spermiation (O'Donnell et al., 2011). Spermatozoa are transported into the epididymis were they mature and become motile.

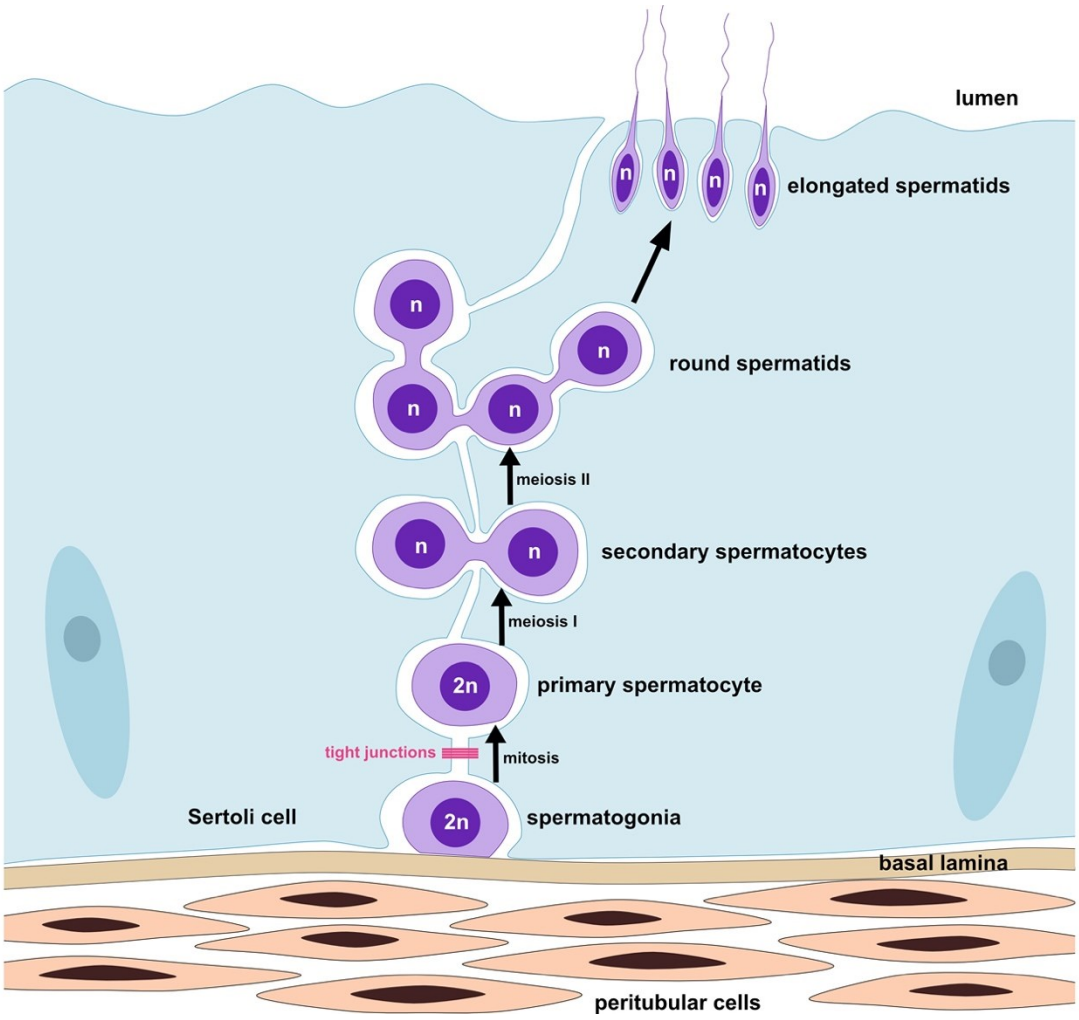

Figure 3: Illustration of the germinal epithelium with a schematic overview of the key steps of spermatogenesis.

1.4. Testicular Peritubular Cells and their Role in the Testis

In primate testes, the lamina propria that surrounds the seminiferous tubules contains five to seven layers of TPCs, each layer surrounded by ECM. The inner layers display a myofibroblastic phenotype, whereas the outer layers are fibroblast-like (Davidoff et al., 1990). The lamina propria is the outermost layer of the seminiferous tubules, which places the TPCs in a functionally strategic position between the germinal epithelium and the interstitial compartment (Mayerhofer, 2020). Key functions of TPCs are structural support, contribution to the ECM, testicular signaling and sperm transport (Mayerhofer, 2013, Fleck et al., 2021). TPCs express smooth muscle cell markers such as smooth muscle actin (ACTA2) and myosin-11 (MYH11) (Schell et al., 2010, Welter et al., 2013). TPCs secrete typical ECM proteins such as laminins, collagens as well as proteoglycans such as decorin (DCN) and biglycan (BGN), which are relevant in

testicular dysfunction and sterile inflammation (Albrecht et al., 2006, Adam et al., 2011, Adam et al., 2012, Mayerhofer, 2013, Mayer et al., 2016).

TPCs further contribute to testicular signaling by producing various factors. One of those factors is the glial cell line-derived neurotrophic factor (GDNF), a growth factor which is crucial for the SSC niche and spermatogonial proliferation and is expressed in both human and mouse testes (Spinnler et al., 2010, Chen et al., 2014). GDNF is also produced by Sertoli cells, but the contribution of TPCs to GDNF signaling is essential in maintaining fertility (Chen et al., 2016). Another factor is the chemokine stromal cell-derived factor 1 (CXCL12), which is involved in the migration of primordial germ cells (Niu et al., 2016). However, its presence and function in secretomes of adult human TPCs needs further elucidation (Flenkenthaler et al., 2014). Pigment epithelium-derived factor (SERPINF1, also known as PEDF), a strong antiangiogenic factor, was also found in TPC secretomes, suggesting a role in preserving the avascularity of the seminiferous tubules (Dawson et al., 1999, Fernandez-Garcia et al., 2007, Flenkenthaler et al., 2014, Windschuttl et al., 2015).

TPCs also express prostaglandin G/H synthase 1 (PTGS1; also known as cyclooxygenase-1 (COX1)) and thereby produce and secrete the pleiotropic factor prostaglandin E_2. This in turn activates the prostaglandin E2 receptor EP1, EP2 and EP4 subtypes, inducing GDNF and ACTA2 expression (Rey-Ares et al., 2018, Mayerhofer, 2020). These findings suggest an important role for prostaglandin E2 in testicular signaling. This hypothesis is further supported by the detrimental effects on the testis of the inhibition of PTGS1 and prostaglandin production through the nonsteroidal anti-inflammatory drug ibuprofen. Sertoli and Leydig cell function were impaired, TPCs were negatively affected and the expression of the TPC markers ACTA2 and MYH11 drastically decreased (Kristensen et al., 2018).

In summary, continuous studies underline that TPCs are an important player in testicular function and regulation, based on their secretory and paracrine effects on other testicular cells. However, despite a recent increase in studies on TPCs, they remain the least explored testicular cell type (Mayerhofer, 2020). Contrary to other testicular cells, they are accessible for *in vitro* studies by isolation from routine biopsies, for instance during re-ligation of vasectomized men (Albrecht et al., 2006).

1.5. Aging of the Male Reproductive System

In Germany, an ever-increasing number of couples postpone parenthood due to socioeconomic reasons (Figure 4). This has led to a steady increase of the average parental age in the last decades, a trend observed in most developed countries (Cedars, 2015, Gunes et al., 2016, Jarak et al., 2018). In Germany in the year 2019, fathers and mothers were on average 34.5 and 31.5 years old, respectively. Due to this trend, the impact of ageing on fertility and offspring health has gained attention. For instance, it is now well established that higher maternal age is associated with an increased risk for miscarriages and chromosomal aberrations. Similarly, there has been increasing evidence that high paternal age can also negatively influence offspring health, implying that the male gonad ages (Paul and Robaire, 2013, Halvaei et al., 2020). However, testicular aging is a controversial topic due to contradictory findings and inconsistent or suboptimal selection criteria, e.g., inclusion of infertile patients in aging studies (Nieschlag et al., 1982, Sharma et al., 2015, Santiago et al., 2019).

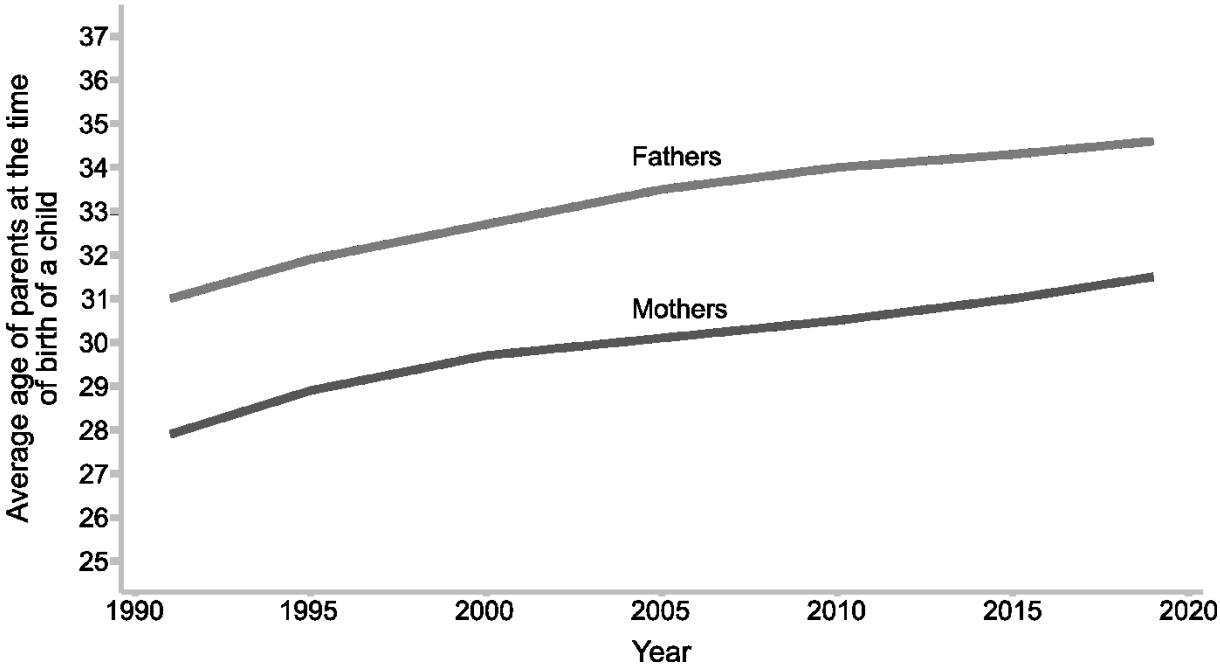

Figure 4: Average age of fathers and mothers at the time of birth of a child in Germany between 1991 and 2019. Data retrieved from Statistisches Bundesamt (destatis.de; site visited 15.12.2020)

Increasing evidence indicates that the aging testis undergoes several morphological and cellular alterations. For instance, most studies have shown a decreased testicular volume in older men, most likely due to a combination of factors such as reduction in testicular cell number and connective tissue alterations (Santiago et al., 2019). Testes

of old men often display a heterogenous assortment of tubular lesions ranging from thickening of the tunica propria to completely sclerosed tubules and as a consequence thereof, partial or complete loss of the germinal epithelium in these involuted tubules (Paniagua et al., 1987, Paniagua et al., 1991, Mularoni et al., 2020). However, these findings were disputed by a study, which did not report any alterations in the seminiferous tubules of older men (Pohl et al., 2019). On the other hand, a recent study showed that HTPCs, the cells of the peritubular wall, undergo profound changes when they become senescent (Schmid et al., 2019).

Moreover, there is an age-dependent decline in various semen parameters such as semen volume, sperm morphology and sperm motility (Kuhnert and Nieschlag, 2004, Johnson et al., 2015) while the sperm concentration, i.e., the spermatogenic output remains stable (Pohl et al., 2019). Increasing paternal age is associated with epigenetic changes, DNA fragmentation, *de novo* mutations and chromosomal aneuploidies in germ cells, all leading to a higher incidence of different disorders in the offspring such as autism and schizophrenia (Paul and Robaire, 2013, Sharma et al., 2015, Johnson et al., 2015, Goldmann et al., 2019, Evenson et al., 2020, Laurentino et al., 2020).

Furthermore, the number of Leydig, Sertoli and germ cells decreases with increasing age (Neaves et al., 1984, Neaves et al., 1985, Paniagua et al., 1991, Dakouane et al., 2005, Mularoni et al., 2020). The loss of Sertoli cells and of Leydig cells strongly correlates, suggesting an attrition mechanism affecting these two somatic cell types (Mularoni et al., 2020). With age some Leydig cells also undergo ultrastructural alterations such as formation of intranuclear Reinke crystals, multiple vacuoles, and accumulation of lipid droplets in the cytoplasm (Paniagua et al., 1986, Paniagua et al., 1991). Studies in the brown Norway rat also showed reduced cholesterol transport into mitochondria and reduced cAMP production after LH stimulation in aged animals (Wang et al., 2017). Similar to Leydig cells, Sertoli cells also display ultrastructural changes in older men: high vacuolation, odd-shaped nuclei, less frequent inter-Sertoli cells tight junctions combined with degenerated lysosomes and endoplasmic reticulum (Jiang et al., 2014, Pohl et al., 2019). The functional impairment of Sertoli cells is indicated by a decline in the Sertoli cell marker Inhibin B and as compensation, substantially increased FSH levels (Kaufman et al., 2019). The loss of integrity of the BTB due to the decreased tight junctions could potentially impair the stem cell niche

microenvironment (Jiang et al., 2014, Santiago et al., 2019). A progressive loss of germ cells was described in old men, starting with a decreased number of spermatids and over time also less differentiated germ cells (Paniagua et al., 1987, Johnson et al., 1987, Paniagua et al., 1991, Jiang et al., 2014). In contrast, a different study reported a constant spermatogenic output, but observed a higher rate of proliferating spermatogonia in older men with proven fertility, indicating a reduced spermatogenic efficiency (Pohl et al., 2019).

Aging in men can further manifest in decreased testosterone levels, but other confounding factors, such as lifestyle and medical history, did also have an impact (Kaufman et al., 2019). Reduced testosterone often stems from a reduced responsiveness of Leydig cells to LH stimulation (Winters and Troen, 1982, Mulligan et al., 2001, Wang et al., 2017). At first, this is compensated by an increased LH secretion leading to a status referred to as compensated hypogonadism (Kaufman et al., 2019). However, when this mechanism is exhausted, it leads to primary hypogonadism, which is characterized by increased LH and lowered testosterone levels (Wu et al., 2008, Tajar et al., 2010).

The age-related decline in spermatogenic and steroidogenic potential is associated with inflamm-aging, characterized by an increased number of testicular macrophages and elevated levels of cytokines such as interleukin-1α, interleukin-1β and tumor necrosis factor (Azenabor et al., 2015, Frungieri et al., 2018). Interleukin-1β induces prostaglandin G/H synthase 2 (PTGS2; also known as cyclooxygenase-2) expression, which negatively affects steroidogenesis in Leydig cells (Wang et al., 2005, Matzkin et al., 2010). Additionally, due to spermatogenesis and steroidogenesis, the ROS production in the testis is comparably high which implies a role for ROS imbalances in testicular aging (Davalli et al., 2016b, Nguyen-Powanda and Robaire, 2020). This is supported by findings in rat testis which show a decrease in anti-oxidative enzymes such as superoxide dismutates (Cao et al., 2004).

Despite evidence about alterations in the aging testis, the topic is still controversial, and the molecular mechanisms involved are still unknown or poorly understood. This is partly due to the difficulty to discern aging effects from other confounding factors such as medical history and lifestyle.

1.6. Exploring Testicular Aging: Human Testicular Peritubular Cells and the Non-Human Primate *Callithrix jacchus*

Triggering cellular senescence in somatic cells *in vitro* is an established method to study age-related alterations (Chen et al., 2013). Among testicular cells, only peritubular cells can be propagated in culture (Albrecht et al., 2006, Mayerhofer, 2013, Mayerhofer, 2020). Morphological and histological studies suggest age-related alterations in the peritubular wall. Since TPCs influence the SSC niche, age-related alterations in TPCs could impact the whole testis. To study this on a molecular level, we passaged human testicular peritubular cells (HTPCs) until senescent and thoroughly characterized using focused ion beam scanning electron microscopy and mass spectrometry-based proteomics (Schmid et al., 2019). The generated data revealed deranged proteostasis, reduced mitochondrial networks and increased number of lysosomes. Additionally, the secretome analysis described a HTPC-specific SASP which included an increased abundance of macrophage migration inhibitory factor (MIF) and dipeptidyl peptidase 4 (DPP4). Both proteins could potentially affect the SSC niche negatively.

These results provided important insight, but an *in vitro* approach does not necessarily reflect the *in vivo* situation. To validate these findings, TPC from young and old individuals should be compared. However, due to ethical reasons, it is impossible to obtain testicular tissue from young and healthy men. This can be overcome by using an appropriate animal model, which also reduces the limitations of confounders associated with human aging such as medical history and lifestyle. While rodents are often the first choice, they are not ideal for studying the testis in general and the peritubular wall and cells in particular. For instance, rodents show differences in spermatogenesis and endocrine signaling (Habert et al., 2014, Fayomi and Orwig, 2018). GDNF expression, an important factor in SSC niche regulation, is induced by androgens in mice testes but not in human testes (Mayer et al., 2018). And lastly, the peritubular wall is structurally different, as rodents possess only one layer of peritubular cells (Mayerhofer, 2013).

The non-human primate *Callithrix jacchus* (common marmoset) is a commonly employed model organism in various fields including cognition, degenerative disease and reproduction (Tardif, 2019). Common marmosets are new world primates of the

family *Callitrichidae* and are native to Northeast Brazil (Schiel and Souto, 2017). They become sexually mature with 18 months and at the age of 8 years they show the first signs of aging such as greying of fur (Abbott et al., 2003, Ross et al., 2012, Nishijima et al., 2012, Mietsch et al., 2020, Moussavi et al., 2020). Like humans, they possess several layers of peritubular cells and their spermatogenesis is relatively similar to the human one. However, TPCs from the marmoset (monkey testicular peritubular cells = MKTPCs) have not been isolated so far and possible molecular differences have not been elucidated yet.

Furthermore, age-related alterations were observed in histological studies covering germ, Sertoli and Leydig cells. Considering how complex testicular signaling and aging are, choosing a more comprehensive approach to investigate these cellular alterations might be beneficial (da Costa et al., 2016). Thus, omics approaches facilitate the characterization of the testicular aging process on the molecular level. The most used and most sensitive omics method is transcriptomics. However, due to the influence of post-transcriptional and post-translational regulation, the prediction of protein abundance is unreliable (Buccitelli and Selbach, 2020). In contrast, proteomics facilitates the direct identification and quantification of proteins. Additionally, data on post-translational modifications and protein secretion is only accessible with proteomics.

1.7. MS-Based Proteomics as a Tool to Characterize Molecular Alterations

There are different experimental strategies to perform mass spectrometry-based proteomics, but the most sensitive and powerful is the so-called bottom-up approach (Aebersold and Mann, 2016). For this approach, proteins are first digested with proteases (mostly trypsin), prior to mass spectrometry analysis. This leads to complex peptide mixtures which are separated with reversed phase nano liquid chromatography, ionized using electro spray ionization and finally analyzed with tandem mass spectrometry. Peptide ions are fragmented with collision induced dissociation, which due to the nature of the peptide bond, leads to predictable fragments (Steen and Mann, 2004, Zhang, 2004). This yields MS/MS spectra, which together with the peptide mass are matched against a protein database using a dedicated search engine (Sadygov et al., 2004).

While in the beginning, proteomics was only capable to identify a few hundred proteins, constant technological advancement has now enabled the identification of thousands of proteins in single LC-MS/MS runs (Mann, 2016, Meier et al., 2018, Mann, 2019). This makes mass spectrometry-based proteomics a valuable and powerful tool to analyze molecular and cellular processes. Proteomics is mainly utilized to analyze tissues and cells but also facilitates the analysis of secreted proteins. The entirety of secreted proteins is referred to as secretome, which is of high relevance for cellular signaling and comprises important factors such as cytokines and growth factors (Uhlén et al., 2019). Especially in the context of aging and senescence where SASP is a typical hallmark, secretome analysis can be highly valuable. The same is true for testicular biology, for instance in HTPCs, which were shown to have complex secretomes, containing various factors and extracellular matrix proteins (Flenkenthaler et al., 2014).

In addition to the identification of proteins, MS-based proteomics also facilitates the quantification of proteins. Most of these approaches generate relative quantification data, which are achieved either via labeling or label-free approaches. Labeling is based on the introduction of stable isotopes, either by metabolically incorporating them, e.g., stable isotope labeling by amino acids in cell culture (SILAC) or by chemically derivatization e.g., using isobaric mass tags (Rauniyar and Yates, 2014). In contrast, label-free approaches either rely on extracted ion counts or MS/MS spectrum counts (spectral counting) (Cox et al., 2014).

1.8. Aim of the Thesis

The major aim of this thesis is to characterize and identify, at the level of the proteome, biochemical alterations associated with testicular aging. Known age-related changes in the human testis include impaired steroidogenesis and spermatogenesis as well as alterations of the seminiferous tubules. Testicular peritubular cells are located in the peritubular wall, transport sperm, contribute to the spermatogonial stem cell niche and interact with other testicular cells to maintain testicular function. Previous *in vitro* experiments indicated that HTPCs are affected by aging. However, samples from young healthy donors are not accessible, therefore a non-human primate model had to be established.

The first aim of this thesis was to evaluate whether MTKPCs from the common marmoset (*Callithrix jacchus*) represent a suitable model for HTPCs. Therefore, the proteome of MKTPCs and HTPCs was compared qualitatively and quantitatively. Further bioinformatic analysis was performed to investigate similarities on a functional level.

The second aim was to assess how the proteomes of MKTPCs are affected by aging. For this purpose, aging of MKTPCs was studied in an *in vitro* and *in vivo* model. Comprehensive proteome and secretome analysis were used to characterize aging of MTKPCs. The results of both approaches were compared and discussed in the context of prior results.

Since testicular aging is not limited to the peritubular wall and TPCs, the third aim of this thesis was to identify age-related alterations in other cell types than TPCs. Since other testicular cells cannot be cultivated *in vitro*, the proteomes of testicular tissue samples from young and old common marmosets were analyzed and compared. Differentially abundant proteins are subjected to functional analysis to identify altered pathways and processes.

2. Materials and Methods

2.1. Materials

2.1.1. Solvent and Reagents

Acetonitrile, LC-MS	Merck, Darmstadt, Germany
Ammonium hydrogen carbonate	Roth, Karlsruhe, Germany
Dithiothreitol (DTT)	Roth, Karlsruhe, Germany
Formic acid (FA)	Merck, Darmstadt, Germany
Iodoacetamide (IAA)	Merck, Darmstadt, Germany
Endopeptidase Lys-C, MS grade	Fujifilm Wako Chemicals, Richmond, USA
Pierce 660 nm Protein Assay Reagent	Thermo Fisher Scientific, Waltham, USA
Tris-(2-carboxyethyl)-phosphine (TCEP)	Roth, Karlsruhe, Germany
Trypsin, modified, sequencing grade	Promega, Madison, USA
Trypsin / Lys-C Mix, mass spec grade	Promega, Madison, USA
Urea	Roth, Karlsruhe, Germany
Water, LC-MS grade	Merck, Darmstadt, Germany

2.1.2. Equipment

Centrifuge 5427 R	Eppendorf, Köln, Germany
Q Exactive HF-X mass spectrometer	Thermo Fisher Scientific, Waltham, USA
Thermomixer 5436	Eppendorf, Köln, Germany
Ultimate 3000 RSLC nano System	Thermo Fisher Scientific, Waltham, USA
5600+ mass spectrometer	Sciex, Concord, Canada
Ultrasonicator Sonopuls UW3200	Bandelin, Berlin, Germany
Vacuum concentrator	Bachofer, Reutlingen, Germany

2.1.3. Plasticware

Amicon Ultra 2 mL Centrifugal Filters (3K)	Merck, Darmstadt, Germany
Amicon® Ultra 0.5 mL Centrifugal Filters (3K)	Merck, Darmstadt, Germany
QIAshredder	QIAGEN, Hilden, Germany
Safe-Lock Tubes (1.5 mL & 2 mL)	Eppendorf, Köln, Germany

2.2. Methods

2.2.1. Cell Culture and Animals

Cell culture of HTPCs and MKTPCs have been performed by Nina Schmid (Biomedical Center; LMU München) as previously described (Albrecht et al., 2006). The animals grew up in the self-sustaining colony at the German Primate Center (Deutsches Primatenzentrum – Leibniz-Institute for Primate Research, DPZ, Göttingen) as previously described (Schmid et al., 2018, Stöckl et al., 2020, Stöckl et al., 2021). Responsible for animal care and tissue collection were Rüdiger Behr and Charis Drummer.

2.2.2. Sample Preparation for Mass Spectrometry Analysis

For lysis of cells and tissue, first, 8 M urea in 50 mM ammonium hydrogen carbonate was added to the samples, which were then lysed using sonication at 4°C using a cup resonator. Cells were pulsed ten times for 10 s with breaks of 20 s in between (total time = 5:40 min). For the tissues, this cycle was repeated until the tissue was completely broken down. The samples were then homogenized with QIAshredder centrifugation devices (4 °C, 2500 g, 1 min).

For the secretome analysis, the supernatants were first concentrated to approximately 500 µL in Amicon 2 mL devices (10 °C; 45 min; 2665 g), then transferred to Amicon 0.5 mL devices and concentrated to 50 µL (4 °C; 30 min; 14000 g). Subsequently, 450 µL of 1 M Urea in 50 mM ammonium hydrogen carbonate were added and the samples were concentrated to a final volume of 50 µL (4 °C; 30 min; 14000 g).

Protein concentration for all samples was assessed with a Pierce 660 nm assay. For digestion, proteins were first reduced in 4 mM DTT/2 mM TCEP for 30 min and then alkylated in 8 mM iodoacetamide for 30 min in the dark (both ambient temperature). Excess IAA was quenched at a final concentration of 10 mM DTT. Cell and tissue samples were digested with Lys-C (1/100, enzyme/protein) for 4 h followed by trypsin (1/50 enzyme/protein) overnight at 37 °C. The secretome samples were digested in a single step using a Lys-C/Trypsin Mix (1/25, enzyme/protein) overnight at 37 °C.

2.3. LC-MS/MS – Proteome Analysis of MKTPCs and Comparison with HTPCs

LC-MS/MS analysis was performed with an Ultimate 3000 RSLC system (Thermo Scientific) coupled to a 5600+ mass spectrometer (Sciex, Concord, Canada). 2.5 µg of peptides were dissolved in 15 µl 0.1% formic acid and trapped on a C18 trap column (µ-Precolumn, C18 PepMap 100, 5 µm, Thermo Scientific, San Jose, CA) at a flow rate of 30 µL/min (mobile phase: 0.1% FA in water). Separation was performed with a C18 nano-flow column (Acclaim PepMap RSLC, 2 µm, 75 µm × 50 cm) at flow rate of 0.2 µL/min with a two-step gradient: 5–25 % B for 285 min and 25–50 % B for 30 min (A: 0.1 % formic acid in water, B: 0.1 % formic acid in acetonitrile). Electrospray ionization was carried out using an uncoated SilicaTip (FS360-20-10-N-20-C15; New Objective, Woburn, MA) and a needle voltage of 2.3 kV. MS data was generated utilizing the data dependent acquisition mode, performing up to 70 MS/MS scans per survey scan.

2.3.1. LC-MS/MS Analysis – Aging Studies

Liquid chromatography (LC) was carried out on an Ultimate 3000 RSLC (Thermo Scientific). From cell lysates, secretomes and testicular tissue, aliquots of 2 µg, 1 µg and 1.5 µg peptides dissolved in 15 µl 0.1% formic acid were injected, respectively. Subsequently, peptides were trapped on a trap column (PepMap 100 C18, 100 µm × 2 cm, 5 µM particles, Thermo Scientific) for 10 min at a flow rate of 5 µL/min (mobile phase: 0.1% formic acid and 1% acetonitrile in water).

Peptides were separated with an EASY-Spray column (PepMap RSLC C18, 75 µm × 50 cm, 2 µm particles, Thermo Scientific) at a flow rate of 250 nL/min using a two-step gradient: Starting with 3 % B to 25 % B in 160 min, followed by a 10 min ramp to 40 % B (A: 0.1% formic acid in water, B: 0.1 % formic acid in acetonitrile). Using the same eluents, the gradient for secretome samples started from 3 % to 25 % B in 30 min, followed by ramping to 40 % B in 5 min.

LC was coupled to a Q Exactive HF-X mass spectrometer (Thermo Scientific), which was run in the data-dependent acquisition mode with a maximum of 15 MS/MS spectra per survey scan for the analysis of cell lysates and testicular tissue. For the secretomes, a maximum of 5 MS/MS spectra was used. Survey scans were measured with a resolution of 60,000 at 200 m/z and product ion spectra were produced with collision induced dissociation and analyzed with a Resolution of 15,000 at 200 m/z.

2.3.2. Data Analysis – Proteome Analysis of MKTPCs and Comparison with HTPCs

Acquired mass spectra were searched with MaxQuant (version: 1.6.0.1) (Tyanova et al., 2016a). Both the “match between runs” feature and the label-free quantification option were turned on, while the rest of the settings were kept at default. Data for MKTPCs and HTPCs were searched separately. To search the MKTPC spectra all entries for *Callithrix jacchus* from Swiss-Prot and TrEMBL were retrieved from UniProt (retrieval date: 06/2017). For HTPCs the human subset of Swiss-Prot was used (retrieval data: 06/2017). Both searches were supplemented with the MaxQuant common contaminants. For quantification the built-in label free quantification module was utilized: the minimum ratio count was set to 1, the remaining settings were kept at default.

Statistical analysis was done with Perseus (1.5.8.5) (Tyanova et al., 2016b). Data from both MTKPC and HTPC were merged into one matrix based on gene name matching. This matrix was used to generate both scatter plot and multi scatter plot.

The “circoletto” graph was generated using the online tool hosted by the bioinformatic analysis team (http://tools.bat.infspire.org/circoletto/). This analysis was limited to the respective 100 most abundant proteins of both MKTPC and HTPC proteomes. Default settings were used with some exceptions: e-value cutoff 10−15; e-value for coloring; use (score-min)/(max-min) ratio to assign colors.

The 25 most abundant proteins in the MKTPC proteome were blasted against the human Swiss-Prot subset using the online tool blastp (https://blast.ncbi.nlm.nih.gov/Blast.cgi) from the National Center for Biotechnology Information (NCBI). The spectral counting approach was performed with Mascot (2.4.0) and Scaffold (4.1.1). The MS data was searched with the same sequence databases as for the MaxQuant analysis. The data was ranked based on average spectral counts. Functional annotation was performed with the “protein analysis through evolutionary relationships” (PANTHER) online tool for gene list analysis (pantherdb.org). With gene names as input the data was annotated using the gene ontology (GO) biological process and GO cellular process as database.

The mass spectrometry proteomics data were deposited to the ProteomeXchange Consortium (http://proteomecentral.proteomexchange.org) via the Proteomics

Identification Database (PRIDE) partner repository with the dataset identifier PXD009394 (Perez-Riverol et al., 2019).

2.3.3. Data Analysis – Publication: "Proteomic Insights into Senescence of Testicular Peritubular Cells from a Nonhuman Primate Model"

Acquired MS spectra were searched with MaxQuant (version: 1.6.5.0) (Tyanova et al., 2016a). Both the "match between runs" feature and the label-free quantification option were turned on, while the rest of the settings were kept at default. For quantification the built-in label free quantification module was utilized. As database, all available entries for *Callithrix jacchus* from both Swiss-Prot and TrEMBL (retrieval: 02/2020) were retrieved from Uniprot (uniprot.org). Additionally, the MaxQuant common contaminants database was used. To match the identified common marmoset proteins to human orthologs several steps were undertaken: first all proteins were subjected to the dbOrtho tool from the biological DataBase network (bioDBnet). From the proteins without a hit, the genes names were matched against the human subset of Swiss-Prot manually (02/2020). If gene names were identical, they were treated as orthologs. Finally, proteins without any match were blasted against the human subset of Swiss-Prot using the blastp online tool from NCBI. Proteins were assumed to be orthologous when they reached at least 85% in identity and query match. Proteins without any matched orthologs were removed prior to annotation analysis.

Statistical analysis was done with Perseus (1.6.5.0) (Tyanova et al., 2016b). Perseus' built-in functions, using default settings, were utilized to generate the PCA and the unsupervised hierarchical clustering. To test for differentially abundant proteins between hp-MKTPCs and lp-MKTPCs (proteomes and secretomes), a modified Welch's *t*-test (s0= 0.1) was used (Tusher et al., 2001). For multiple testing correction a permutation-based approach was chosen with a final false discovery rate (FDR) of < 0.05. Volcano plots for the comparison of young and old MKTPCs were analyzed using a cut-off curve, which was calculated utilizing a modified *t*-test and an FDR-based approach to correct for multiple testing (s0= 0.1, FDR < 0.05) (Tusher et al., 2001).

Annotation analysis of differentially abundant proteins was performed using the functional clustering tool of the "Database for Annotation, Visualization and Integrated Discovery" (DAVID) (Huang da et al., 2009). The following categories were used: GO biological process, GO cellular component, GO molecular function, and REACTOME. The resulting clusters were labeled according to the term with the smallest p-value and

plotted with R (3.6.3) and the R library tidyverse (1.3.0). The data of the comparison of MKTPCs from young and old animals were analyzed with a gene set enrichment analysis (GSEA) (Subramanian et al., 2005). The following gene sets were used: KEGG, REACTOME, GO biological process, GO cellular component, GO molecular function (all retrieved from http://www.gsea-msigdb.org/gsea/msigdb/collections.jsp; /04/2020). The number of permutations was 50000 and as metric "tTest" was chosen. The resulting terms were converted to GO IDs with the R package GO.db and subsequently summarized with REVIGO (similarity= 0.4) (Supek et al., 2011). The results were again plotted with R.

The differentially abundant proteins in the secretomes of hp-MKTPCs were subjected to the tools SignalP and SecretomeP to predict signal peptides and nonclassical protein secretion, respectively (Bendtsen et al., 2004, Almagro Armenteros et al., 2019).

The mass spectrometry proteomics data were deposited to the ProteomeXchange Consortium (http://proteomecentral.proteomexchange.org) via the Proteomics Identification Database partner repository with the dataset identifier PXD022165 (Perez-Riverol et al., 2019).

2.3.4. Data analysis – Publication: "Age-Related Alterations in the Testicular Proteome of a Non-Human Primate"

Acquired MS spectra were searched with MaxQuant (version: 1.6.5.0) (Tyanova et al., 2016a). Both the "match between runs" feature and the label-free quantification option were turned on, while the rest of the settings were kept at default. For quantification the built-in label free quantification module was utilized. As database, all available entries for *Callithrix jacchus* from both Swiss-Prot and TrEMBL (retrieval: 09/2020) were retrieved from Uniprot (uniprot.org). Additionally, the MaxQuant common contaminants database was used. Where possible, identified proteins were matched with human orthologs, in the same manner as described above.

Statistical analysis was done with Perseus (1.6.5.0) (Tyanova et al., 2016b). Perseus' built-in functions, using default settings, were utilized to generate the PCA and unsupervised hierarchical clustering. For identification of differentially abundant proteins, first a volcano plot was generated. Using built-in functionalities, a significance cut-off curve was generated. The cut-off was calculated utilizing a modified *t*-test and an FDR-based approach to correct for multiple testing (s0= 0.1, FDR < 0.05) (Tusher

et al., 2001). Proteins above the curve were considered significantly altered in abundance in the old testes.

The differentially abundant proteins were further analyzed and annotated using DAVID's functional clustering tool (Huang da et al., 2009) with the following settings: GO biological process, GO cellular component, GO molecular function, REACTOME and UniProt keyword entries as categories; high classification stringency. The resulting clusters were labeled according to the term with the smallest p-value and plotted with R (4.0.1).

All differentially abundant proteins were analyzed with the "Search Tool for the Retrieval of Interacting Genes/Proteins" (STRING) database. All available interactions with the exceptions of neighborhood and gene fusion were included. The results were illustrated in a network. Nodes without significant interactions were removed.

The mass spectrometry proteomics data were deposited to the ProteomeXchange Consortium (http://proteomecentral.proteomexchange.org) via the Proteomics Identification Database partner repository with the dataset identifier PXD024844 (Perez-Riverol et al., 2019).

3. Results

3.1. Proteome Analysis of MKTPCs and Comparison with HTPCs

Section 3.1 has been adapted from: Schmid N, Stöckl JB*, Flenkenthaler F, Dietrich KG, Schwarzer JU, Köhn FM, Drummer C, Fröhlich T, Arnold GJ, Behr R, Mayerhofer A. Characterization of a non-human primate model for the study of testicular peritubular cells-comparison with human testicular peritubular cells Mol Hum Reprod. 2018 Aug, 1;24(8):401-410. doi: 10.1093/molehr/gay025. PMID: 29846669.*

**Contributed equally*

Proteins of MKTPCs from six individual donors were investigated by LC-MS/MS. In total 2437 protein groups were identified (FDR < 1 %) in MKTPCs, of which 1825 protein groups could be quantified in at least three individual samples. The inter-individual variance was investigated by a multi scatter plot analysis of all protein LFQ intensities between all MKTPC individuals (Figure 5 A). The Pearson correlation coefficient ranged between 0.93 and 0.97.

Additionally, a set of HTPCs from 7 individual human donors was analyzed using exactly the same parameters and compared to the results of the MKTPCs. From 3374 protein groups, which were identified in HTPCs, 2137 are contained in the MKTPC dataset, demonstrating that 88 % (2137 out of 2437) of the proteins in MKTPCs are represented in the HTPC data. The inter-individual variance was again assessed using a multi scatter plot between all individual donors, which resulted in a Pearson correlation coefficient between 0.93 and 0.96 (Figure 5 B).

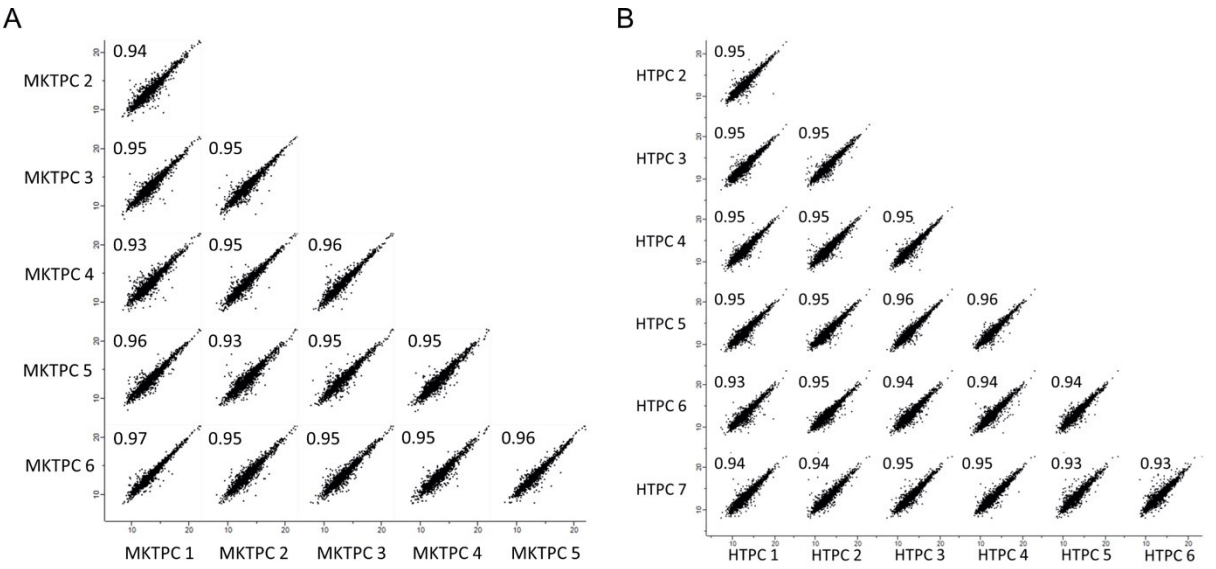

Figure 5: (A) Multi scatter plot of log_2 Max-Quant LFQ protein intensity values of MKTPCs from 6 donors. The number in the upper left corner of each individual scatterplot shows the Pearson correlation. (B) Multi scatter plot of log_2 Max-Quant LFQ protein intensity values of HTPCs from 7 donors.

The means of the MaxQuant LFQ values were scatter plotted against each other, which resulted in a correlation coefficient of 0.78 (Figure 6) between human and marmoset cells. To investigate the variability of this inter-species comparison, each individual of MKTPCs were plotted against all individual HTPC donors. The found mean Pearson correlation was 0.75 with no significant outliers (Grubbs' test for outliers; 99% confidence) and therefore showing a very homologous correlation pattern (Figure 7).

From both datasets the 100 most abundant proteins were retrieved and analyzed with the circoletto tool to visualize sequence homology of highly expressed proteins between HTPC and MKTPC (Figure 8). The resulting network shows sequence homologies (< e-value 10-15) between the most abundant proteins found in both species, of which a vast majority shows high degree of similarity. Furthermore, a BLAST analysis of the 25 most abundant MKTPC using the Human Swiss-Prot database reveals that 22 are showing sequence identities > 95% (Table 1). Two further proteins could be matched to their human counterparts with >85 % identity and represent members of the tropomyosin family, and only one single protein (F7FP14; uncharacterized protein) could not unambiguously be assigned to a human protein.

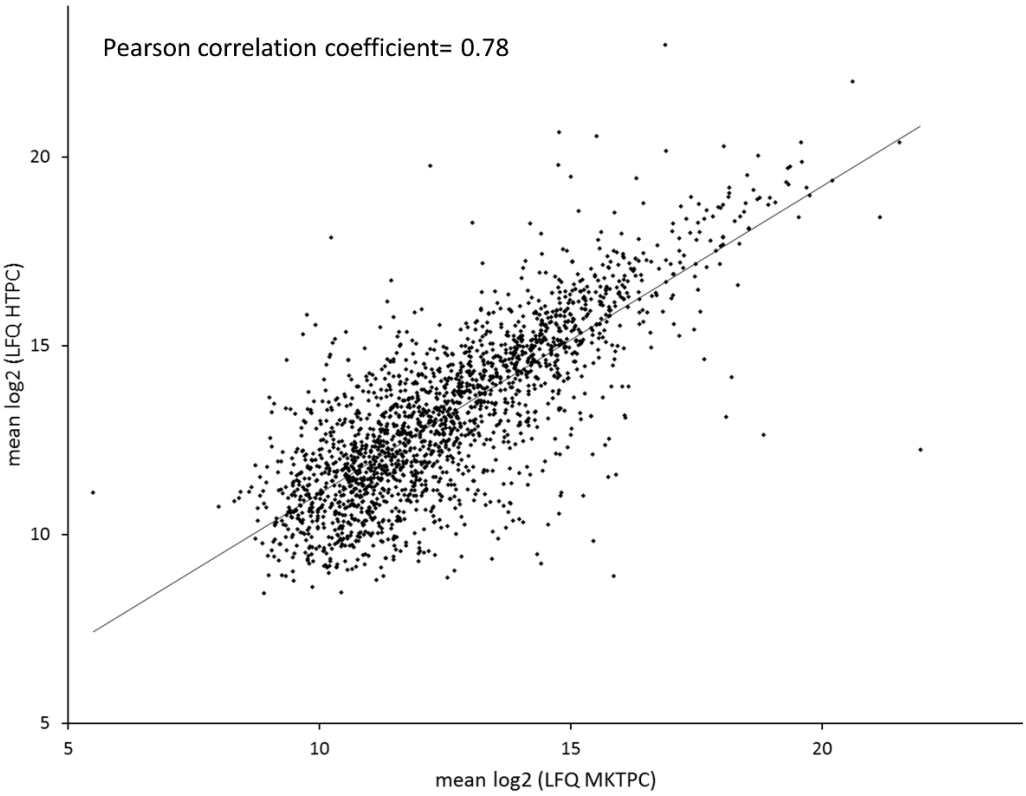

Figure 6: Scatter plot of averaged log_2 LFQ protein intensity values of MKTPCs and HTPCs. The number in the left corner of an individual scatterplot shows the Pearson correlation. Note the correlation at the protein level between cells of both species.

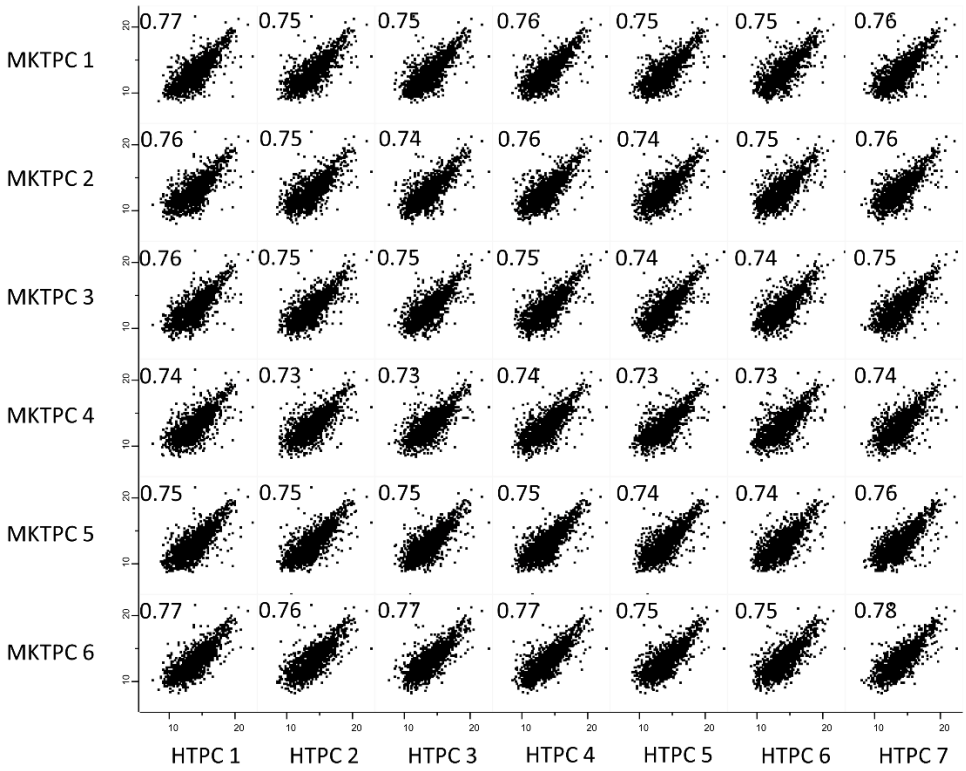

Figure 7: Multi scatter plot showing individual MKTPCs compared against individual HTPCs. The number in the upper left corner of each individual scatterplot shows the Pearson correlation.

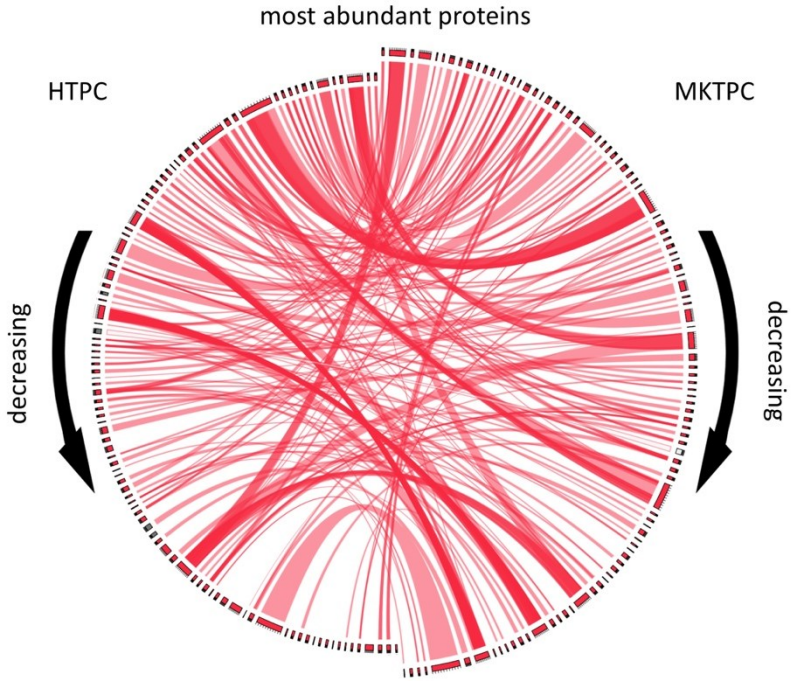

Figure 8: Circoletto analysis of the top 100 protein identifications found in HTPC and MKTPC. The left half circle shows HTPC proteins sorted by their abundance from highest at the top to the lowest at the bottom. The right half circle lists the top 100 proteins identified in MKTPC in the same order. Both groups are compared with respect to protein sequence similarity. Proteins are represented by boxes on the circle. The length of the boxes indicates the length of the protein sequences. Sequence similarities between two corresponding proteins (MKTPC vs. HTPC) are represented by a ribbon connecting the two boxes (cutoff e-value 10^{-15}).

To review if the most abundant proteins in MKTPCs are also high abundant in HTPCs, the identified MKTPC and HTPC protein groups were sorted according to their MS/MS spectral count values, a measure for their abundance. Comparison of both datasets revealed that 21 out of the top 25 MKTPC protein groups are contained in the top 50 HTPC protein groups (Table 2). Only transgelin (TAGLN), caldesmon (CALD1) and the tropomyosins TPM1 and TPM4 ranked noticeably lower in HTPCs compared to MKTPC.

To assess similarities between MKTPCs and HTPCs at the functional level, the identified proteins were analyzed with the PANTHER analysis tool using the “Biological Process” and “Cellular Process” Gene Ontology Databases. The proteins of both MKTPC and HTPC show highly similar distributions concerning related biological and cellular processes, suggesting strong biochemical and functional similarities between MKTPC and HTPC (Figure 9).

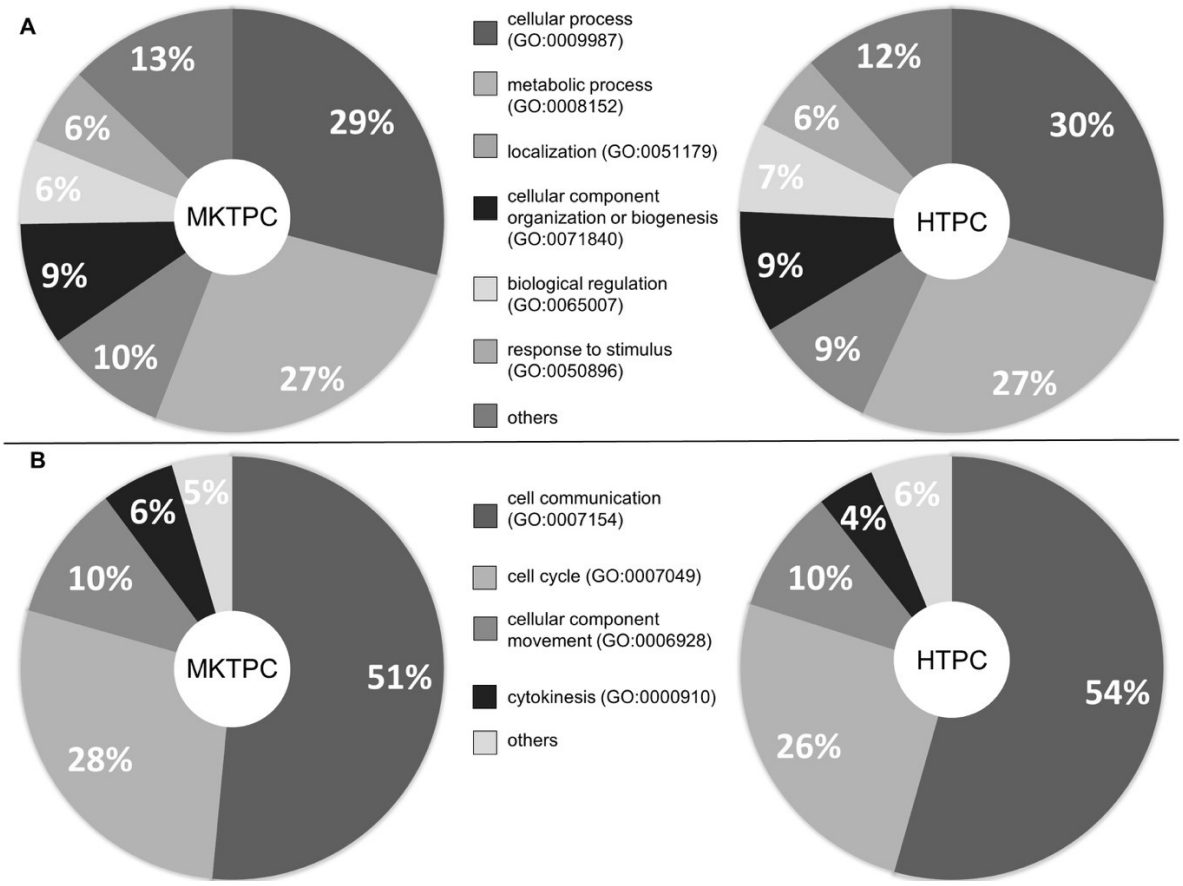

Figure 9: (A) GO analysis using the “biological process” database for MKTPC (left) and HTPC (right) proteomes. **(B)** GO analysis regarding the “cellular process” subset for MKTPC (left) and HTPC (right).

Table 1: The top 25 most abundant proteins in MKTPC are shown. Sequence similarities with corresponding human proteins were determined by BLAST analysis and are indicated as "% identity".

Callithrix jacchus **UniProt accession**	***Callithrix jacchus*** **Gene name**	***Callithrix jacchus*** **protein name**	**human UniProt accession**	**% Identity**
F7IH64	ACTA2	Actin, alpha 2, smooth muscle, aorta	P62736	100
B0KWW5	FLNA	Filamin-A isoform 1,2	P21333	98.79
F7BQY8	VIM	Vimentin	P08670	99.36
F6ZZ90	MYH9	Myosin heavy chain 9	P35579	99.49
F7I1Q9	TAGLN	Transgelin	Q01995	99.5
F7I9U1	TPM2	Tropomyosin beta chain isoform 2	P07951	87.32
F7HTQ3	CALD1	Caldesmon 1	Q05682	95.33
F7I0W8	LOC100409006	Uncharacterized protein	P63261	100
U3EQM9	ACTN4	Alpha-actinin-4	O43707	99.89
F6YS84	TPM1	Tropomyosin 1	P09493	85.92
U3BZ94	TUBB4B	Tubulin beta chain	P68371	99.33
U3CYB6	ENO1	Alpha-enolase isoform 1	P06733	99.31
F7I318	LGALS1	Galectin	P09382	99.07
F7HZP3	TUBA1B	Tubulin alpha chain	P68363	100
F6RMA3	ANXA2	Annexin	P07355	99.71
F7IHK8	PRDX1	Peroxiredoxin 1	Q06830	97.99
U3EKQ0	ACTN1	Actinin alpha 1	P12814	99.78
F7CXD3	EEF1A1	Elongation factor 1-alpha	P68104	100
F6SQW1	PPIA	Peptidyl-prolyl cis-trans isomerase	P62937	99.78
U3FXT1	HSPA5	78 kDa glucose-regulated protein; Heat shock protein family A (Hsp70) member 5	P11021	99.39
F7HVD2	HSPA8	Heat shock protein family A (Hsp70) member 8	P11142	99.85
F7FP14		Uncharacterized protein	Q8N386	62.38
F6YTV2	LMNA	Lamin A/C	P02545	98.65
F6XL35	PKM	Pyruvate kinase	P14618	99.06
U3D5Z3	TLN1	Talin-1	Q9Y490	99.21

Table 2: The top 25 most abundant MKTPC protein groups and their number of group members are shown. The abundance ranks of MKTPC protein groups are compared to the ranks of the corresponding protein groups in HTPCs.

Rank in MKTPC	Rank in HTPC	Protein Group	# Proteins in Group
1	2	Actin, cytoplasmic 1	11
2	4	Filamin-A	3
3	7	Myosin 9	5
4	9	Alpha-actinin-4	7
5	1	Vimentin	45
6	3	Tubulin beta	19
7	4	Uncharacterized protein homologue to human neuroblast differentiation-associated protein AHNAK	3
8	63	Transgelin	1
9	93	Tropomyosin alpha-4 chain	5
10	42	Myosin-10	3
11	239	Tropomyosin alpha-1 chain	4
12	23	Filamin-C	2
13	26	Alpha-enolase	6
14	12	Talin-1	1
15	14	Heat shock protein family A (Hsp70) member 5	1
16	113	Caldesmon	3
17	44	Filamin-B	4
18	6	Plectin	2
19	19	Clathrin heavy chain	2
20	11	Tubulin alpha chain	7
21	15	Heat shock protein 90	4
22	21	Cytoplasmic dynein 1 heavy chain 1	1
23	8	Pyruvate kinase	5
24	20	Lamin isoform A	3
25	27	Heat shock protein family A (Hsp70) member 8	3

3.2. Proteomic Insights into Senescence of Testicular Peritubular Cells from a Non-Human Primate Model

Section 3.2 has been adapted from: Stöckl, J.B.; Schmid, N.; Flenkenthaler, F.; Drummer, C.; Behr, R.; Mayerhofer, A.; Arnold, G.J.; Fröhlich, T. Proteomic Insights into Senescence of Testicular Peritubular Cells from a Nonhuman Primate Model. Cells 2020, 9, 2498. https://doi.org/10.3390/cells9112498

3.2.1. Proteome Analysis of Cells and Secretomes from Low- vs. High-Passage MKTPCs

A proteome analysis of low-passage-number MKTPCs (lp-MKTPCs) and high-passage-number MKTPCs (hp-MKTPCs) was conducted, using MKTPCs derived from five young healthy donors. Secretomes and proteomes were analyzed by LC–MS/MS from cells of the same donors after 2–3 and after 10–12 passages, respectively. MKTPCs proliferated in culture showed, after more than 10 passages, a significant increase in cell size and changes in cell shape, expressed considerable amounts of senescence-associated beta galactosidase, and stopped dividing (Figure 10).

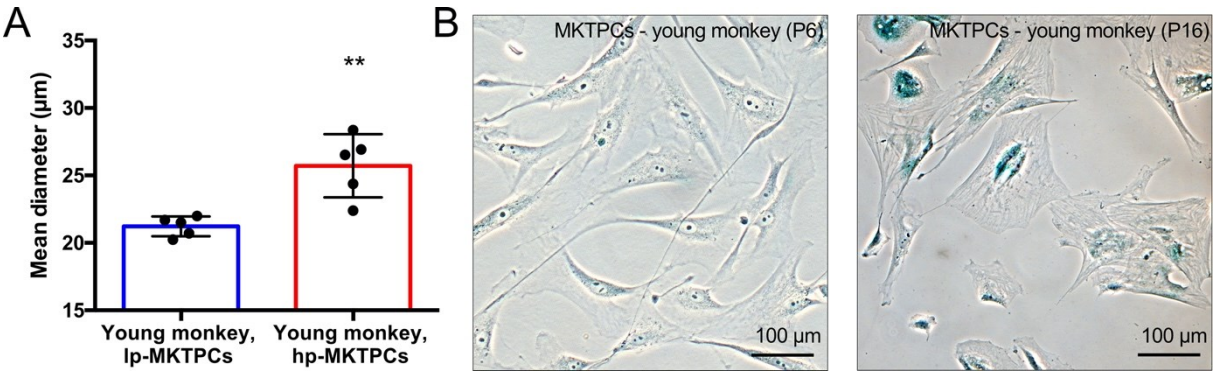

Figure 10: (A) Cell size measurement of low-passage-number vs high-passage-number testicular peritubular cells from the common marmoset (lp-MKTPCs vs. hp-MKTPCs) from the same donor animal. A significant increase in cellular diameter of hp-MKTPCs was shown. Columns indicate the mean; bars indicate the standard deviation; for statistics, a paired *t*-test was used. **(B)** Light micrograph of senescence-associated β-galactosidase staining of lp-MKTPCS and hp-MKTPCs. **: p-value < 0.005; Experiments performed by Nina Schmid (Biomedical Center; LMU München)

In total, 4916 and 1132 proteins and 66,240 and 8786 peptides were identified from the proteome and secretome, respectively (Supplementary Info 1). Typical testicular peritubular cell markers, namely, calponin 1 (CNN1), smooth muscle actin (ACTA2), and myosin heavy chain 11 (MYH11), were identified. A principal component analysis

(PCA) based on the quantitative protein abundance data showed clear separation of the proteomes and secretomes of hp-MKTPCs and lp-MKTPCs (Figure 11 A, B). For both cellular proteome and secretome, unsupervised hierarchical clustering indicated clustering of lp-MKTPCs and hp-MKTPCs (Figure 11 C, D).

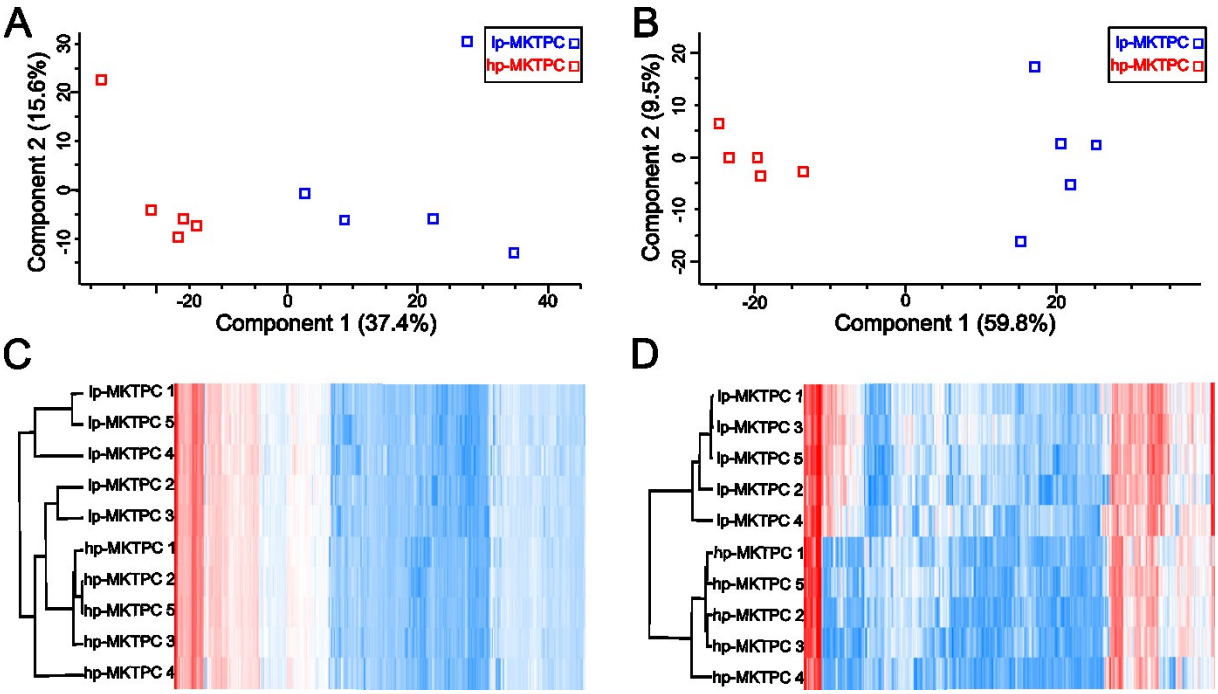

Figure 11: Principal component analysis (PCA) of cellular proteomes **(A)** and secretomes **(B)** of MKTPCs derived from lp-MKTPCs and hp-MKTPCs; each square represents an individual donor. Heat map and unsupervised hierarchical clustering of cellular proteomes **(C)** and secretome **(D)**.

Volcano plot analysis using the paired Welch *t*-tests resulted in the detection of 421 and 212 proteins significantly altered in abundance in the hp-MKTPC cell proteomes and secretomes, respectively (Figure 12 A, B). A complete list of differentially abundant proteins for proteomes and secretomes can be found in Supplementary Info 1. The secretome of hp-MKTPCs showed a nearly fivefold increased number of proteins reduced in abundance (176) compared to proteins increased in abundance (36). For the hp-MKTPC proteome, where 174 proteins were less abundant and 247 more abundant, the disparity was less pronounced. Strikingly, proteins involved in smooth muscle activity such as CNN1, ACTA2, MYH11, and desmin (DES) were found to be less abundant in the hp-MKTPC proteome. Further proteins with decreased abundance were factors such as nuclear factor (NF)-κB (NFKB1) and elongation factor 1-alpha 1 (EEF1A1), while regulatory proteins such as EGF-like repeat and discoidin I-like domain-containing protein 3 (EDIL3), ubiquitin-conjugating enzyme E2 J2

(UBE2J2), and plasminogen activator inhibitor 1 (SERPINE1) were found to be more abundant in the proteome of passaged MKTPCs.

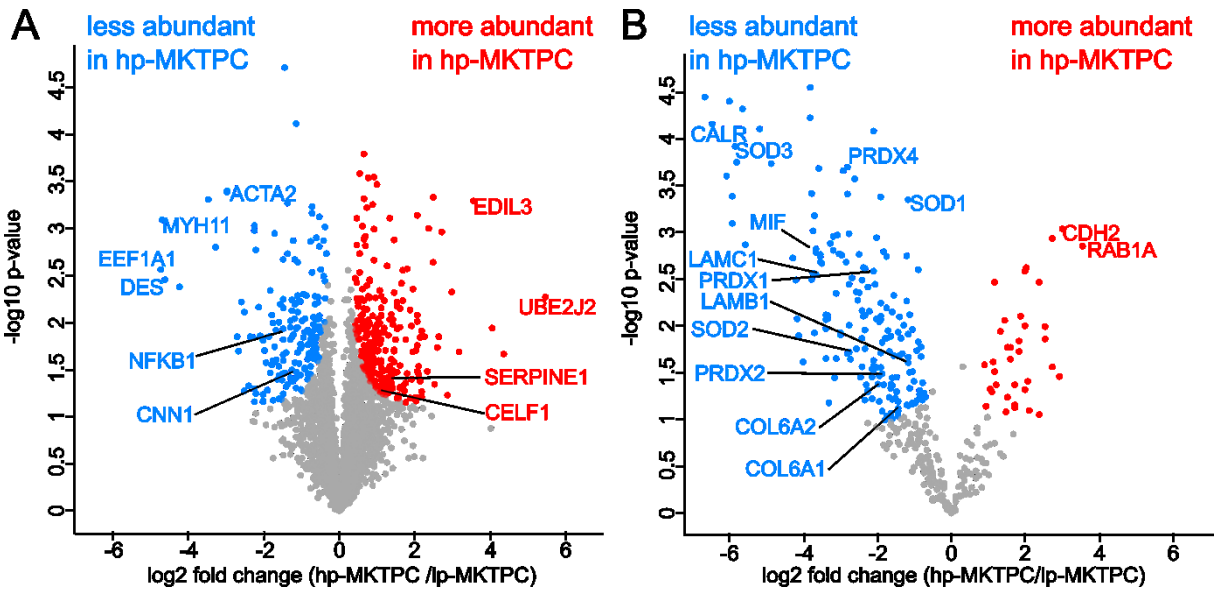

Figure 12: Volcano plots of hp-MKTPC vs. lp-MKTPC proteomes (**A**) and secretomes (**B**). For statistics, a paired Welch *t*-test was used. Results were corrected for multiple testing with a false discovery rate (FDR) of 0.05. Each colored dot represents a differentially abundant protein fulfilling the significance criteria.

In order to examine how much abundance alterations in the secretomes were due to protein secretion rather than cell degradation, all differentially abundant proteins of the secretome were annotated for “extracellular region” (GO:0005576) and the UniProt keyword “secreted”. Accordingly, proteins secreted via classical secretory pathway and via nonclassical secretion were predicted by SignalP and SecretomeP, respectively. In total, 66 classically secreted proteins and 35 proteins with nonclassical secretion were found. Only 31 from 212 proteins had neither of the four annotations, indicating only minor contaminations of proteins released from dying cells. In the secretomes, several members of the collagen family and laminins, e.g., collagen alpha-1(VI) chain (COL6A1), collagen alpha-2(VI) chain (COL6A2), laminin subunit beta-1 (LAMB1), and laminin subunit gamma-1 (LAMC1), were found to be less abundant in hp-MKTPCs. Superoxide dismutases (SOD1, SOD2, and SOD3), peroxiredoxins (PRDX1, PRDX2, PRDX4, and PRDX6), and macrophage migration inhibitory factor (MIF) were also found to be less abundant. Calreticulin (CALR) showed one of the strongest declines in abundance ($\log_2$ fold change: −6.5). Prominent proteins with increased abundance in hp-MKTPC secretomes were regulatory proteins such as cadherin-2 (CDH2) and Ras-related protein Rab-1A (RAB1A).

To obtain deeper insight into the biochemical pathways related to the observed changes, a DAVID annotation cluster analysis of the proteins, which were altered in the proteomes, was performed. This resulted in 20 enriched functional clusters (Figure 13). In the group of proteins more abundant in hp-MKTPCs, different metabolic processes, including the mitochondrial tricarboxylic acid cycle, reactions involving GTPases, and endoplasmic-reticulum-related terms such as retinol metabolic process, as well as extracellular matrix proteoglycans, were significantly enriched (Figure 13 A). In contrast, proteins related to glycolysis, cell cycle, RNA, and splicing processes were found to be enriched in the set of proteins less abundant in hp-MKTPCs (Figure 13 B). Additionally, actins, proteins binding to actin filaments, and proteins related to the term "cell–cell adherens junction" were found to be significantly enriched in the datasets of both up- and downregulated proteins.

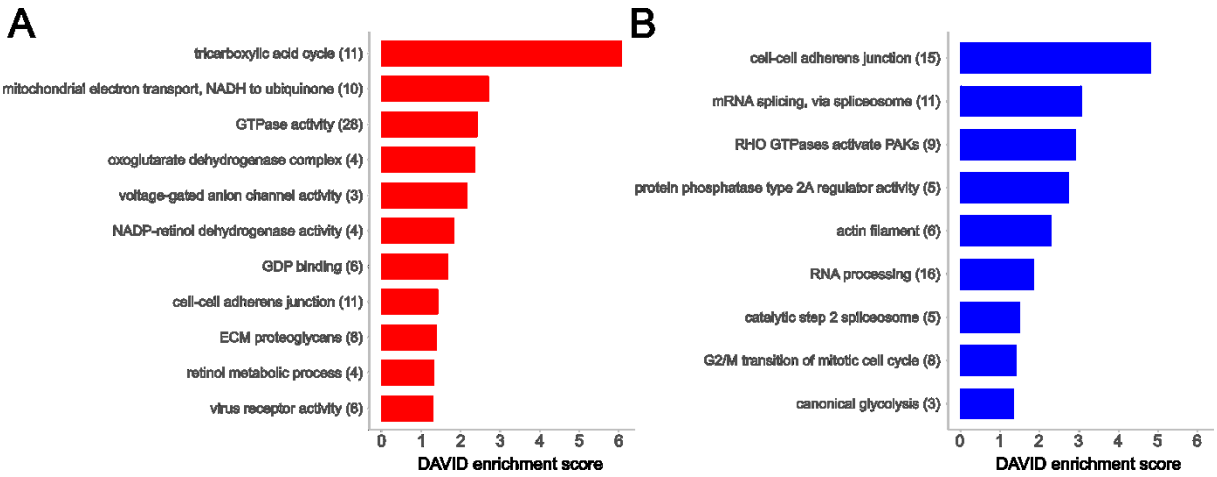

Figure 13: Enriched Database for Annotation, Visualization, and Integrated Discovery (DAVID) annotation clusters from proteins more abundant (**A**) and less abundant (**B**) in hp-MKTPCs. The number in brackets behind the term indicates the number of proteins in one cluster. Results with an enrichment score >1.3 were considered significant. Categories used for the DAVID tool were as follows: Gene Ontology (GO) biological process, GO cellular component, GO molecular function, and REACTOME. NADH: nicotinamide-adenine dinucleotide, reduced, GDP: guanosine diphosphate PAK: p21 activated kinase

3.2.2. Proteome Analysis of Cells and Secretomes of MKTPCs from Young and Old Donors

To further investigate aging-related changes in TPCs, we compared MKTPCs from six young and six old *Callithrix jacchus* individuals. Young donors were either 2 or 3 years old, while the old donors were between 9 and 15 years old. The MKTPCs from older donors showed a significantly increased cell size (Figure 14 A) and expressed a

significantly increased amount of senescence-associated beta galactosidase (Figure 14 B, C). MKTPCs from young individuals entered cell-cycle arrest and showed clear signs of senescence after 11–14 passages, while only 3–7 passages were needed to trigger senescence of MKTPCs from old animals (Figure 14 D). The proteome and the secretome of MKTPCs from young and old donors were analyzed and led to the identification of 4534 and 1192 proteins with 51,801 and 9729 peptides, respectively (Supplementary Info 1). However, in contrast to the lp-MKTPC vs. hp-MKTPC comparison, the principal component analysis showed no clear separation between TPC proteomes and secretomes from young and old individuals (Figure 15). Strikingly, the quantitative protein profiles of the older individuals showed higher variation in components one and two than the protein profiles of the young individuals.

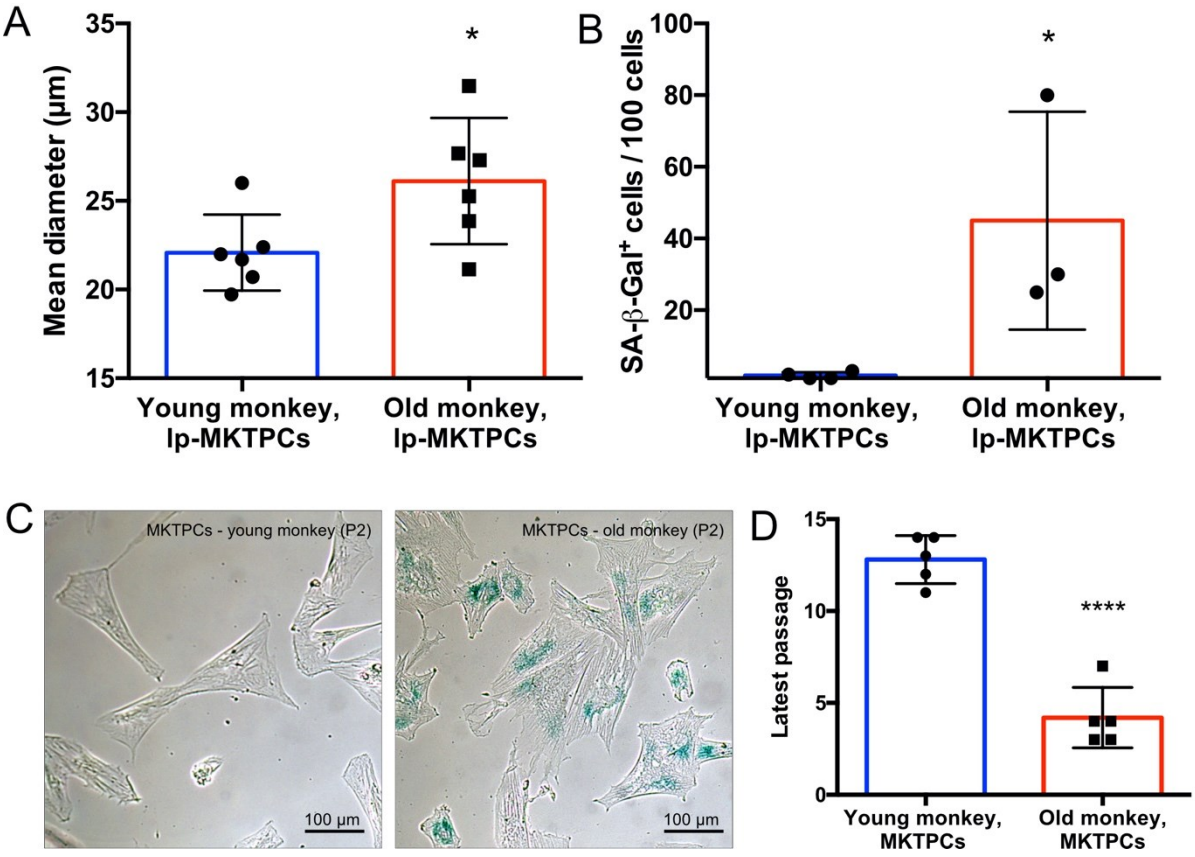

Figure 14: (**A**) Cell size measurement of MKTPCs from young vs. old monkeys revealed significantly increased cell size of MKTPCs from older monkeys. (**B**) Proportion of β-galactosidase-positive MKTPCs from young vs. old monkeys. (**C**) Light micrograph of senescence-associated β-galactosidase staining of MKTPCs from young (3 years) and old (11 years) monkey in passage 2. (**D**) Maximal passage numbers before offset of cell division. Columns indicate the mean; bars indicate the standard deviation. For statistical analysis, unpaired *t*-tests were used (**A**, **B**, **D**). *: p-value < 0.05; ***:_p-value < 0.00005; Experiments performed by Nina Schmid (Biomedical Center; LMU München)

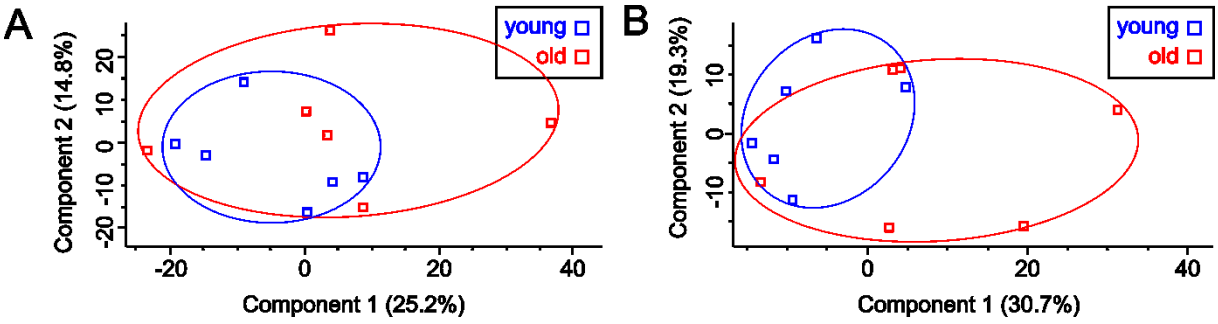

Figure 15: Principal component analysis of cell proteomes (**A**) and secretomes (**B**) of MKTPCs derived from young and older individual donors.

The statistical evaluation of the data using unpaired Welch modified *t*-tests did not lead to the detection of proteins significantly (FDR < 5%) altered in abundance. A Volcano plot analysis also did not show any significant abundance alterations (Figure 16) after correction for multiple testing (FDR < 5%). However, while the cell proteome plot was quite symmetrical, the plot of secretomes was skewed toward negative $\log_2$ fold changes. This indicates a reduced secretion activity of MKTPCs of old animals, for which *p*-values of individual proteins were too high to be considered as significant after *p*-value correction for multiple testing.

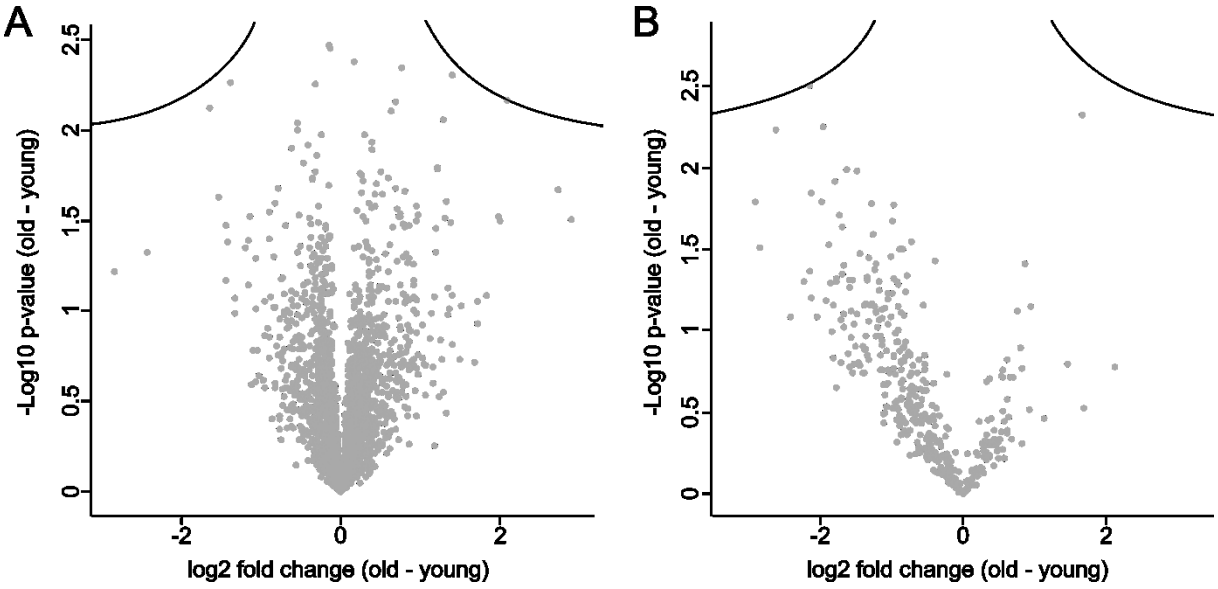

Figure 16: Volcano plot analysis of proteomes (**A**) and secretomes (**B**) of MKTPCs from older and younger individual donors. Proteins above the significance cutoff curve (s = 0.1; FDR < 0.05) are considered significant.

To perform a statistical analysis at the level of related functional terms rather than at the level of individual proteins, a Gene Set Enrichment Analysis (GSEA) was performed. While the analysis of the secretome data resulted in only a small amount

of regulated gene sets (data not shown), the MKPTC proteome analysis resulted in 560 enriched gene sets at an FDR < 0.05 (351 increased and 209 decreased, Supplementary Info 1). The most prominent gene sets within the proteins more abundant in samples from old animals were related to metabolic processes such as the tricarboxylic acid cycle (TCA) and lipid metabolic processes, but also contained terms related to membrane and secretion (Figure 17). Enriched terms from the set of downregulated proteins contained RNA- and DNA-centered processes and, to a lesser extent, terms of metabolic processes related to nitrogen and carbohydrate compounds.

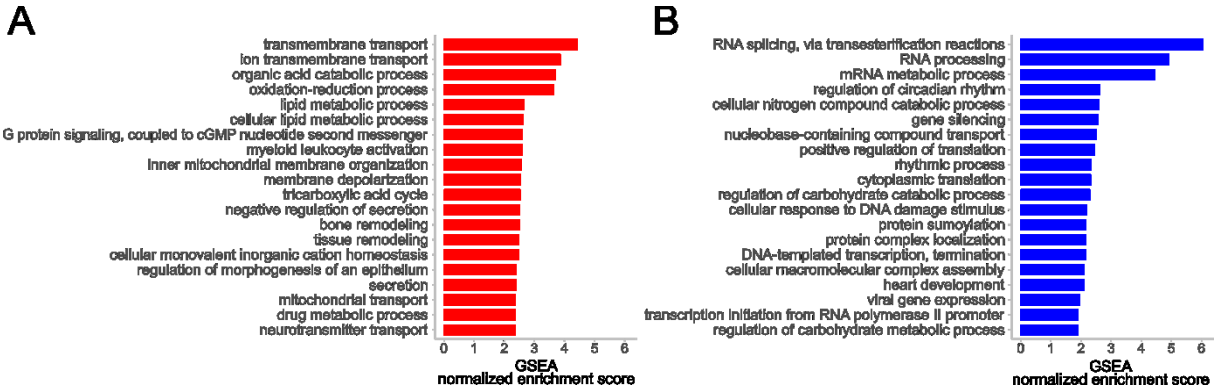

Figure 17: The 20 most significant gene set hits of MKTPC proteomes from older vs. young individual donors. Significant Gene Set Enrichment Analysis (GSEA) results (FDR q-value < 0.05) were summarized by reducing redundancy with REVIGO. Only gene sets from the GO biological process category were utilized. Gene sets enriched in the MKTPC proteome of old donors (**A**) and enriched gene sets in the MKTPC proteome of young donors (**B**) are displayed.

3.3. Age-Related Alterations in the Testicular Proteome of a Non-Human Primate

Section 3.3 has been adapted from: Stöckl, J.B.; Schmid, N.; Flenkenthaler, F.; Drummer, C.; Behr, R.; Mayerhofer, A.; Arnold, G.J.; Fröhlich, T. Age-Related Alterations in the Testicular Proteome of a Non-Human Primate. Cells 2021, 10, 1306. https://doi.org/10.3390/cells10061306

3.3.1. Histology Reveals Ongoing Spermatogenesis in All Samples and Slightly Increased Tubular Diameters in Old Animals

Histological evaluation of testis sections from six young (2 to 3 years) and four old (10 to 12 years) monkeys indicated ongoing spermatogenesis in all specimens (Figure 18). Due to the handling of the testes, germ cells were occasionally detached and were observed in the lumen. However, measurements of tubular diameters were possible and revealed slightly increased diameters in the older individuals ($p < 0.05$) (Figure 18 A).

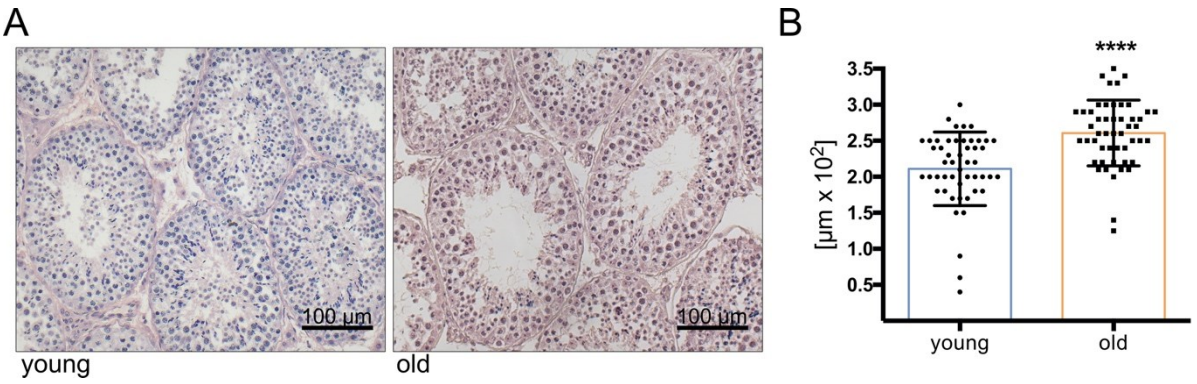

Figure 18: Light micrograph of HE stained sections of testes from young (3 years, left) and old *C. jacchus* (11 years, right) (**A**) Scale bar indicates 100 µm. Tubular diameters of young (2 - 3 years, n= 5) and old (10 - 12 years, n= 4) *C. jacchus.* (**B**) Tubular diameter was slightly increased in the old *C. jacchus* (**** $p < 0.0001$; unpaired *t*-test); individual diameters are shown, and bars indicate the mean and SD; Experiments performed by Nina Schmid (Biomedical Center; LMU München)

3.3.2. Comprehensive Proteome Analysis of Testes of Young and Old Individual Donors

The proteomes of testicular tissue derived from six young (age: on average 2.8 years old) and four old (age: on average 11.2 years old) *Callithrix jacchus* individuals were analyzed by LC MS/MS leading to the identification of 63,510 peptides and 5924 proteins (Supplementary Info 2). Several of the identified proteins are characteristic of

specific testicular cell types (Table 1). For instance, ATP-dependent RNA helicase DDX4 (DDX4) and melanoma-associated antigen 4 (MAGEA4) are in the testis specific for germ cells (Eildermann et al., 2012, Langenstroth et al., 2014), cholesterol side-chain cleavage enzyme, mitochondrial (CYP11A1) and insulin-like 3 (INSL3) are markers specific for Leydig cells (Davidoff et al., 2004, Ivell et al., 2013). Furthermore, cyclin-dependent kinase inhibitor 1B (CDKN1B) and aortic smooth muscle actin (ACTA2, also referred to as alpha-smooth muscle actin) are common markers for adult Sertoli cells and peritubular cells, respectively (Sharpe et al., 2003, Mayerhofer, 2013). Additionally, vimentin (VIM) is common in somatic testicular cell types such as peritubular cells, Sertoli cells and interstitial cells (Kossack et al., 2013).

Table 3: Overview of identified markers for different testicular cell types

Cell type	**Markers**
Leydig cells	CYP11A1, CYP17A1, INSL3
Sertoli cells	VIM, CDKN1B
Peritubular cells	VIM, ACTA2
Germ cells	DDX4, MAGEA4, UTF1

Proteins were quantified using a label-free quantification approach and filtered with the criteria: having at least 90 % valid values among either old or young samples. This resulted in 3217 sufficiently quantified proteins. The quantitative data was analyzed using unsupervised hierarchical clustering and principal component analysis (PCA) (Figure 19 A, Figure 20). PCA shows a separation of testes proteome profiles from old and young donors (Figure 19 A). In contrast, the heatmap shows three main clusters (Figure 20). While proteome profiles from two old individuals are separated from those of the other eight, one cluster contains three young and two old individuals and a third cluster three samples from young individuals.

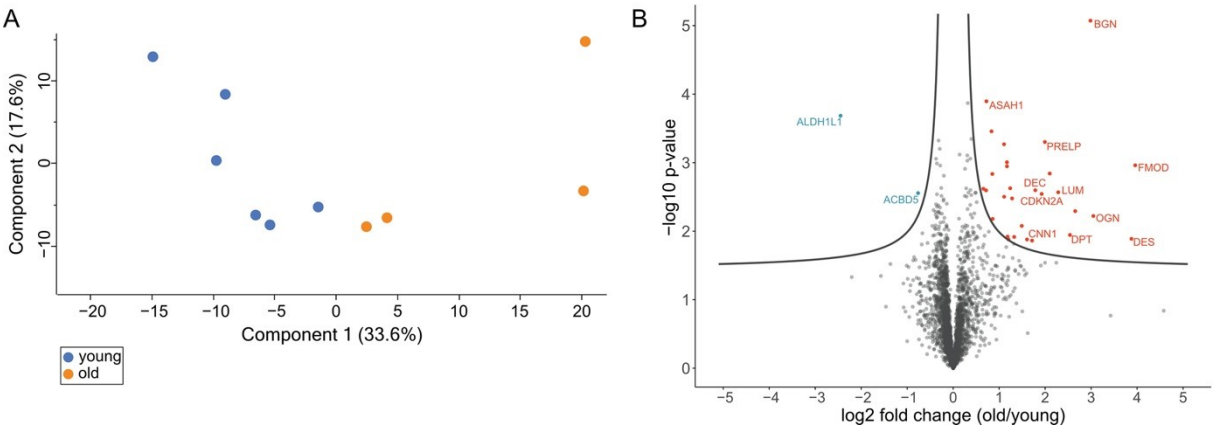

Figure 19: (A) Principal component analysis of old (red dots) and young (blue dots) *C. jacchus* testicular proteome profiles. Numbers in parentheses indicate the percentage of variation each component explains. **(B)** Volcano plot of old vs young testis proteomes. Significance cut off curve was generated using the parameters FDR < 0.05 and s_0 = 0.1. Proteins above the curve are considered significant, red color indicates higher abundance in old donors, blue color indicates lower abundance in old donors.

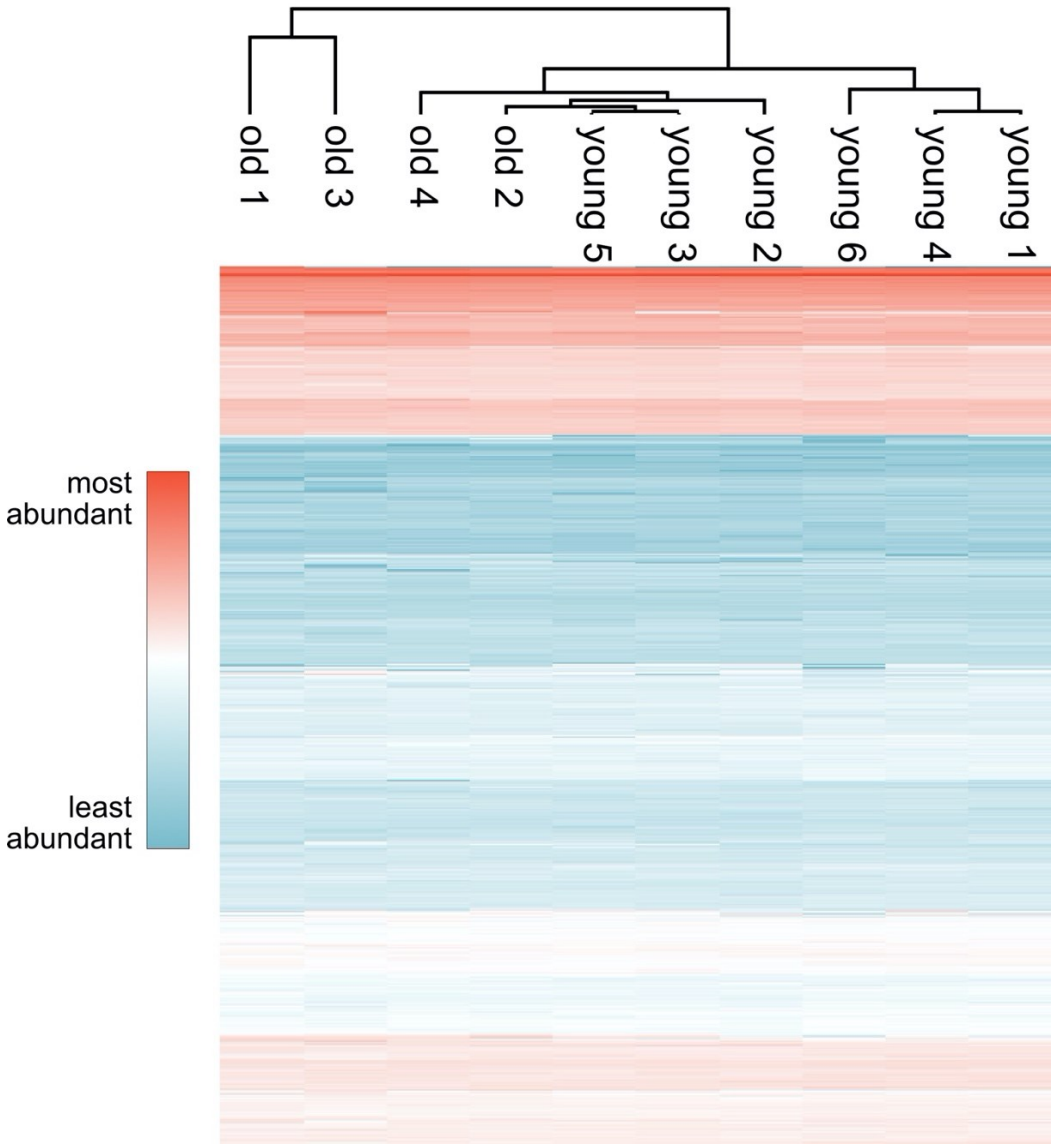

Figure 20: Unsupervised hierarchical clustering of old and young *C. jacchus* testicular proteome profiles

3.3.3. Volcano Plot Analysis Reveals Significant Alterations in the Testis Proteome of Older Individuals

A volcano plot analysis revealed 31 differentially abundant proteins in the testicular proteomes of the older individuals compared to the proteomes of the young testes (Figure 19 B, Supplementary Info 2) (FDR < 0.05). All these proteins were clustered in a z-score normalized heatmap, illustrating the strong differences in abundance (Figure 21 A). Furthermore, a higher variance in the abundance of these proteins within the samples from old individuals compared to samples from the young individuals became apparent. Conspicuously, only two of the differentially abundant proteins were less abundant in the testis samples of aged animals: i) cytosolic 10-formyltetrahydrofolate dehydrogenase (ALDH1L1) and ii) acyl-CoA-binding domain-containing protein 5 (ACBD5). The 29 more abundant proteins could predominantly be assigned to three protein families: four proteins from the actin-binding calponin repeat family, three tropomyosins and several members of the small leucine-rich proteoglycans (SLRPs). A Gene Ontology analysis using the PANTHER online tool was used to classify the differentially abundant proteins (Figure 21 B).

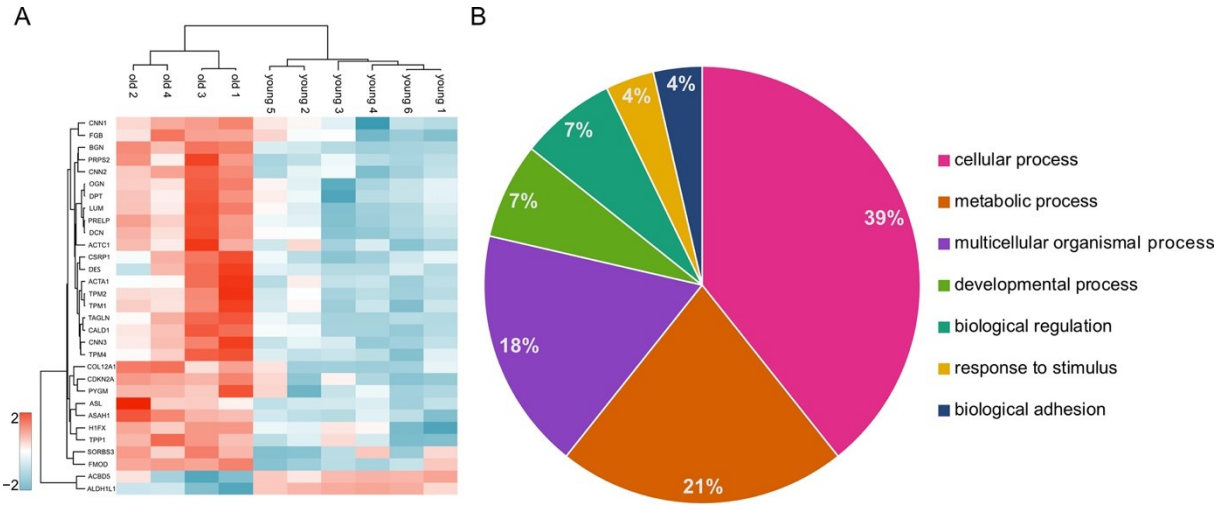

Figure 21: (**A**) Heatmap and unsupervised hierarchical clustering of differentially abundant proteins for the comparison old vs young testicular proteomes. Data was z-scored prior to the analysis. (**B**) PANTHER analysis of differentially abundant proteins using GO biological process as database. The numbers indicate the percentage of proteins annotated with the corresponding GO term.

3.3.4. DAVID Analysis Reveals Clusters of Enriched Functional Terms

The data was annotated and analyzed with DAVID resulting in functionally enriched terms which were subsequently clustered (Figure 22, Supplementary Info 2). Six clusters were found to be significantly enriched and the most significant term was used to label the cluster. Out of the 31 differentially abundant proteins, 21 are represented in at least one of these clusters. The cluster named “muscle filament sliding” showed the highest enrichment score and comprises desmin (DES), actins and three tropomyosins. These three tropo-myosins were also found in the cluster “muscle thin filament tropomyosin”. In the second most enriched cluster “extracellular matrix”, all above mentioned SLRPs, collagen al-pha-1(XII) chain (COL12A1), dermatopontin (DPT) and fibrinogen beta chain (FGB) were found. The cluster “keratan sulfate catabolic process” contained four differentially abundant SLRPs: lumican (LUM), fibromodulin (FMOD), mimecan (OGN) and prolargin (PRELP). However, in our dataset, no enzyme of this pathway was identified. The cluster “cell-cell adhesion” comprises actin-binding proteins like calponins and caldesmon (CALD1). The cluster “secreted” includes enzymes like tripeptidyl-peptidase 1 (TPP1) and acid ceramidase (ASAH1) in addition to the proteins of the cluster “extracellular matrix”.

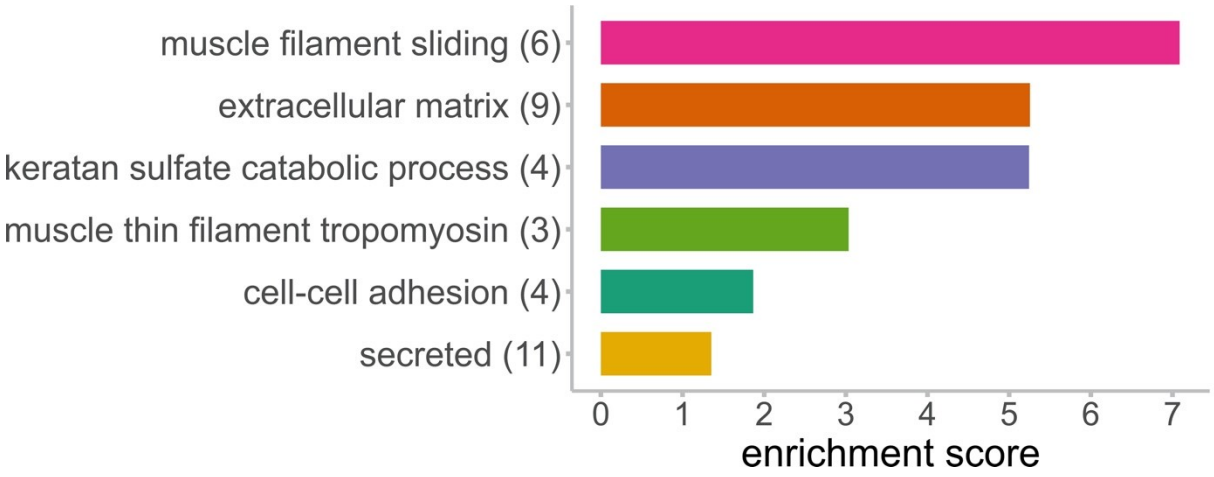

Figure 22: Clusters of functionally enriched terms generated from proteins differentially abundant in testes of old donors. Numbers in brackets indicate the number of identified proteins in one cluster. Categories used for the DAVID tool were: GO biological process, GO cellular component, GO molecular function, REACTOME, UniProt keywords

3.3.5. STRING Analysis Results in a Rich Interaction Network

The 31 differentially abundant proteins were analyzed with STRING (Figure 23). This resulted in significantly more interactions than expected by chance (PPI enrichment p-value: 1.0 x e-16, expected number of edges: 5, number of edges found: 73). From 31 proteins, 23 had at least one interaction with another differentially abundant protein. Strikingly, two distinct networks can be observed, of which the smaller contained all the differentially abundant SLRPs together with DPT and COL12A1. All of them are annotated to be secreted, and some are known to be involved in “supramolecular fiber organization”, while others are part of “glycosaminoglycan catabolic process”. LUM and FMOD are part of both gene sets. The other network comprises various cytoskeletal proteins, of which around half are also known to be involved in “supramolecular fiber organization”. Cysteine and glycine-rich protein 1 (CSRP1) is not annotated in the four chosen categories but is, e.g., involved in actin cytoskeleton organization.

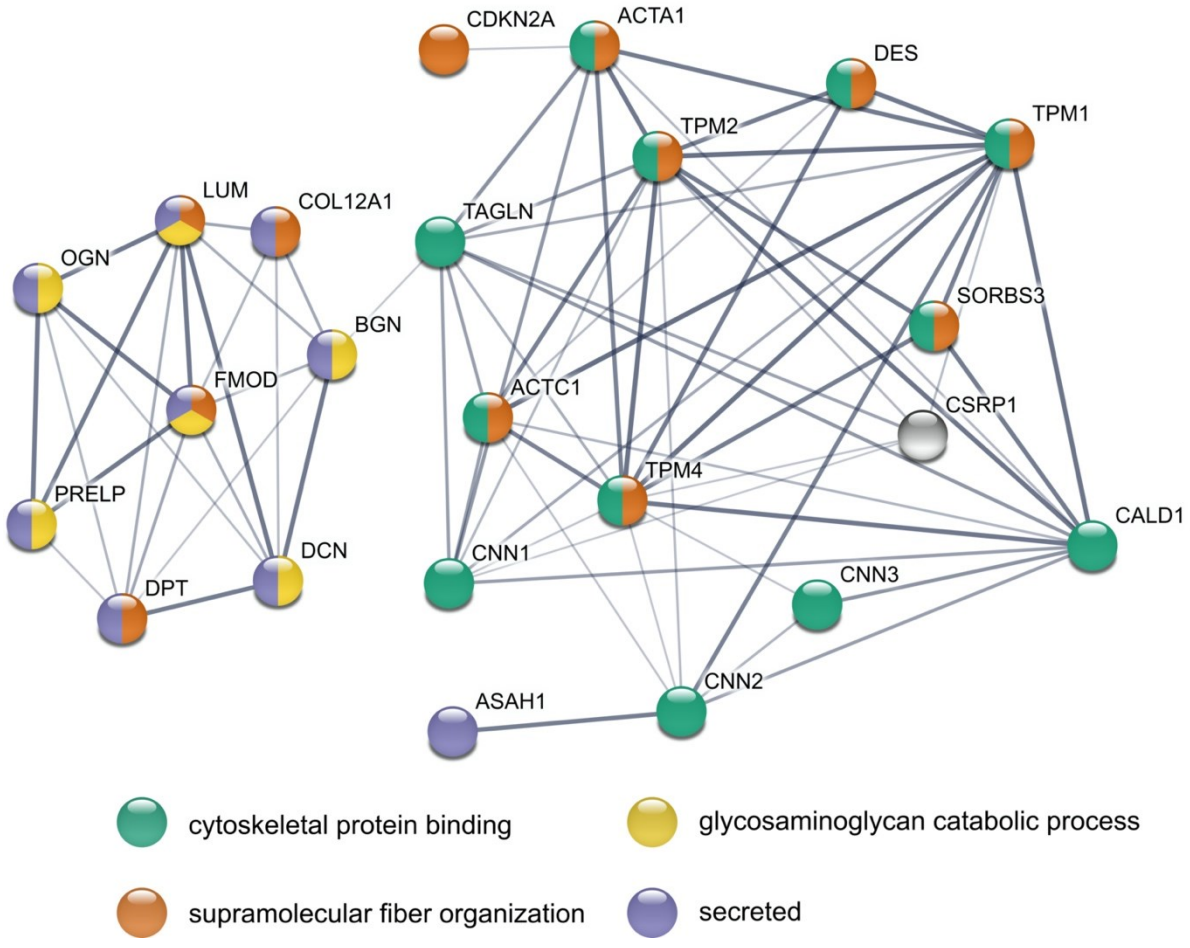

Figure 23: STRING analysis of all differentially abundant proteins in the testis of old vs. young donors. Nodes represent individual proteins and are colored based on the four annotations indicated at the bottom of the figure. Line strength indicates confidence level from low (0.150) to highest (0.900).

3.3.6. Immunostaining Illustrates the Increased Abundance of Extracellular Matrix Proteins

Immunohistochemistry revealed expression of CNN1 in testicular peritubular cells of young and old *Callithrix jacchus* (Figure 24 A, a, B, b). Smooth muscle cells of testicular blood vessels were also immunopositive for CNN1 and served as internal staining control. In the young individuals, not all peritubular cells were immunopositive. In contrast, in the old individuals all peritubular cells were stained.

OGN was detected mainly within the interstitial space of both, young and old individuals (Figure 24 C, c, D, d). More intensive staining of larger interstitial areas indicates higher abundance of OGN. Both findings nicely corroborate our proteome analysis, where CNN1 (log_2 fold change: 1.61; p-value: 0.013) and OGN (log_2 fold change: 3.05; p-value: 0.0060) were found to be more abundant in the old testes.

Collagen alpha-1(I) chain (COL1A1) was localized in the peritubular wall compartment and the interstitial space, with higher abundance in old individuals (Figure 24 E, e, F, f,). In the proteome analysis, a trend (p-value: 0.14; log_2 fold change: 0.72) towards an increased COL1A1 abundance was found.

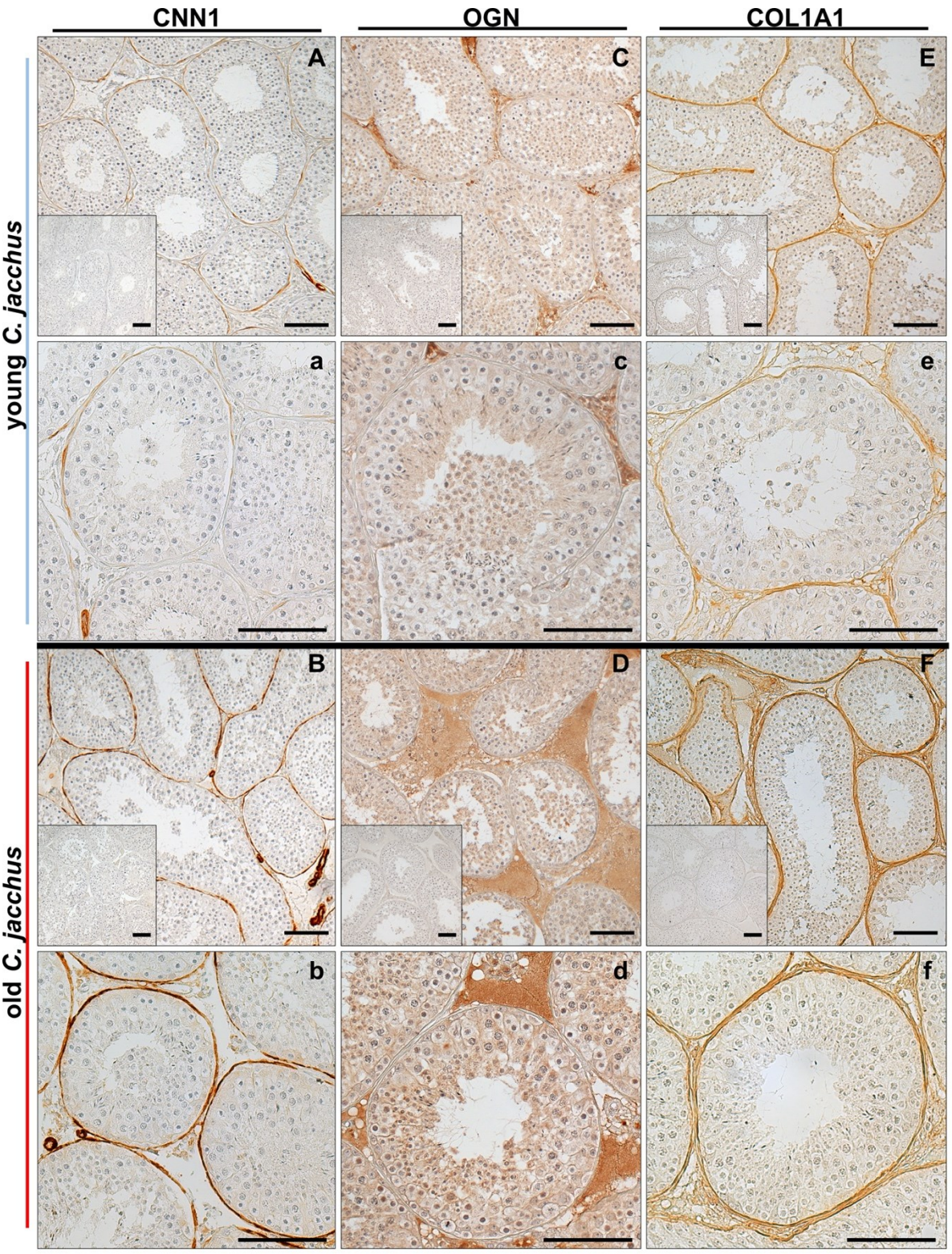

Figure 24: Representative light micrographs of immunohistochemistry. Testicular sections from young (2-3 years) and old (10-12 years) *C. jacchus* were stained with specific antibodies against CNN1, OGN and COL1A1. CNN1 staining was found in most peritubular cells from young *C. jacchus* (A, a, (higher magnification)). In old *C. jacchus*, CNN1 was expressed in all peritubular cells (B, b (higher magnification)). OGN was detected mainly within the interstitial space of testes of young *C. jacchus* (C, c (higher magnification)). The level increased in the testes of old *C. jacchus* (D, d (higher magnification)). COL1A1 was detected in peritubular cells from young (E, e (higher magnification)) and old (F, f (higher

magnification)) *C. jacchus*. In old individuals, COL1A1 expression increased in the interstitial space. Nuclei were slightly stained with hematoxylin. Inserts: negative controls. Scale bars = 100 µm; Experiments performed by Nina Schmid (Biomedical Center; LMU München)

4. Discussion

4.1. Proteome Analysis of MKTPCs and Comparison with HTPCs

Section 4.1 has been adapted from: Schmid N, Stöckl JB*, Flenkenthaler F, Dietrich KG, Schwarzer JU, Köhn FM, Drummer C, Fröhlich T, Arnold GJ, Behr R, Mayerhofer A. Characterization of a non-human primate model for the study of testicular peritubular cells-comparison with human testicular peritubular cells Mol Hum Reprod. 2018 Aug, 1;24(8):401-410. doi: 10.1093/molehr/gay025. PMID: 29846669.*

**Contributed equally*

A main indicator for the suitability of MKTPCs as a model for HTPCs would be a close resemblance between their proteomes. In a first step to investigate this, the proteomes of MKTPCs were characterized, using cells obtained from 6 individual young adult *Callithrix jacchus* donors. In order to focus on the most abundant proteins being easily assessable with a single-run LC-MS/MS method, the proteomics workflow was kept as simple as possible and there was no pre-fractionation at the protein or the peptide level. Nevertheless, the analysis of the acquired mass spectra led to the identification of 2437 MKTPC protein groups (FDR < 1 %). For the chosen approach, this represents a fairly high number of protein IDs and reflects the suitability of the *Callithrix jacchus* database for LC-MS based proteome analysis of MKTPC samples. Additionally, a multi scatter plot analysis (Figure 5 A) between the donors revealed very reproducible protein expression patterns, demonstrating the robustness of isolation and cultivation methods as well as a low inter-individual variability between the individual donors.

For the suitability of the animal model, the similarity between MKTPC and HTPC at the proteome level is an important indicator. To assess this, HTPC proteomes from 7 human donors were analyzed using exactly the same methodology. Inter-individual correlation analysis shows clear homogeneity and reproducibility similar to MKTPCs (Figure 5 B), with the latter one being more accessible and generated under monitored conditions. The inter-species scatter plot analysis of protein intensity values between MKTPC and HTPC showed a Pearson correlation coefficient of 0.78 (Figure 6) indicating similar abundance patterns of MKTPC and HTPC proteins. A further MKTPC

vs. HTPC multi scatter plot analysis at the level of individuals (Figure 7) showed in all cases very similar Pearson correlation coefficients with no outliers. Taken together, the correlation analyses reveal a clear conformity between MKTPC and HTPC on the level of protein expression patterns and a high degree of inter-individual reproducibility of MKTPCs.

A circoletto network analysis (Figure 8) as well as a BLAST analysis of the 25 most abundant proteins showed high sequence homology between HTPC and MKTPC proteins, indicating a high degree of functional similarity (Table 1). Using a spectral count quantification approach combined with homology-based protein grouping, we could further demonstrate that the broad majority of the 25 most abundant MKTPC protein groups are also highly expressed in HTPCs (Table 2). Only transgelin (TAGLN), caldesmon (CALD1) and the two tropomyosins (TPM1 and TPM4) showed lower spectral counts in MKTPC. Since all of these four proteins are actin binders this finding may reflect slight differences in the cytoskeleton between MKTPC and HTPCs. Finally, the PANTHER GO analysis of MKTPC and HTPC proteins lead to almost identical results (Figure 9), suggesting a strong resemblance at the level of biological and biochemical processes between MKTPCs and HTPCs.

Overall, the proteome data demonstrates a high similarity between MKTPCs and HTPCs. This was published alongside data on the isolation of MKTPCs as well as a characterization of MKTPCs using RT-PCR, immunohistochemistry, and immunofluorescence (Schmid et al., 2018). Just like HTPCs, MKTPCs can be isolated from testicular fractions and, in resemblance of the proteome data, express typical markers such as calponin-1 (CNN1), aortic smooth muscle actin (ACTA2), and androgen receptor (AR). They also produce characteristic factors such as glial cell line-derived neurotrophic factor (GDNF) and decorin (DEC). In summary, MKTPCs closely resemble their human counterparts and are therefore a suitable model for HTPCs. MKTPCs are isolated from adult marmosets, which live in a controlled environment. Therefore, contrary to HTPCs, cells from both young and old individuals are obtainable, while the influence of confounding factors is also reduced.

4.2. Proteomic Insights into Senescence of Testicular Peritubular Cells from a Non-Human Primate Model

Section 4.2 has been adapted from: Stöckl, J.B.; Schmid, N.; Flenkenthaler, F.; Drummer, C.; Behr, R.; Mayerhofer, A.; Arnold, G.J.; Fröhlich, T. Proteomic Insights into Senescence of Testicular Peritubular Cells from a Nonhuman Primate Model. Cells 2020, 9, 2498. https://doi.org/10.3390/cells9112498

4.2.1. General Remarks

In the present study we compared MKTPCs derived from young donors of high (hp-MKTPC) and low passages (lp-MKTPC). As this *in vitro* model may not exactly reflect *in vivo* aging, we further analyzed MKTPCs from young donors with MKTPCs from old donors (nine to fifteen years). As captive marmosets show signs of aging already at the age of 8 years, the animals in the older group can be considered aged or even old (Ross et al., 2012, Moussavi et al., 2020, Mietsch et al., 2020). The comparison of data from both sample sets enabled us to clarify to what extent repeated passaging reflects *in vivo* TPC aging. We focused on the analysis of TPC proteomes using a straightforward label-free mass spectrometry-based approach and detected over 5000 proteins. This high number of identified proteins corresponds to the analytical depth achieved by recent proteomic studies in the testes of other species (Jarvis et al., 2020, Schmid et al., 2020, Zhou et al., 2020). Among the identified proteins, we found MYH11, ACTA2 and CNN1, all related to the typical smooth muscle-like phenotype of TPCs. Furthermore, we detected low abundant factors, e.g., NF-κB, demonstrating the sensitivity of our approach. In addition to cell lysates, we analyzed conditioned cell culture media to further monitor age-related alterations of the TPCs secretory activity. Out of these secretomes, we were able to identify nearly 1200 proteins, among them low abundant factors such as the important immune signaling factor MIF, demonstrating the analytical depths and biological relevance of our dataset.

4.2.2. Alterations in the Proteome of hp-MKTPC Point to Impaired Signaling, Reduced Contractility, and Altered RNA Processing in Senescent MKTPC

Among the proteins more abundant in hp-MKTPCs compared to lp-MKTPCs, several are related to mitochondrial energy production via the TCA-cycle and the electron transport chain (Figure 13 A). In contrast, senescent HTPCs showed a decrease in

mitochondrial proteins and a degrading mitochondrial ultrastructure (Schmid et al., 2019). This is in line with mitochondrial dysfunction described as a classic hallmark of senescence (Chapman et al., 2019, Lopez-Otin et al., 2013). Nevertheless, since only a small subclass of mitochondrial proteins was found to be altered in abundance in hp-MKTPCs, monkey TPC mitochondria may have been less affected by passaging than their human counterparts.

Many other findings in hp-MKTPC, e.g., the increased abundance of Ras-related and GDP binding proteins (Figure 13 A), are in line with the results of senescent HTPCs (Schmid et al., 2019). In detail, we found the Ras-related proteins Rab-1A, Rab-21, Rab-5B, Rab-32, Rab-31, Rab-5C, and Rab-5A, more abundant in hp-MKTPC. Ras-related proteins are small GTPases, which regulate vesicle formation and membrane trafficking and can have a variety of functions (Homma et al., 2020). For example, Ras-related protein Rab-1A (RAB1A), is involved not only in interleukin 8 and growth hormone secretion but also in autophagy and cell migration (Dong et al., 2012, Yang et al., 2016). Furthermore, many Ras-related proteins are known to act as oncogenes and tumor suppressive regulators (Gopal Krishnan et al., 2020). Considering the broad role of this protein class in disease and male fertility, alterations in their abundance may reflect higher risks of tumorigenesis and an impaired spermatogenesis of the aging testis (Simanshu et al., 2017, Bae et al., 2019).

The functional enrichment analysis of the proteins with higher abundance in hp-MKTPCs revealed an overrepresentation of extracellular matrix (ECM) proteins associated with the REACTOME term “ECM proteoglycans”. Among them, we found the transmembrane receptors integrin alpha-2 (ITGA2) and integrin beta-5 (ITGB5) as well as dystroglycan (DAG1) and laminin subunit beta-1 (LAMB1). The two latter proteins are known to be localized at the basement membrane. In addition to its structural functions and its proximity to TPCs, the basement membrane further acts as a platform for complex signaling and is an important player for extracellular matrix organization.

Since the maintenance of the ECM is a key feature of TPCs, the observed abundance alterations may reflect irregularities in this task. Additionally, we found an increased abundance of SERPINE1 in hp-MKTPCs, which is a downstream target of p53

triggered senescence (Kortlever et al., 2006). Together with the alterations in Ras-related proteins, all these findings clearly indicate impairments in hp-MTKPC signaling. This finding is further supported by a decreased abundance of the p105 subunit of NF-κB (NFKB1) in hp-MKTPC. NF-κB is a pleiotropic transcription factor which is regulated by various signal transduction pathways and fulfills roles in various biological processes. Interestingly, NFKB1-deficient mice show an early onset of aging (Bernal et al., 2014). From the set of proteins less abundant in hp-MKTPC, we found proteins related to the Gene Ontology terms “RNA processing” and “catalytic step 2 spliceosome” less abundant in hp-MKTPCs. An age-related downregulation of alternative splicing has already been described and was also found in HTPCs of high passage number (Harries et al., 2011, Holly et al., 2013, Schmid et al., 2019). In this context two proteins are particularly interesting: Heterogeneous nuclear ribonucleoprotein D0 (HNRNPD) and serine/arginine-rich splicing factor 7 (SRSF7). In a recent study, HNRNPD was knocked down in human endothelial cells, which resulted in an increased occurrence of senescence (Latorre et al., 2018). Furthermore, SRFSF7 is known to play a role in the regulation of alternative splicing of p53 and in the regulation of senescence (Chen et al., 2017). These findings strongly suggest that RNA-binding proteins and alternative splicing play an important role in the development of senescence in TPCs.

In addition to changes related to RNA processing and splicing, the functional enrichment analysis revealed a significantly high proportion of proteins of the REACTOME pathway “RHO GTPases activates PAKs” (Figure 13 B). This pathway is mainly involved in cytoskeletal reorganization and contains several proteins characteristic for TPCs such as myosin-10 (MYH10), myosin-11 (MYH11) and calmodulin-1 (CALM1), all found less abundant in hp-MKTPC. The pathway also includes myosin regulatory light chain 12B (MYL12B) and smooth muscle myosin light chain kinase (MYLK). Both regulate smooth muscle cell contraction and were less abundant. Proteins which are not part of this pathway but are also essential for contractility such as smooth muscle actin (ACTA2), desmin (DES) and calponin-1 (CNN1) were also less abundant in hp-MKTPCs. ACTA2, CNN1 and MYH11 are commonly described as contractility markers and are known to be reduced in patients with impaired spermatogenesis (Schell et al., 2010, Welter et al., 2013). Furthermore, a decrease in DES positive cells in elderly men’s testes was reported, making it a clear

indicator of testicular aging (Arenas et al., 1997). Overall, the broad decrease in various structural and regulatory proteins points towards a reduced contractility. Contrary to the study in the human system (Schmid et al., 2019), we provide clear evidence for the decreased abundance of key contractility markers.

4.2.3. The Secretome of hp-MKTPC Indicates Alteration in ROS Handling and Signaling

Strikingly, similar to the proteomes, many alterations in abundances found in hp-MKTPC secretomes were previously found in HTPCs, which underlines the relevance of our non-human primate model for the human system. For instance, a lower abundance of different alpha collagens and laminins was found in hp-MKPTCs, highlighting the impact of TPC senescence on the ECM (Figure 14 B)(Schmid et al., 2019). In contrast to the HTPC results, macrophage migration inhibitory factor (MIF) was found in lower abundance in hp-MKTPCs, while it was more abundant in senescent HTPC secretomes. Since MIF is a pro-inflammatory cytokine which can activate NF-κB, this could indicate a different role for immune signaling in the young MKTPC donors compared to the aged HTPC donors (Salminen and Kaarniranta, 2011). Another protein involved in NF-κB signaling is the calcium-binding chaperone calreticulin (CALR). It is one of the proteins with the most reduced abundance (log_2 fold change: -6.5) in hp-MKTPC secretomes. With respect to the regulation of CDK-Inhibitor 1 (p21), CALR competes with CUGBP Elav-like family member 1 (CELF1), which was found to be more abundant in the hp-MKTPC proteome (Iakova et al., 2004). The binding of CELF1 instead of CALR to p21 RNA leads to growth arrest and consequently to senescence. Therefore, the observed change in the ratio of CALR/CELF1 may reflect a reduced CALR repression of p21 translation and clearly indicates an involvement of p21 in the cellular senescence of MKTPCs.

Among the proteins less abundant in hp-MKTPC secretomes were several peroxiredoxins and superoxide dismutases, all involved in the degradation of reactive oxygen species (ROS). This is in line with results from several studies which support the idea that increased ROS is not necessarily the cause, but the result of aging and possibly caused by a reduced abundance of ROS handling enzymes in senescent cells (Hekimi et al., 2011). However, it is known that a knockdown of Cu-Zn superoxide dismutase (SOD1) leads to senescence, which supports the common hypothesis that excessive ROS triggers senescence (Blander et al., 2003, Davalli et al., 2016a). Even

though this study cannot resolve if ROS are the product or the inducer of senescence in hp-MKTPCs, it emphasizes the role of ROS in senescent MKTPCs.

Strikingly, in hp-MKTPC secretomes, we found a considerably higher number of proteins decreased rather than increased in abundance compared to lp-MKTPC. This hints to a lower capability of senescent cells to secrete proteins. Furthermore, cadherin-2 (CDH2), a protein important for cell-cell adhesion, and Ras-related protein Rab-1A (RAB1) which was also more abundant in hp-MKTPC proteomes, were the two proteins with the strongest increase in abundance in hp-MKTPC secretomes (Tamura et al., 1998). These proteins, so far not reported in the context of cellular senescence, illustrate that senescence-induced protein secretion may also influence other cell types in the testis. Several proteins with decreased abundance in the secretome of hp-MKTPCs, i.e., fibronectin, laminins, collagens, and MIF also imply a senescence-associated secretory phenotype (SASP) affecting testicular signaling (Coppé et al., 2008, Coppé et al., 2010).

4.2.4. Proteomics Reveals Reduced Contractility Markers and Impaired Secretion as Subtle Signs of Senescence in the Proteome of Older MKTPCs

Like hp-MKTPCs, MKTPCs from old donors showed characteristic hallmarks of senescence, namely beta galactosidase expression and increased cell size (Figure 14). However, in contrast to the passaged MKTPCs, PCA did not lead to a clear separation of proteomes and secretomes of MKTPCs from old and young donors (Figure 15). Additionally, neither statistical Welch's *t*-tests nor volcano plot analyses revealed differentially abundant proteins (Figure 16). Thus, alterations in the old MKTPC group were less pronounced than in *in vitro* induced senescence in hp-MKTPC.

In contrast to their young counterparts, the proteome and secretome profiles from the old MKTPC group showed higher variations, which may be related to the fact that this group was composed of donors with an age range of nine to fifteen years and therefore somewhat heterogeneous. Additionally, similar to the passaged MKTPCs, the asymmetrical volcano plot of the secretome suggests a reduced secretory activity of MKTPCs from old animals as compared to young animals. In combination with the fact that MKTPCs of old individuals could be significantly less often passaged and showed other clear signs of senescence, these observations suggest differences in the

corresponding cell proteomes. Indeed, a gene set enrichment analysis comparing datasets of older vs. young MKTPCs led to several significantly enriched gene sets in the cell proteome (Figure 17).

Similar to the results from the passaged MKTPCs, several enriched gene sets are related to metabolic pathways, especially mitochondrial pathways such as the TCA cycle, which was the most enriched pathway in hp-MKTPCs. Particularly interesting is the enrichment of proteins related to the term “negative regulation of secretion”, which fits the decreased secretion observed for many proteins. The set of proteins less abundant in older MKTPC showed an enrichment for various terms related to RNA processing and splicing, which was also detected in hp-MKTPCs and was discussed as a sign of aging and senescence (see above). Furthermore, proteins related to smooth muscle cell contraction were found in the terms “heart development” and in the REACTOME term “smooth muscle contraction”, both significantly decreased (FDR < 0.05), again indicating a possible loss of contractility. Incidentally, three of the enriched proteins in the downregulated term “regulation of circadian rhythm” were non-POU domain-containing octamer-binding protein (NONO), splicing factor, proline- and glutamine-rich (SFPQ), and paraspeckle component 1 (PSPC1). All three proteins were previously reported to be expressed in Sertoli cells and play a role in androgen receptor signaling (Kuwahara et al., 2006). The androgen receptor also plays an active role in TPCs which makes these three proteins an interesting new target for follow-up studies to explore their specific roles in TPCs (Mayer et al., 2018). Two negatively enriched gene sets were REACTOME “cellular senescence” and “cell cycle”. One prominent member of these enriched terms was again NF-κB, which was already found significantly lower abundant in senescent MKTPCs and HTPCs, indicating again alterations in the immune signaling of senescent TPCs.

4.2.5. Concluding Remarks

This study demonstrates that replicative senescence in hp-MKTPCs is associated with a variety of alterations in the proteome and secretome. The detected alterations showed a high degree of similarity to results previously obtained in human TPC, which demonstrates that the non-human *Callithrix jacchus* model reliably reflects the human system (Schmid et al., 2019). The detected proteome and secretome alterations in senescent MKTPCs strongly suggest impairments of protein secretion and ECM modulation, as well as a decreased capacity to handle ROS. Furthermore, our results

provide evidence for changes in RNA processing and alternative splicing, for NF-κB-modulated immune signaling and for a reduced capability of senescent MKTPC to contract.

In addition to studies on TPC senescence induced by repeated cell passaging, the common marmoset model facilitates studies and comparisons of young and older TPCs aged *in vivo.* Even though the alterations within the proteomes and secretomes of *in vivo* aged MKTPCs are less pronounced than in *in vitro* aged TPCs, we again found evidence for an impaired protein secretion, for alterations in splicing and for a reduced contractility of *in vivo* aged MKTPCs. These findings demonstrate the involvement of TPCs in testicular aging.

However, it has to be considered that even though proteomics is a powerful research tool, facilitating the quantification of thousands of proteins, proteome alterations alone cannot completely characterize the entire mechanism of a complex process such as cellular aging. Nevertheless, the detected senescence-related proteome alterations and the associated biochemical pathways are particularly valuable and can serve as a basis for future functional and mechanistic experiments dedicated to improving the understanding of cellular aging.

4.3. Age-Related Alterations in the Testicular Proteome of a Non-Human Primate

Section 4.3 has been adapted from: Stöckl, J.B.; Schmid, N.; Flenkenthaler, F.; Drummer, C.; Behr, R.; Mayerhofer, A.; Arnold, G.J.; Fröhlich, T. Age-Related Alterations in the Testicular Proteome of a Non-Human Primate. Cells 2021, 10, 1306. https://doi.org/10.3390/cells10061306

4.3.1. General Remarks

This study was performed to examine age-related changes in testicular proteins. We analyzed the testicular proteomes of six young (2 to 3 years) and four old (10 to 12 years) *Callithrix jacchus* individuals. Captive marmosets show the first signs of aging around the age of 8 years, and therefore, the older animals can be regarded as old, healthily aged individuals (Ross et al., 2012, Mietsch et al., 2020, Moussavi et al., 2020). We were able to directly compare testicular tissues from young and old individuals grown up under well-characterized conditions in the same colony and thereby minimizing influences of lifestyle. Using a bottom-up mass spectrometry approach, we identified 5924 proteins, among them several specific for germ cells and somatic cells, like Leydig and Sertoli cells, in the testis. This indicates a profound analytical depth, shows that all major testicular cell types are captured by our analysis and thus demonstrates the relevance of our dataset. Principal component analysis (PCA) of LFQ intensity values led to a clear separation between old and young testicular proteomes, indicating significant alterations between the testis proteomes of young and old donors (Figure 19 A). Further statistical evaluation revealed 31 differentially abundant proteins. The large majority (29 proteins) was more abundant in the testes of old animals (Figure 19 B). Strikingly, most of these proteins belong to just a few enriched protein families and categories (Figure 21 B, Figure 22, Figure 23). The abundance of common Sertoli and Leydig cell markers (Mularoni et al., 2020), as well as of germ cell-specific proteins, was not altered in older animals. This result is in line with the observed ongoing spermatogenesis in both age-groups.

4.3.2. Levels of Anti-Proliferative Proteins are Increased in Testes from Older Individuals

Among proteins more abundant in old testes are various proteins known to inhibit cell proliferation. The most prominent one is CDKN2A (log_2 fold change: 1.92; p-value: 0.0029), also called $p16^{INK4a}$, which is a strong interactor of cyclin dependent kinase 4 and 6 (Rayess et al., 2012). This interaction directly regulates the transition of a cell from G1 phase into S1 phase (Rayess et al., 2012). Therefore, an increase of this protein is typically associated with a growth cycle arrest, a characteristic attribute of cellular senescence (Hall et al., 2016b, Ohtani et al., 2004). Additionally, in skin, CDKN2A has been described as an *in vivo* biomarker for cellular senescence since its expression in dermis and epidermis cells positively correlates with chronological aging (Ressler et al., 2006). We attempted to localize this protein in sections of testes by immunohistochemistry, yet the findings did not yield specific results. Hence the nature of cells, in which CDKN2A increases, remains to be defined.

Furthermore, three extracellular proteins increased in old testes, show anti-proliferative activity, namely, the two SLRPs PRELP and OGN as well as DPT. PRELP is known to be typically located near basement membranes and is supposed to act as an anchor to connective tissue (Bengtsson et al., 2002). The inhibitory effect of PRELP on proliferation was recently shown for hepatocellular carcinoma cells but otherwise its biological function is not well known (Hong et al., 2020). Another extracellular protein known to play a role in inhibition of proliferation is DPT, which is involved in the organization of collagen fibrils in the extracellular matrix (Okamoto and Fujiwara, 2006, Okamoto et al., 1999). Additionally, it was demonstrated that an increased abundance of DPT is associated with testicular dysfunction (Okamoto et al., 1999, Tzen and Huang, 2004, Cai et al., 2016). OGN was shown to inhibit proliferation in cardiac smooth muscle tissue and influences apoptosis and cell migration (Zhang et al., 2015, Zuo et al., 2018). A strong increase of OGN in old testes was also shown by immunostaining. OGN was predominantly found in the interstitial compartment, which contains extracellular matrix and fibroblasts, next to Leydig cells, macrophages, and blood vessels. Taken together, the alterations in proteins regulating cell proliferation indicate that mitotic events in old testes are slowed down or even arrested.

Associated with testicular dysfunction is the enzyme ASAH1, which was increased in old testes. ASAH1 is a regulator of steroidogenic capacity by controlling the turnover of ceramide and sphingosine. It may also influence steroidogenesis directly by binding to NR5A1 (Lucki et al., 2012a, Lucki et al., 2012b). Its substrate, ceramide, is a bioactive lipid which regulates apoptosis, differentiation but also proliferation (Li et al., 1999, Cirillo et al., 2021). In human ovarian granulosa cells, it induced cell death (Bagnjuk et al., 2019).

4.3.3. Testis Proteomes of Aged Individuals Show a Broad Increase of Actin-Binding Proteins

The proteomics analysis showed an increase of actin-binding proteins in the old testes, including all three calponin isoforms. One of them, calponin-1 (CNN1) is specific for smooth muscle cells, a fact reflected by the immunostaining of testicular peritubular cells and typical smooth muscle cells of blood vessels (Figure 24 A, a, B, b). Previously, a decline of peritubular cell CNN1 was shown in infertile patients, which went hand in hand with a partial loss of other contractility proteins of peritubular cells and indicated loss of the smooth muscle phenotype, in general (Welter et al., 2013). In the present study, stronger staining of CNN1 in peritubular cells of old testes was observed, whereas in young testes not all peritubular cells were positive for CNN1. This implies that CNN1 expression increases with advanced age. For ACTA2, another contractility protein (Schlatt et al., 1993, Welter et al., 2020), expression was reported upon onset of puberty in non-human primates, but other age-depending changes are not well known. By binding actins, CNN1 plays an important role in the cytoskeleton (North et al., 1994). Specifically, it has an inhibitory role in smooth muscle contraction and responsiveness regulation (Liu and Jin, 2016). An increase of CNN1 thus may suggest reduced contractile abilities. Calponin-2 (CNN2) also binds actin but has a different functional profile and is involved in cell proliferation, cell motility and immune modulation (reviewed in (Liu and Jin, 2016)). Calponin-3 (CNN3) is the least explored. It regulates the actin cytoskeleton and is involved in cell fusion and myogenesis (Liu and Jin, 2016). The functions of CNN2/3 in the testis are not known.

Another more abundant protein in aged testes and a member of the calponin repeat family is transgelin (TAGLN). TAGLN is an actin-binding cytoskeletal protein involved in differentiation, apoptosis, and proliferation (Mitarai et al., 2017, Elsafadi et al., 2016,

Dvorakova et al., 2014). The three isoforms of the actin-binding tropomyosin family, tropomyosin alpha-1 chain (TPM1), tropomyosin beta chain (TPM2) and tropomyosin alpha-4 chain (TPM4), were also more abundant in old testes. Tropomyosins are known to be involved in regulating cell migration and apoptosis (reviewed in (Lin et al., 2008, Gunning et al., 2015)). Together with the also increased CALD1, they regulate smooth muscle contraction and contribute to the stabilization of the cytoskeleton (Marston et al., 1998). By interacting with tropomyosins, CALD1 inhibits the contraction of smooth muscle cells, and an increase of CALD1 is associated with a higher inhibitory effect (Horiuchi et al., 1995, Marston and Redwood, 1992, Alahyan et al., 2006).

Several actin-binding cytoskeletal proteins, including CNN2, TAGLN, CALD1 and TPM1, which were more abundant in old testes, also have anti-proliferative functions. CNN2 and CALD1 are linked to inhibition of proliferation in smooth muscle cells (Yamashiro et al., 2001, Yokouchi et al., 2006, Hossain et al., 2003). For CNN2, this effect was also shown in fibroblasts and prostate cancer cells (Moazzem Hossain et al., 2014). Furthermore, the potential involvement of TPM1 in the inhibition of cancer and vascular smooth muscle cell proliferation has been demonstrated (Wang et al., 2019, Schevzov et al., 2015, Wang et al., 2011).

Taken together, the increase of several actin-binding proteins, specifically CNN1, CALD1, tropomyosins, which can inhibit smooth muscle cell proliferation and contraction, may indicate a reduced capacity of cells, presumably peritubular cells, and typical smooth muscle cells of blood vessels, to contract in aged testes.

4.3.4. Proteomic Alterations in old Testes Point to Specific Age-Related Changes of Peritubular Cells

TPCs are smooth muscle-like cells, which form a small compartment, the peritubular wall of the seminiferous tubules. They are able to contract and thereby crucial for sperm transport (Fleck et al., 2021). They also secrete extracellular matrix components and various signaling factors (Mayerhofer, 2013, Flenkenthaler et al., 2014). Importantly, they express several of the above discussed proteins, namely, CNN1, CNN2, TPM1, TAGLN and CALD1.

Replicative senescence of isolated MKTPCs and furthermore a comparison of TPCs isolated from old and young animals was discussed in the previous chapter (4.2). These results revealed alterations of proteins related to impairments of protein secretion and, of note, reduced levels of proteins related to contractility (Stöckl et al., 2020). The proteins identified include CNN1, MYH11, ACTA2 and DES. Hence, both studies, addressing either whole testes or isolated TPCs, evidence a reduction in contractility-associated proteins. This points to reduced contractile abilities of TPCs in old animals.

In this context, the slight but significantly increased diameter of the seminiferous tubules in old animals is of note (Figure 18). It may indicate a reduced contractile state or tone of peritubular cells but could be due to other reasons as well, including alterations in the composition of the tubular wall. The immunostaining showed an increase of COL1A1 in the peritubular wall in older testes. Increased abundance of collagen is associated with fibrosis, (Haider et al., 1999), which is typically observed in the testes of infertile men (de Kretser et al., 1975, Kisseleva and Brenner, 2008, Schell et al., 2010). Such changes could potentially impair the ability to contract in the old testes, as well. Fibrosis, including the interstitial areas, is indicated by higher levels of SLRPs, namely, decorin (DCN), biglycan (BGN), fibromodulin (FMOD) and lumican (LUM), which are involved in the maintenance of collagen I fibrils (Svensson et al., 2000, Chakravarti, 2002, Chen and Birk, 2013, Robinson et al., 2017) and might play a role in the observed alterations of the peritubular wall. The function of FMOD and LUM in the testis is unknown, but DCN and BGN are known products of TPCs (Adam et al., 2012, Mayer et al., 2016). They serve structural roles but can also interfere with signaling factors and receptors, as shown in HTPCs (Adam et al., 2011). Increased amounts thus imply that the local signaling in the testis and functions of TPCs, in particular, may be impaired.

Whether and to what degree smooth muscle cells of blood vessels, present in whole testes, may contribute to the proteomic changes remains to be studied. This warrants additional studies to address the question, whether aging of the testes may include alterations of blood vessels and hence blood flow.

4.3.5. Concluding Remarks

To investigate the mechanisms which underly healthy testicular aging in a translational non-human primate model, we performed a proteome analysis complemented by immunohistochemistry. Our data demonstrates that testicular aging is associated with proteome alterations, including increased levels of a variety of anti-proliferative proteins. Furthermore, several proteins which can impair smooth muscle cell contraction, and extracellular matrix proteins were more abundant in old testes. They point to age-associated changes specifically in smooth muscle cells and smooth-muscle-like cells of the peritubular wall. While proteomics is a powerful tool to gain new insights into complex biochemical networks, additional studies are now necessary to obtain mechanistic insights.

5. Summary

Age-related changes in the human testis include altered steroidogenesis, and impaired spermatogenesis. Furthermore, fibrosis and enlargement of the tubular wall are commonly observed in aging men. The major aim of this thesis was to comprehensively characterize proteomic alterations of the aging testis as a means to get new biochemical insights associated with the observed age effects. Since samples from young healthy human donors are not accessible, a translational, non-human primate *Callithrix jacchus* model was used. The *Callithrix jacchus* model has three key advantages: (i) reduced impact of confounding factors on the aging process, since the animals grow up and age in a controlled environment; (ii) possibility of a direct comparison between young and old animals; and (iii) it better reflects human testicular biology than rodent models. In a first step, we focused on testicular peritubular cells (TPCs), which are smooth muscle like cells fulfilling essential testicular functions, including sperm transport, contributions to the spermatogonial stem cell niche, and paracrine interactions within the testis. Another feature of TPCs is that, in contrast to other testicular cell types, they can be isolated and cultivated *in vitro*.

To confirm the suitability of monkey testicular peritubular cells (MKTPCs) as a model for the human system, a comprehensive proteome analysis was performed. The proteome of MKTPCs from six individual donors was characterized with high reproducibility and low inter-individual variability. Human testicular peritubular cells (HTPCs) from 7 donors were analyzed in the same manner and the results were compared to the MKTPC data. Correlation analysis showed homogeneity and reproducibility across species and a clear conformity in protein expression patterns. Further bioinformatic analysis demonstrated a high similarity on a functional level between HTPCs and MKTPCs. In summary, the data indicates that MKTPCs are a suitable model for HTPCs.

To investigate possible age-related proteome alterations in MKTPCs, an *in vitro* model, as well samples collected from young and aged monkeys were investigated. For the *in vitro* model, cells were aged by repeatedly passaging, which represents a common approach to trigger senescence in various cell types. Comprehensive proteome and secretome analysis revealed extensive alterations between MKTPCs of high and low

passage numbers. More specifically, high passage MKTPCs showed an impaired secretion, and the proteomic data pointed to a reduced contractility, and lower capacity of high passage cells to handle reactive oxygen species. Additionally, evidence for alterations in alternative splicing, RNA processing, NF-κB-modulated signaling and extracellular matrix modulation was found. Since this *in vitro* approach might not completely reflect the *in vivo* situation, MKTPC proteomes isolated from both young and old animals were also analyzed and compared. This approach revealed less strong alterations in the proteome and secretome, but similarly indicated impaired secretion, altered alternative splicing, and reduced contractility of cells from aged donors. In summary, this study provided evidence for specific age-related changes in TPCs.

However, testicular aging may not only be reflected in TPCs, but also in further testicular cell types. To assess this, testicular tissue from six young and four old *Callithrix jacchus* animals was analyzed and compared using proteomics, leading to the detection of a variety of proteins differentially abundant in older testes. Most of these proteins were more abundant and could be assigned to the following groups: extracellular proteins, small leucine rich proteoglycans (SLRPs) and actin-binding proteins. Functional annotation further revealed that several of the increased proteins are known to inhibit proliferation, indicating slowed or halted proliferation in the aging testis. The most important protein of this group is CDKN2A, a common marker for cellular senescence, which was increased nearly two-fold in the older testes. Additionally, the increase in SLRPs and other extracellular proteins points towards fibrotic events and impaired cell migration. These findings were confirmed by immunohistochemistry. Furthermore, proteins with inhibitory roles in smooth muscle cells contraction were increased in older testes indicating a reduced contractility of testicular peritubular cells.

In summary, the comprehensive analysis of MKTPC and whole testis proteomes performed in this thesis, provides a whole series of novel insights into testicular aging and underlying molecular mechanisms.

6. References

ABBOTT, D. H., BARNETT, D. K., COLMAN, R. J., YAMAMOTO, M. E. & SCHULTZ-DARKEN, N. J. 2003. Aspects of common marmoset basic biology and life history important for biomedical research. *Comp Med,* 53**,** 339-50.

ACOSTA, J. C., BANITO, A., WUESTEFELD, T., GEORGILIS, A., JANICH, P., MORTON, J. P., ATHINEOS, D., KANG, T.-W., LASITSCHKA, F., ANDRULIS, M., PASCUAL, G., MORRIS, K. J., KHAN, S., JIN, H., DHARMALINGAM, G., SNIJDERS, A. P., CARROLL, T., CAPPER, D., PRITCHARD, C., INMAN, G. J., LONGERICH, T., SANSOM, O. J., BENITAH, S. A., ZENDER, L. & GIL, J. 2013. A complex secretory program orchestrated by the inflammasome controls paracrine senescence. *Nature Cell Biology,* 15**,** 978-990.

ACOSTA, J. C., O'LOGHLEN, A., BANITO, A., GUIJARRO, M. V., AUGERT, A., RAGUZ, S., FUMAGALLI, M., DA COSTA, M., BROWN, C., POPOV, N., TAKATSU, Y., MELAMED, J., D'ADDA DI FAGAGNA, F., BERNARD, D., HERNANDO, E. & GIL, J. 2008. Chemokine signaling via the CXCR2 receptor reinforces senescence. *Cell,* 133**,** 1006-18.

ADAM, M., SCHWARZER, J. U., KÖHN, F. M., STRAUSS, L., POUTANEN, M. & MAYERHOFER, A. 2011. Mast cell tryptase stimulates production of decorin by human testicular peritubular cells: possible role of decorin in male infertility by interfering with growth factor signaling. *Hum Reprod,* 26**,** 2613-25.

ADAM, M., URBANSKI, H. F., GARYFALLOU, V. T., WELSCH, U., KÖHN, F. M., ULLRICH SCHWARZER, J., STRAUSS, L., POUTANEN, M. & MAYERHOFER, A. 2012. High levels of the extracellular matrix proteoglycan decorin are associated with inhibition of testicular function. *Int J Androl,* 35**,** 550-61.

ADAMS, P. D. 2009. Healing and Hurting: Molecular Mechanisms, Functions, and Pathologies of Cellular Senescence. *Molecular Cell,* 36**,** 2-14.

AEBERSOLD, R. & MANN, M. 2016. Mass-spectrometric exploration of proteome structure and function. *Nature,* 537**,** 347-55.

ALAHYAN, M., WEBB, M. R., MARSTON, S. B. & EL-MEZGUELDI, M. 2006. The mechanism of smooth muscle caldesmon-tropomyosin inhibition of the elementary steps of the actomyosin ATPase. *J Biol Chem,* 281**,** 19433-48.

ALBRECHT, M., RAMSCH, R., KOHN, F. M., SCHWARZER, J. U. & MAYERHOFER, A. 2006. Isolation and cultivation of human testicular peritubular cells: a new model for the investigation of fibrotic processes in the human testis and male infertility. *J Clin Endocrinol Metab,* 91**,** 1956-60.

ARAUJO, A. B. & WITTERT, G. A. 2011. Endocrinology of the aging male. *Best Pract Res Clin Endocrinol Metab,* 25**,** 303-19.

ARENAS, M. I., BETHENCOURT, F. R., DE MIGUEL, M. P., FRAILE, B., ROMO, E. & PANIAGUA, R. 1997. Immunocytochemical and quantitative study of actin, desmin and vimentin in the peritubular cells of the testes from elderly men. *Reproduction,* 110**,** 183-193.

AZENABOR, A., EKUN, A. O. & AKINLOYE, O. 2015. Impact of Inflammation on Male Reproductive Tract. *J Reprod Infertil,* 16**,** 123-9.

BAE, J. W., KIM, S. H., KIM, D. H., HA, J. J., YI, J. K., HWANG, S., RYU, B. Y., PANG, M. G. & KWON, W. S. 2019. Ras-related proteins (Rab) are key proteins related to male fertility following a unique activation mechanism. *Reprod Biol,* 19**,** 356-362.

BAGNJUK, K., STÖCKL, J. B., FRÖHLICH, T., ARNOLD, G. J., BEHR, R., BERG, U., BERG, D., KUNZ, L., BISHOP, C., XU, J. & MAYERHOFER, A. 2019. Necroptosis in primate luteolysis: a role for ceramide. *Cell Death Discov,* 5**,** 67.

BAKER, D. J., CHILDS, B. G., DURIK, M., WIJERS, M. E., SIEBEN, C. J., ZHONG, J., SALTNESS, R. A., JEGANATHAN, K. B., VERZOSA, G. C., PEZESHKI, A., KHAZAIE, K., MILLER, J. D. & VAN DEURSEN, J. M. 2016. Naturally occurring p16(Ink4a)-positive cells shorten healthy lifespan. *Nature,* 530**,** 184-9.

BAKER, D. J., WIJSHAKE, T., TCHKONIA, T., LEBRASSEUR, N. K., CHILDS, B. G., VAN DE SLUIS, B., KIRKLAND, J. L. & VAN DEURSEN, J. M. 2011. Clearance of p16Ink4a-positive senescent cells delays ageing-associated disorders. *Nature,* 479**,** 232-236.

BEAUSÉJOUR, C. M., KRTOLICA, A., GALIMI, F., NARITA, M., LOWE, S. W., YASWEN, P. & CAMPISI, J. 2003. Reversal of human cellular senescence: roles of the p53 and p16 pathways. *The EMBO Journal,* 22**,** 4212-4222.

BENGTSSON, E., MÖRGELIN, M., SASAKI, T., TIMPL, R., HEINEGÅRD, D. & ASPBERG, A. 2002. The leucine-rich repeat protein PRELP binds perlecan and collagens and may function as a basement membrane anchor. *J Biol Chem,* 277**,** 15061-8.

BERNAL, G. M., WAHLSTROM, J. S., CRAWLEY, C. D., CAHILL, K. E., PYTEL, P., LIANG, H., KANG, S., WEICHSELBAUM, R. R. & YAMINI, B. 2014. Loss of Nfkb1 leads to early onset aging. *Aging (Albany NY),* 6**,** 931-43.

BHADRA, M., HOWELL, P., DUTTA, S., HEINTZ, C. & MAIR, W. B. 2020. Alternative splicing in aging and longevity. *Hum Genet,* 139**,** 357-369.

BIRAN, A., ZADA, L., ABOU KARAM, P., VADAI, E., ROITMAN, L., OVADYA, Y., PORAT, Z. & KRIZHANOVSKY, V. 2017. Quantitative identification of senescent cells in aging and disease. *Aging Cell,* 16**,** 661-671.

BLACKBURN, E. H., GREIDER, C. W. & SZOSTAK, J. W. 2006. Telomeres and telomerase: the path from maize, Tetrahymena and yeast to human cancer and aging. *Nat Med,* 12**,** 1133-8.

BLANDER, G., DE OLIVEIRA, R. M., CONBOY, C. M., HAIGIS, M. & GUARENTE, L. 2003. Superoxide dismutase 1 knock-down induces senescence in human fibroblasts. *J Biol Chem,* 278**,** 38966-9.

BRUNET, A. & BERGER, S. L. 2014. Epigenetics of Aging and Aging-related Disease. *The Journals of Gerontology: Series A,* 69**,** S17-S20.

BUCCITELLI, C. & SELBACH, M. 2020. mRNAs, proteins and the emerging principles of gene expression control. *Nature Reviews Genetics,* 21**,** 630-644.

BURD, C. E., SORRENTINO, J. A., CLARK, K. S., DARR, D. B., KRISHNAMURTHY, J., DEAL, A. M., BARDEESY, N., CASTRILLON, D. H., BEACH, D. H. & SHARPLESS, N. E. 2013. Monitoring tumorigenesis and senescence in vivo with a p16(INK4a)-luciferase model. *Cell,* 152**,** 340-51.

BURTNER, C. R. & KENNEDY, B. K. 2010. Progeria syndromes and ageing: what is the connection? *Nat Rev Mol Cell Biol,* 11**,** 567-78.

CAI, J., LIU, W., HAO, J., CHEN, M. & LI, G. 2016. Increased expression of dermatopontin and its implications for testicular dysfunction in mice. *Mol Med Rep,* 13**,** 2431-8.

CALDEIRA-BRANT, A. L., MARTINELLI, L. M., MARQUES, M. M., REIS, A. B., MARTELLO, R., ALMEIDA, F. & CHIARINI-GARCIA, H. 2020. A subpopulation of human Adark spermatogonia behaves as the reserve stem cell. *Reproduction,* 159**,** 437-451.

CAMPISI, J. 2001. Cellular senescence as a tumor-suppressor mechanism. *Trends Cell Biol,* 11**,** S27-31.
CAO, L., LEERS-SUCHETA, S. & AZHAR, S. 2004. Aging alters the functional expression of enzymatic and non-enzymatic anti-oxidant defense systems in testicular rat Leydig cells. *J Steroid Biochem Mol Biol,* 88**,** 61-7.
CEDARS, M. I. 2015. Introduction: Childhood implications of parental aging. *Fertility and Sterility,* 103**,** 1379-1380.
CHAKRAVARTI, S. 2002. Functions of lumican and fibromodulin: lessons from knockout mice. *Glycoconj J,* 19**,** 287-93.
CHAPMAN, J., FIELDER, E. & PASSOS, J. F. 2019. Mitochondrial dysfunction and cell senescence: deciphering a complex relationship. *FEBS Letters,* 593**,** 1566-1579.
CHEN, H., LI, Y. & TOLLEFSBOL, T. O. 2013. Cell senescence culturing methods. *Methods Mol Biol,* 1048**,** 1-10.
CHEN, J., CRUTCHLEY, J., ZHANG, D., OWZAR, K. & KASTAN, M. B. 2017. Identification of a DNA Damage-Induced Alternative Splicing Pathway That Regulates p53 and Cellular Senescence Markers. *Cancer Discov,* 7**,** 766-781.
CHEN, L.-Y., BROWN, P. R., WILLIS, W. B. & EDDY, E. M. 2014. Peritubular Myoid Cells Participate in Male Mouse Spermatogonial Stem Cell Maintenance. *Endocrinology,* 155**,** 4964-4974.
CHEN, L.-Y., WILLIS, W. D. & EDDY, E. M. 2016. Targeting the Gdnf Gene in peritubular myoid cells disrupts undifferentiated spermatogonial cell development. 113**,** 1829-1834.
CHEN, S. & BIRK, D. E. 2013. The regulatory roles of small leucine-rich proteoglycans in extracellular matrix assembly. *Febs j,* 280**,** 2120-37.
CHEN, S. R. & LIU, Y. X. 2015. Regulation of spermatogonial stem cell self-renewal and spermatocyte meiosis by Sertoli cell signaling. *Reproduction,* 149**,** R159-67.
CHEN, Y., GENG, A., ZHANG, W., QIAN, Z., WAN, X., JIANG, Y. & MAO, Z. 2020. Fight to the bitter end: DNA repair and aging. *Ageing Research Reviews,* 64**,** 101154.
CHO, S. & HWANG, E. S. 2012. Status of mTOR activity may phenotypically differentiate senescence and quiescence. *Molecules and Cells,* 33**,** 597-604.
CIRILLO, F., PICCOLI, M., GHIROLDI, A., MONASKY, M. M., ROTA, P., LA ROCCA, P., TARANTINO, A., D'IMPERIO, S., SIGNORELLI, P., PAPPONE, C. & ANASTASIA, L. 2021. The antithetic role of ceramide and sphingosine-1-phosphate in cardiac dysfunction. *J Cell Physiol*.
COPPÉ, J.-P., DESPREZ, P.-Y., KRTOLICA, A. & CAMPISI, J. 2010. The Senescence-Associated Secretory Phenotype: The Dark Side of Tumor Suppression. *Annual Review of Pathology: Mechanisms of Disease,* 5**,** 99-118.
COPPÉ, J.-P., PATIL, C. K., RODIER, F., SUN, Y., MUÑOZ, D. P., GOLDSTEIN, J., NELSON, P. S., DESPREZ, P.-Y. & CAMPISI, J. 2008. Senescence-Associated Secretory Phenotypes Reveal Cell-Nonautonomous Functions of Oncogenic RAS and the p53 Tumor Suppressor. *PLoS Biology,* 6**,** e301.
COUNTOURIS, N. & HOLSTEIN, A. F. 1985. Wieviel Lobuli testis enthält ein menschlicher Hoden? Nachuntersuchung eines alten Problems. *Andrologia,* 17**,** 525-531.
COX, J., HEIN, M. Y., LUBER, C. A., PARON, I., NAGARAJ, N. & MANN, M. 2014. Accurate proteome-wide label-free quantification by delayed normalization and

maximal peptide ratio extraction, termed MaxLFQ. *Mol Cell Proteomics,* 13**,** 2513-26.
D'ADDA DI FAGAGNA, F. 2008. Living on a break: cellular senescence as a DNA-damage response. *Nature Reviews Cancer,* 8**,** 512-522.
DA COSTA, J. P., VITORINO, R., SILVA, G. M., VOGEL, C., DUARTE, A. C. & ROCHA-SANTOS, T. 2016. A synopsis on aging-Theories, mechanisms and future prospects. *Ageing Res Rev,* 29**,** 90-112.
DAKOUANE, M., BICCHIERAY, L., BERGERE, M., ALBERT, M., VIALARD, F. & SELVA, J. 2005. A histomorphometric and cytogenetic study of testis from men 29-102 years old. *Fertil Steril,* 83**,** 923-8.
DAVALLI, P., MITIC, T., CAPORALI, A., LAURIOLA, A. & D'ARCA, D. 2016a. ROS, Cell Senescence, and Novel Molecular Mechanisms in Aging and Age-Related Diseases. *Oxid Med Cell Longev,* 2016**,** 3565127.
DAVALLI, P., MITIC, T., CAPORALI, A., LAURIOLA, A. & D'ARCA, D. 2016b. ROS, Cell Senescence, and Novel Molecular Mechanisms in Aging and Age-Related Diseases. *Oxidative Medicine and Cellular Longevity,* 2016**,** 3565127.
DAVIDOFF, M. S., BREUCKER, H., HOLSTEIN, A. F. & SEIDL, K. 1990. Cellular architecture of the lamina propria of human seminiferous tubules. *Cell and Tissue Research,* 262**,** 253-261.
DAVIDOFF, M. S., MIDDENDORFF, R., ENIKOLOPOV, G., RIETHMACHER, D., HOLSTEIN, A. F. & MÜLLER, D. 2004. Progenitor cells of the testosterone-producing Leydig cells revealed. *J Cell Biol,* 167**,** 935-44.
DAWSON, D. W., VOLPERT, O. V., GILLIS, P., CRAWFORD, S. E., XU, H., BENEDICT, W. & BOUCK, N. P. 1999. Pigment epithelium-derived factor: a potent inhibitor of angiogenesis. *Science,* 285**,** 245-8.
DE HAAN, G. & LAZARE, S. S. 2018. Aging of hematopoietic stem cells. *Blood,* 131**,** 479-487.
DE KRETSER, D. M., KERR, J. B. & PAULSEN, C. A. 1975. The Peritubular Tissue in the Normal and Pathological Human Testis. An Ultrastructural Study. *Biology of Reproduction,* 12**,** 317-324.
DE MAGALHAES, J. P. & PASSOS, J. F. 2018. Stress, cell senescence and organismal ageing. *Mech Ageing Dev,* 170**,** 2-9.
DEMARIA, M., OHTANI, N., YOUSSEF, SAMEH A., RODIER, F., TOUSSAINT, W., MITCHELL, JAMES R., LABERGE, R.-M., VIJG, J., VAN STEEG, H., DOLLÉ, MARTIJN E. T., HOEIJMAKERS, JAN H. J., DE BRUIN, A., HARA, E. & CAMPISI, J. 2014. An Essential Role for Senescent Cells in Optimal Wound Healing through Secretion of PDGF-AA. *Developmental Cell,* 31**,** 722-733.
DI MICCO, R., KRIZHANOVSKY, V., BAKER, D. & D'ADDA DI FAGAGNA, F. 2021. Cellular senescence in ageing: from mechanisms to therapeutic opportunities. *Nature Reviews Molecular Cell Biology,* 22**,** 75-95.
DIMRI, G. P., LEE, X., BASILE, G., ACOSTA, M., SCOTT, G., ROSKELLEY, C., MEDRANO, E. E., LINSKENS, M., RUBELJ, I., PEREIRA-SMITH, O. & ET AL. 1995. A biomarker that identifies senescent human cells in culture and in aging skin in vivo. *Proc Natl Acad Sci U S A,* 92**,** 9363-7.
DONG, N., ZHU, Y., LU, Q., HU, L., ZHENG, Y. & SHAO, F. 2012. Structurally distinct bacterial TBC-like GAPs link Arf GTPase to Rab1 inactivation to counteract host defenses. *Cell,* 150**,** 1029-41.
DRUELLE, C., DRULLION, C., DESLÉ, J., MARTIN, N., SAAS, L., CORMENIER, J., MALAQUIN, N., HUOT, L., SLOMIANNY, C., BOUALI, F., VERCAMER, C., HOT, D., POURTIER, A., CHEVET, E., ABBADIE, C. & PLUQUET, O. 2016.

ATF6α regulates morphological changes associated with senescence in human fibroblasts. *Oncotarget,* 7.
DVORAKOVA, M., NENUTIL, R. & BOUCHAL, P. 2014. Transgelins, cytoskeletal proteins implicated in different aspects of cancer development. *Expert Rev Proteomics,* 11**,** 149-65.
DYM, M. 1974. The fine structure of monkey sertoli cells in the transitional zone at the junction of the seminiferous tubules with the tubuli recti. *American Journal of Anatomy,* 140**,** 1-25.
EFEYAN, A., COMB, W. C. & SABATINI, D. M. 2015. Nutrient-sensing mechanisms and pathways. *Nature,* 517**,** 302-10.
EILDERMANN, K., GROMOLL, J. & BEHR, R. 2012. Misleading and reliable markers to differentiate between primate testis-derived multipotent stromal cells and spermatogonia in culture. *Human Reproduction,* 27**,** 1754-1767.
ELSAFADI, M., MANIKANDAN, M., DAWUD, R. A., ALAJEZ, N. M., HAMAM, R., ALFAYEZ, M., KASSEM, M., ALDAHMASH, A. & MAHMOOD, A. 2016. Transgelin is a TGFβ-inducible gene that regulates osteoblastic and adipogenic differentiation of human skeletal stem cells through actin cytoskeleston organization. *Cell Death Dis,* 7**,** e2321.
EVENSON, D. P., DJIRA, G., KASPERSON, K. & CHRISTIANSON, J. 2020. Relationships between the age of 25,445 men attending infertility clinics and sperm chromatin structure assay (SCSA®) defined sperm DNA and chromatin integrity. *Fertil Steril,* 114**,** 311-320.
FAFIÁN-LABORA, J. A. & O'LOGHLEN, A. 2020. Classical and Nonclassical Intercellular Communication in Senescence and Ageing. *Trends Cell Biol,* 30**,** 628-639.
FAGAGNA, F. D. A. D., REAPER, P. M., CLAY-FARRACE, L., FIEGLER, H., CARR, P., VON ZGLINICKI, T., SARETZKI, G., CARTER, N. P. & JACKSON, S. P. 2003. A DNA damage checkpoint response in telomere-initiated senescence. *Nature,* 426**,** 194-198.
FAYOMI, A. P. & ORWIG, K. E. 2018. Spermatogonial stem cells and spermatogenesis in mice, monkeys and men. *Stem Cell Research,* 29**,** 207-214.
FERNANDEZ-GARCIA, N. I., VOLPERT, O. V. & JIMENEZ, B. 2007. Pigment epithelium-derived factor as a multifunctional antitumor factor. *J Mol Med (Berl),* 85**,** 15-22.
FERRUCCI, L., GONZALEZ-FREIRE, M., FABBRI, E., SIMONSICK, E., TANAKA, T., MOORE, Z., SALIMI, S., SIERRA, F. & DE CABO, R. 2020. Measuring biological aging in humans: A quest. *Aging Cell,* 19**,** e13080.
FLECK, D., KENZLER, L., MUNDT, N., STRAUCH, M., UESAKA, N., MOOSMANN, R., BRUENTGENS, F., MISSEL, A., MAYERHOFER, A., MERHOF, D., SPEHR, J. & SPEHR, M. 2021. ATP activation of peritubular cells drives testicular sperm transport. *Elife,* 10.
FLENKENTHALER, F., WINDSCHUTTL, S., FROHLICH, T., SCHWARZER, J. U., MAYERHOFER, A. & ARNOLD, G. J. 2014. Secretome analysis of testicular peritubular cells: a window into the human testicular microenvironment and the spermatogonial stem cell niche in man. *J Proteome Res,* 13**,** 1259-69.
FRANCESCHI, C., BONAFÈ, M., VALENSIN, S., OLIVIERI, F., DE LUCA, M., OTTAVIANI, E. & DE BENEDICTIS, G. 2000. Inflamm-aging. An evolutionary perspective on immunosenescence. *Ann N Y Acad Sci,* 908**,** 244-54.

FRUNGIERI, M. B., CALANDRA, R. S., BARTKE, A. & MATZKIN, M. E. 2018. Ageing and inflammation in the male reproductive tract. *Andrologia,* 50**,** e13034.

GIL, J. 2019. Cellular senescence causes ageing. *Nat Rev Mol Cell Biol,* 20**,** 388.

GOLDMANN, J. M., VELTMAN, J. A. & GILISSEN, C. 2019. De Novo Mutations Reflect Development and Aging of the Human Germline. *Trends Genet,* 35**,** 828-839.

GOODELL, M. A. & RANDO, T. A. 2015. Stem cells and healthy aging. *Science,* 350**,** 1199-204.

GOPAL KRISHNAN, P. D., GOLDEN, E., WOODWARD, E. A., PAVLOS, N. J. & BLANCAFORT, P. 2020. Rab GTPases: Emerging Oncogenes and Tumor Suppressive Regulators for the Editing of Survival Pathways in Cancer. *Cancers (Basel),* 12.

GORGOULIS, V., ADAMS, P. D., ALIMONTI, A., BENNETT, D. C., BISCHOF, O., BISHOP, C., CAMPISI, J., COLLADO, M., EVANGELOU, K., FERBEYRE, G., GIL, J., HARA, E., KRIZHANOVSKY, V., JURK, D., MAIER, A. B., NARITA, M., NIEDERNHOFER, L., PASSOS, J. F., ROBBINS, P. D., SCHMITT, C. A., SEDIVY, J., VOUGAS, K., VON ZGLINICKI, T., ZHOU, D., SERRANO, M. & DEMARIA, M. 2019. Cellular Senescence: Defining a Path Forward. *Cell,* 179**,** 813-827.

GRISWOLD, M. D. 2016. Spermatogenesis: The Commitment to Meiosis. *Physiol Rev,* 96**,** 1-17.

GUNES, S., HEKIM, G. N., ARSLAN, M. A. & ASCI, R. 2016. Effects of aging on the male reproductive system. *J Assist Reprod Genet,* 33**,** 441-54.

GUNNING, P. W., HARDEMAN, E. C., LAPPALAINEN, P. & MULVIHILL, D. P. 2015. Tropomyosin - master regulator of actin filament function in the cytoskeleton. *J Cell Sci,* 128**,** 2965-74.

HABERT, R., MUCZYNSKI, V., GRISIN, T., MOISON, D., MESSIAEN, S., FRYDMAN, R., BENACHI, A., DELBES, G., LAMBROT, R., LEHRAIKI, A., N'TUMBA-BYN, T., GUERQUIN, M. J., LEVACHER, C., ROUILLER-FABRE, V. & LIVERA, G. 2014. Concerns about the widespread use of rodent models for human risk assessments of endocrine disruptors. *Reproduction,* 147**,** R119-29.

HAIDER, S. G., TALATI, J. & SERVOS, G. 1999. Ultrastructure of peritubular tissue in association with tubular hyalinization in human testis. *Tissue Cell,* 31**,** 90-8.

HALL, B. M., BALAN, V., GLEIBERMAN, A. S., STROM, E., KRASNOV, P., VIRTUOSO, L. P., RYDKINA, E., VUJCIC, S., BALAN, K., GITLIN, I., LEONOVA, K., POLINSKY, A., CHERNOVA, O. B. & GUDKOV, A. V. 2016a. Aging of mice is associated with p16(Ink4a)- and beta-galactosidase-positive macrophage accumulation that can be induced in young mice by senescent cells. *Aging (Albany NY),* 8**,** 1294-315.

HALL, B. M., BALAN, V., GLEIBERMAN, A. S., STROM, E., KRASNOV, P., VIRTUOSO, L. P., RYDKINA, E., VUJCIC, S., BALAN, K., GITLIN, I., LEONOVA, K., POLINSKY, A., CHERNOVA, O. B. & GUDKOV, A. V. 2016b. Aging of mice is associated with p16(Ink4a)- and β-galactosidase-positive macrophage accumulation that can be induced in young mice by senescent cells. *Aging,* 8**,** 1294-1315.

HALVAEI, I., LITZKY, J. & ESFANDIARI, N. 2020. Advanced paternal age: effects on sperm parameters, assisted reproduction outcomes and offspring health. *Reprod Biol Endocrinol,* 18**,** 110.

HARLEY, C. B., FUTCHER, A. B. & GREIDER, C. W. 1990. Telomeres shorten during ageing of human fibroblasts. *Nature,* 345**,** 458-60.
HARRIES, L. W., HERNANDEZ, D., HENLEY, W., WOOD, A. R., HOLLY, A. C., BRADLEY-SMITH, R. M., YAGHOOTKAR, H., DUTTA, A., MURRAY, A., FRAYLING, T. M., GURALNIK, J. M., BANDINELLI, S., SINGLETON, A., FERRUCCI, L. & MELZER, D. 2011. Human aging is characterized by focused changes in gene expression and deregulation of alternative splicing. *Aging Cell,* 10**,** 868-78.
HAYFLICK, L. & MOORHEAD, P. S. 1961. The serial cultivation of human diploid cell strains. *Exp Cell Res,* 25**,** 585-621.
HEKIMI, S., LAPOINTE, J. & WEN, Y. 2011. Taking a “good” look at free radicals in the aging process. *Trends in Cell Biology,* 21**,** 569-576.
HERBIG, U., JOBLING, W. A., CHEN, B. P. C., CHEN, D. J. & SEDIVY, J. M. 2004. Telomere Shortening Triggers Senescence of Human Cells through a Pathway Involving ATM, p53, and p21CIP1, but Not p16INK4a. *Molecular Cell,* 14**,** 501-513.
HERNANDEZ-SEGURA, A., DE JONG, T. V., MELOV, S., GURYEV, V., CAMPISI, J. & DEMARIA, M. 2017. Unmasking Transcriptional Heterogeneity in Senescent Cells. *Curr Biol,* 27**,** 2652-2660.e4.
HERNANDEZ-SEGURA, A., NEHME, J. & DEMARIA, M. 2018. Hallmarks of Cellular Senescence. *Trends Cell Biol,* 28**,** 436-453.
HERRANZ, N. & GIL, J. 2018. Mechanisms and functions of cellular senescence. *J Clin Invest,* 128**,** 1238-1246.
HOARE, M., ITO, Y., KANG, T. W., WEEKES, M. P., MATHESON, N. J., PATTEN, D. A., SHETTY, S., PARRY, A. J., MENON, S., SALAMA, R., ANTROBUS, R., TOMIMATSU, K., HOWAT, W., LEHNER, P. J., ZENDER, L. & NARITA, M. 2016. NOTCH1 mediates a switch between two distinct secretomes during senescence. *Nat Cell Biol,* 18**,** 979-92.
HOARE, M. & NARITA, M. 2013. Transmitting senescence to the cell neighbourhood. *Nature Cell Biology,* 15**,** 887-889.
HOLLY, A. C., MELZER, D., PILLING, L. C., FELLOWS, A. C., TANAKA, T., FERRUCCI, L. & HARRIES, L. W. 2013. Changes in splicing factor expression are associated with advancing age in man. *Mech Ageing Dev,* 134**,** 356-66.
HOMMA, Y., HIRAGI, S. & FUKUDA, M. 2020. Rab family of small GTPases: an updated view on their regulation and functions. *Febs j*.
HONG, R., GU, J., NIU, G., HU, Z., ZHANG, X., SONG, T., HAN, S., HONG, L. & KE, C. 2020. PRELP has prognostic value and regulates cell proliferation and migration in hepatocellular carcinoma. *J Cancer,* 11**,** 6376-6389.
HORIUCHI, K. Y., WANG, Z. & CHACKO, S. 1995. Inhibition of smooth muscle actomyosin ATPase by caldesmon is associated with caldesmon-induced conformational changes in tropomyosin bound to actin. *Biochemistry,* 34**,** 16815-20.
HOSSAIN, M. M., HWANG, D. Y., HUANG, Q. Q., SASAKI, Y. & JIN, J. P. 2003. Developmentally regulated expression of calponin isoforms and the effect of h2-calponin on cell proliferation. *Am J Physiol Cell Physiol,* 284**,** C156-67.
HWANG, E. S., YOON, G. & KANG, H. T. 2009. A comparative analysis of the cell biology of senescence and aging. *Cellular and Molecular Life Sciences,* 66**,** 2503-2524.
IAKOVA, P., WANG, G. L., TIMCHENKO, L., MICHALAK, M., PEREIRA-SMITH, O. M., SMITH, J. R. & TIMCHENKO, N. A. 2004. Competition of CUGBP1 and

calreticulin for the regulation of p21 translation determines cell fate. *Embo j,* 23**,** 406-17.
IVELL, R., WADE, J. D. & ANAND-IVELL, R. 2013. INSL3 as a biomarker of Leydig cell functionality. *Biol Reprod,* 88**,** 147.
JARAK, I., ALMEIDA, S., CARVALHO, R. A., SOUSA, M., BARROS, A., ALVES, M. G. & OLIVEIRA, P. F. 2018. Senescence and declining reproductive potential: Insight into molecular mechanisms through testicular metabolomics. *Biochimica et Biophysica Acta (BBA) - Molecular Basis of Disease,* 1864**,** 3388-3396.
JARVIS, S., GETHINGS, L. A., SAMANTA, L., PEDRONI, S. M. A., WITHERS, D. J., GRAY, N., PLUMB, R. S., WINSTON, R. M. L., WILLIAMSON, C. & BEVAN, C. L. 2020. High fat diet causes distinct aberrations in the testicular proteome. *Int J Obes (Lond),* 44**,** 1958-1969.
JIANG, H., ZHU, W. J., LI, J., CHEN, Q. J., LIANG, W. B. & GU, Y. Q. 2014. Quantitative histological analysis and ultrastructure of the aging human testis. *Int Urol Nephrol,* 46**,** 879-85.
JIN, K. 2010. Modern Biological Theories of Aging. *Aging Dis,* 1**,** 72-74.
JOHNSON, L., NGUYEN, H. B., PETTY, C. S. & NEAVES, W. B. 1987. Quantification of human spermatogenesis: germ cell degeneration during spermatocytogenesis and meiosis in testes from younger and older adult men. *Biol Reprod,* 37**,** 739-47.
JOHNSON, S. L., DUNLEAVY, J., GEMMELL, N. J. & NAKAGAWA, S. 2015. Consistent age-dependent declines in human semen quality: a systematic review and meta-analysis. *Ageing Res Rev,* 19**,** 22-33.
KAUFMAN, J.-M., LAPAUW, B., MAHMOUD, A., T'SJOEN, G. & HUHTANIEMI, I. T. 2019. Aging and the Male Reproductive System. *Endocrine Reviews,* 40**,** 906-972.
KAUPPILA, T. E. S., KAUPPILA, J. H. K. & LARSSON, N.-G. 2017. Mammalian Mitochondria and Aging: An Update. *Cell Metabolism,* 25**,** 57-71.
KAUR, G., THOMPSON, L. A. & DUFOUR, J. M. 2014. Sertoli cells--immunological sentinels of spermatogenesis. *Seminars in cell & developmental biology,* 30**,** 36-44.
KAUSHIK, S. & CUERVO, A. M. 2015. Proteostasis and aging. *Nature Medicine,* 21**,** 1406-1415.
KIM, N., PIATYSZEK, M., PROWSE, K., HARLEY, C., WEST, M., HO, P., COVIELLO, G., WRIGHT, W., WEINRICH, S. & SHAY, J. 1994. Specific association of human telomerase activity with immortal cells and cancer. *Science,* 266**,** 2011-2015.
KIRKWOOD, T. B. 2005. Understanding the odd science of aging. *Cell,* 120**,** 437-47.
KISSELEVA, T. & BRENNER, D. A. 2008. Mechanisms of fibrogenesis. *Exp Biol Med (Maywood),* 233**,** 109-22.
KLAIPS, C. L., JAYARAJ, G. G. & HARTL, F. U. 2017. Pathways of cellular proteostasis in aging and disease. *Journal of Cell Biology,* 217**,** 51-63.
KOROLCHUK, V. I., MIWA, S., CARROLL, B. & VON ZGLINICKI, T. 2017. Mitochondria in Cell Senescence: Is Mitophagy the Weakest Link? *EBioMedicine,* 21**,** 7-13.
KORTLEVER, R. M., HIGGINS, P. J. & BERNARDS, R. 2006. Plasminogen activator inhibitor-1 is a critical downstream target of p53 in the induction of replicative senescence. *Nature Cell Biology,* 8**,** 877-884.
KOSSACK, N., TERWORT, N., WISTUBA, J., EHMCKE, J., SCHLATT, S., SCHÖLER, H., KLIESCH, S. & GROMOLL, J. 2013. A combined approach

facilitates the reliable detection of human spermatogonia in vitro. *Hum Reprod,* 28**,** 3012-25.
KRISHNAMURTHY, J., TORRICE, C., RAMSEY, M. R., KOVALEV, G. I., AL-REGAIEY, K., SU, L. & SHARPLESS, N. E. 2004. Ink4a/Arf expression is a biomarker of aging. *The Journal of Clinical Investigation,* 114**,** 1299-1307.
KRISTENSEN, D. M., DESDOITS-LETHIMONIER, C., MACKEY, A. L., DALGAARD, M. D., DE MASI, F., MUNKBØL, C. H., STYRISHAVE, B., ANTIGNAC, J.-P., LE BIZEC, B., PLATEL, C., HAY-SCHMIDT, A., JENSEN, T. K., LESNÉ, L., MAZAUD-GUITTOT, S., KRISTIANSEN, K., BRUNAK, S., KJAER, M., JUUL, A. & JÉGOU, B. 2018. Ibuprofen alters human testicular physiology to produce a state of compensated hypogonadism. *Proceedings of the National Academy of Sciences,* 115**,** E715-E724.
KUBBEN, N. & MISTELI, T. 2017. Shared molecular and cellular mechanisms of premature ageing and ageing-associated diseases. *Nature Reviews Molecular Cell Biology,* 18**,** 595-609.
KUHNERT, B. & NIESCHLAG, E. 2004. Reproductive functions of the ageing male. *Hum Reprod Update,* 10**,** 327-39.
KURZ, D. J., DECARY, S., HONG, Y. & ERUSALIMSKY, J. D. 2000. Senescence-associated (beta)-galactosidase reflects an increase in lysosomal mass during replicative ageing of human endothelial cells. *J Cell Sci,* 113 (Pt 20)**,** 3613-22.
KUWAHARA, S., IKEI, A., TAGUCHI, Y., TABUCHI, Y., FUJIMOTO, N., OBINATA, M., UESUGI, S. & KURIHARA, Y. 2006. PSPC1, NONO, and SFPQ are expressed in mouse Sertoli cells and may function as coregulators of androgen receptor-mediated transcription. *Biol Reprod,* 75**,** 352-9.
LABBADIA, J. & MORIMOTO, R. I. 2015. The biology of proteostasis in aging and disease. *Annu Rev Biochem,* 84**,** 435-64.
LANGENSTROTH, D., KOSSACK, N., WESTERNSTRÖER, B., WISTUBA, J., BEHR, R., GROMOLL, J. & SCHLATT, S. 2014. Separation of somatic and germ cells is required to establish primate spermatogonial cultures. *Hum Reprod,* 29**,** 2018-31.
LATORRE, E., TORREGROSSA, R., WOOD, M. E., WHITEMAN, M. & HARRIES, L. W. 2018. Mitochondria-targeted hydrogen sulfide attenuates endothelial senescence by selective induction of splicing factors HNRNPD and SRSF2. *Aging (Albany NY),* 10**,** 1666-1681.
LAURENTINO, S., CREMERS, J. F., HORSTHEMKE, B., TÜTTELMANN, F., CZELOTH, K., ZITZMANN, M., POHL, E., RAHMANN, S., SCHRÖDER, C., BERRES, S., REDMANN, K., KRALLMANN, C., SCHLATT, S., KLIESCH, S. & GROMOLL, J. 2020. A germ cell-specific ageing pattern in otherwise healthy men. *Aging Cell,* 19**,** e13242.
LEE, B. Y., HAN, J. A., IM, J. S., MORRONE, A., JOHUNG, K., GOODWIN, E. C., KLEIJER, W. J., DIMAIO, D. & HWANG, E. S. 2006. Senescence-associated beta-galactosidase is lysosomal beta-galactosidase. *Aging Cell,* 5**,** 187-95.
LI, C. M., PARK, J. H., HE, X., LEVY, B., CHEN, F., ARAI, K., ADLER, D. A., DISTECHE, C. M., KOCH, J., SANDHOFF, K. & SCHUCHMAN, E. H. 1999. The human acid ceramidase gene (ASAH): structure, chromosomal location, mutation analysis, and expression. *Genomics,* 62**,** 223-31.
LI, Z., ZHANG, Z., REN, Y., WANG, Y., FANG, J., YUE, H., MA, S. & GUAN, F. 2021. Aging and age-related diseases: from mechanisms to therapeutic strategies. *Biogerontology*.

LIN, J. J., EPPINGA, R. D., WARREN, K. S. & MCCRAE, K. R. 2008. Human tropomyosin isoforms in the regulation of cytoskeleton functions. *Adv Exp Med Biol,* 644**,** 201-22.
LIU, R. & JIN, J. P. 2016. Calponin isoforms CNN1, CNN2 and CNN3: Regulators for actin cytoskeleton functions in smooth muscle and non-muscle cells. *Gene,* 585**,** 143-153.
LOPEZ-OTIN, C., BLASCO, M. A., PARTRIDGE, L., SERRANO, M. & KROEMER, G. 2013. The hallmarks of aging. *Cell,* 153**,** 1194-217.
LUCKI, N. C., BANDYOPADHYAY, S., WANG, E., MERRILL, A. H. & SEWER, M. B. 2012a. Acid ceramidase (ASAH1) is a global regulator of steroidogenic capacity and adrenocortical gene expression. *Mol Endocrinol,* 26**,** 228-43.
LUCKI, N. C., LI, D., BANDYOPADHYAY, S., WANG, E., MERRILL, A. H. & SEWER, M. B. 2012b. Acid ceramidase (ASAH1) represses steroidogenic factor 1-dependent gene transcription in H295R human adrenocortical cells by binding to the receptor. *Mol Cell Biol,* 32**,** 4419-31.
LUKÁŠOVÁ, E., KOVAŘÍK, A. & KOZUBEK, S. 2018. Consequences of Lamin B1 and Lamin B Receptor Downregulation in Senescence. *Cells,* 7.
MANN, M. 2016. Origins of mass spectrometry-based proteomics. *Nat Rev Mol Cell Biol,* 17**,** 678.
MANN, M. 2019. The ever expanding scope of electrospray mass spectrometry—a 30 year journey. *Nature Communications,* 10**,** 3744.
MARSTON, S., BURTON, D., COPELAND, O., FRASER, I., GAO, Y., HODGKINSON, J., HUBER, P., LEVINE, B., EL-MEZGUELDI, M. & NOTARIANNI, G. 1998. Structural interactions between actin, tropomyosin, caldesmon and calcium binding protein and the regulation of smooth muscle thin filaments. *Acta Physiol Scand,* 164**,** 401-14.
MARSTON, S. B. & REDWOOD, C. S. 1992. Inhibition of actin-tropomyosin activation of myosin MgATPase activity by the smooth muscle regulatory protein caldesmon. *J Biol Chem,* 267**,** 16796-800.
MATZKIN, M. E., MAYERHOFER, A., ROSSI, S. P., GONZALEZ, B., GONZALEZ, C. R., GONZALEZ-CALVAR, S. I., TERRADAS, C., PONZIO, R., PUIGDOMENECH, E., LEVALLE, O., CALANDRA, R. S. & FRUNGIERI, M. B. 2010. Cyclooxygenase-2 in testes of infertile men: evidence for the induction of prostaglandin synthesis by interleukin-1β. *Fertil Steril,* 94**,** 1933-6.
MAYER, C., ADAM, M., GLASHAUSER, L., DIETRICH, K., SCHWARZER, J. U., KOHN, F. M., STRAUSS, L., WELTER, H., POUTANEN, M. & MAYERHOFER, A. 2016. Sterile inflammation as a factor in human male infertility: Involvement of Toll like receptor 2, biglycan and peritubular cells. *Sci Rep,* 6**,** 37128.
MAYER, C., ADAM, M., WALENTA, L., SCHMID, N., HEIKELA, H., SCHUBERT, K., FLENKENTHALER, F., DIETRICH, K. G., GRUSCHKA, S., ARNOLD, G. J., FROHLICH, T., SCHWARZER, J. U., KOHN, F. M., STRAUSS, L., WELTER, H., POUTANEN, M. & MAYERHOFER, A. 2018. Insights into the role of androgen receptor in human testicular peritubular cells. *Andrology,* 6**,** 756-765.
MAYERHOFER, A. 2013. Human testicular peritubular cells: more than meets the eye. *Reproduction,* 145**,** R107-16.
MAYERHOFER, A. 2020. Peritubular cells of the human testis: prostaglandin E(2) and more. *Andrology,* 8**,** 898-902.
MAZAUD-GUITTOT, S., MEUGNIER, E., PESENTI, S., WU, X., VIDAL, H., GOW, A. & LE MAGUERESSE-BATTISTONI, B. 2010. Claudin 11 Deficiency in Mice

Results in Loss of the Sertoli Cell Epithelial Phenotype in the Testis1. *Biology of Reproduction,* 82**,** 202-213.
MEIER, F., GEYER, P. E., VIRREIRA WINTER, S., COX, J. & MANN, M. 2018. BoxCar acquisition method enables single-shot proteomics at a depth of 10,000 proteins in 100 minutes. *Nat Methods*.
MENSÀ, E., LATINI, S., RAMINI, D., STORCI, G., BONAFÈ, M. & OLIVIERI, F. 2019. The telomere world and aging: Analytical challenges and future perspectives. *Ageing Research Reviews,* 50**,** 27-42.
MIETSCH, M., PAQUÉ, K., DRUMMER, C., STAHL-HENNIG, C. & ROSHANI, B. 2020. The aging common marmoset's immune system: From junior to senior. *American Journal of Primatology,* 82**,** e23128.
MITARAI, H., WADA, N., HASEGAWA, D., YOSHIDA, S., SONODA, M., TOMOKIYO, A., HAMANO, S., SERITA, S., MIZUMACHI, H. & MAEDA, H. 2017. Transgelin mediates transforming growth factor-β1-induced proliferation of human periodontal ligament cells. *J Periodontal Res,* 52**,** 984-993.
MOAZZEM HOSSAIN, M., WANG, X., BERGAN, R. C. & JIN, J. P. 2014. Diminished expression of h2-calponin in prostate cancer cells promotes cell proliferation, migration and the dependence of cell adhesion on substrate stiffness. *FEBS Open Bio,* 4**,** 627-36.
MOORADIAN, A. D., MORLEY, J. E. & KORENMAN, S. G. 1987. Biological Actions of Androgens. *Endocrine Reviews,* 8**,** 1-28.
MORIN, G. B. 1989. The human telomere terminal transferase enzyme is a ribonucleoprotein that synthesizes TTAGGG repeats. *Cell,* 59**,** 521-529.
MOUSSAVI, A., MIETSCH, M., DRUMMER, C., BEHR, R., MYLIUS, J. & BORETIUS, S. 2020. Cardiac MRI in common marmosets revealing age-dependency of cardiac function. *Scientific Reports,* 10**,** 10221.
MULARONI, V., ESPOSITO, V., DI PERSIO, S., VICINI, E., SPADETTA, G., BERLOCO, P., FANELLI, F., MEZZULLO, M., PAGOTTO, U., PELUSI, C., NIELSEN, J. E., RAJPERT-DE MEYTS, E., JORGENSEN, N., JORGENSEN, A. & BOITANI, C. 2020. Age-related changes in human Leydig cell status. *Hum Reprod,* 35**,** 2663-2676.
MULLIGAN, T., IRANMANESH, A. & VELDHUIS, J. D. 2001. Pulsatile iv infusion of recombinant human LH in leuprolide-suppressed men unmasks impoverished Leydig-cell secretory responsiveness to midphysiological LH drive in the aging male. *J Clin Endocrinol Metab,* 86**,** 5547-53.
NARITA, M. & LOWE, S. W. 2005. Senescence comes of age. *Nat Med,* 11**,** 920-2.
NEAVES, W. B., JOHNSON, L. & PETTY, C. S. 1985. Age-related change in numbers of other interstitial cells in testes of adult men: evidence bearing on the fate of Leydig cells lost with increasing age. *Biol Reprod,* 33**,** 259-69.
NEAVES, W. B., JOHNSON, L., PORTER, J. C., PARKER, C. R., JR. & PETTY, C. S. 1984. Leydig cell numbers, daily sperm production, and serum gonadotropin levels in aging men. *J Clin Endocrinol Metab,* 59**,** 756-63.
NEUROHR, G. E., TERRY, R. L., LENGEFELD, J., BONNEY, M., BRITTINGHAM, G. P., MORETTO, F., MIETTINEN, T. P., VAITES, L. P., SOARES, L. M., PAULO, J. A., HARPER, J. W., BURATOWSKI, S., MANALIS, S., VAN WERVEN, F. J., HOLT, L. J. & AMON, A. 2019. Excessive Cell Growth Causes Cytoplasm Dilution And Contributes to Senescence. *Cell,* 176**,** 1083-1097.e18.
NGUYEN-POWANDA, P. & ROBAIRE, B. 2020. Oxidative Stress and Reproductive Function in the Aging Male. *Biology,* 9**,** 282.

NIESCHLAG, E., LAMMERS, U., FREISCHEM, C. W., LANGER, K. & WICKINGS, E. J. 1982. Reproductive functions in young fathers and grandfathers. *J Clin Endocrinol Metab,* 55**,** 676-81.
NISHIJIMA, K., SAITOH, R., TANAKA, S., OHSATO-SUZUKI, M., OHNO, T. & KITAJIMA, S. 2012. Life span of common marmoset (Callithrix jacchus) at CLEA Japan breeding colony. *Biogerontology,* 13**,** 439-43.
NIU, Z., GOODYEAR, S. M., AVARBOCK, M. R. & BRINSTER, R. L. 2016. Chemokine (C-X-C) Ligand 12 Facilitates Trafficking of Donor Spermatogonial Stem Cells. *Stem Cells Int,* 2016**,** 5796305.
NORTH, A. J., GIMONA, M., CROSS, R. A. & SMALL, J. V. 1994. Calponin is localised in both the contractile apparatus and the cytoskeleton of smooth muscle cells. *J Cell Sci,* 107 (Pt 3)**,** 437-44.
O'DONNELL, L., NICHOLLS, P. K., O'BRYAN, M. K., MCLACHLAN, R. I. & STANTON, P. G. 2011. Spermiation: The process of sperm release. *Spermatogenesis,* 1**,** 14-35.
OATLEY, J. M. & BRINSTER, R. L. 2012. The germline stem cell niche unit in mammalian testes. *Physiol Rev,* 92**,** 577-95.
OHANNA, M., GIULIANO, S., BONET, C., IMBERT, V., HOFMAN, V., ZANGARI, J., BILLE, K., ROBERT, C., BRESSAC-DE PAILLERETS, B., HOFMAN, P., ROCCHI, S., PEYRON, J.-F., LACOUR, J.-P., BALLOTTI, R. & BERTOLOTTO, C. 2011. Senescent cells develop a PARP-1 and nuclear factor-κB-associated secretome (PNAS). *Genes & Development,* 25**,** 1245-1261.
OHTANI, N., YAMAKOSHI, K., TAKAHASHI, A. & HARA, E. 2004. The p16INK4a-RB pathway: molecular link between cellular senescence and tumor suppression. *J Med Invest,* 51**,** 146-53.
OKAMOTO, O. & FUJIWARA, S. 2006. Dermatopontin, a novel player in the biology of the extracellular matrix. *Connect Tissue Res,* 47**,** 177-89.
OKAMOTO, O., FUJIWARA, S., ABE, M. & SATO, Y. 1999. Dermatopontin interacts with transforming growth factor beta and enhances its biological activity. *Biochem J,* 337 (Pt 3)**,** 537-41.
OLOVNIKOV, A. M. 1973. A theory of marginotomy: The incomplete copying of template margin in enzymic synthesis of polynucleotides and biological significance of the phenomenon. *Journal of Theoretical Biology,* 41**,** 181-190.
OU, H.-L. & SCHUMACHER, B. 2018. DNA damage responses and p53 in the aging process. *Blood,* 131**,** 488-495.
PANIAGUA, R., AMAT, P., NISTAL, M. & MARTIN, A. 1986. Ultrastructure of Leydig cells in human ageing testes. *J Anat,* 146**,** 173-83.
PANIAGUA, R., NISTAL, M., AMAT, P., RODRIGUEZ, M. C. & MARTIN, A. 1987. Seminiferous Tubule Involution in Elderly Men1. *Biology of Reproduction,* 36**,** 939-947.
PANIAGUA, R., NISTAL, M., SAEZ, F. J. & FRAILE, B. 1991. Ultrastructure of the aging human testis. *J Electron Microsc Tech,* 19**,** 241-60.
PAUL, C. & ROBAIRE, B. 2013. Ageing of the male germ line. *Nat Rev Urol,* 10**,** 227-34.
POHL, E., HÖFFKEN, V., SCHLATT, S., KLIESCH, S., GROMOLL, J. & WISTUBA, J. 2019. Ageing in men with normal spermatogenesis alters spermatogonial dynamics and nuclear morphology in Sertoli cells. *Andrology,* 7**,** 827-839.
RAO, S. G. & JACKSON, J. G. 2016. SASP: Tumor Suppressor or Promoter? Yes! *Trends in Cancer,* 2**,** 676-687.

RATO, L., ALVES, M. G., SOCORRO, S., DUARTE, A. I., CAVACO, J. E. & OLIVEIRA, P. F. 2012. Metabolic regulation is important for spermatogenesis. *Nature Reviews Urology,* 9**,** 330-338.

RAUNIYAR, N. & YATES, J. R. 2014. Isobaric Labeling-Based Relative Quantification in Shotgun Proteomics. *Journal of Proteome Research,* 13**,** 5293-5309.

RAYESS, H., WANG, M. B. & SRIVATSAN, E. S. 2012. Cellular senescence and tumor suppressor gene p16. *Int J Cancer,* 130**,** 1715-25.

REN, R., OCAMPO, A., LIU, G.-H. & IZPISUA BELMONTE, J. C. 2017. Regulation of Stem Cell Aging by Metabolism and Epigenetics. *Cell Metabolism,* 26**,** 460-474.

RESSLER, S., BARTKOVA, J., NIEDEREGGER, H., BARTEK, J., SCHARFFETTER-KOCHANEK, K., JANSEN-DÜRR, P. & WLASCHEK, M. 2006. p16INK4A is a robust in vivo biomarker of cellular aging in human skin. *Aging Cell,* 5**,** 379-89.

REY-ARES, V., ROSSI, S. P., DIETRICH, K. G., KÖHN, F. M., SCHWARZER, J. U., WELTER, H., FRUNGIERI, M. B. & MAYERHOFER, A. 2018. Prostaglandin E(2) (PGE(2)) is a testicular peritubular cell-derived factor involved in human testicular homeostasis. *Mol Cell Endocrinol,* 473**,** 217-224.

ROBINSON, K. A., SUN, M., BARNUM, C. E., WEISS, S. N., HUEGEL, J., SHETYE, S. S., LIN, L., SAEZ, D., ADAMS, S. M., IOZZO, R. V., SOSLOWSKY, L. J. & BIRK, D. E. 2017. Decorin and biglycan are necessary for maintaining collagen fibril structure, fiber realignment, and mechanical properties of mature tendons. *Matrix Biology,* 64**,** 81-93.

ROSS, C. N., DAVIS, K., DOBEK, G. & TARDIF, S. D. 2012. Aging Phenotypes of Common Marmosets (Callithrix jacchus). *Journal of Aging Research,* 2012**,** 567143.

SADAIE, M., SALAMA, R., CARROLL, T., TOMIMATSU, K., CHANDRA, T., YOUNG, A. R., NARITA, M., PÉREZ-MANCERA, P. A., BENNETT, D. C., CHONG, H., KIMURA, H. & NARITA, M. 2013. Redistribution of the Lamin B1 genomic binding profile affects rearrangement of heterochromatic domains and SAHF formation during senescence. *Genes Dev,* 27**,** 1800-8.

SADYGOV, R. G., COCIORVA, D. & YATES, J. R., 3RD 2004. Large-scale database searching using tandem mass spectra: looking up the answer in the back of the book. *Nat Methods,* 1**,** 195-202.

SALAMA, R., SADAIE, M., HOARE, M. & NARITA, M. 2014. Cellular senescence and its effector programs. *Genes Dev,* 28**,** 99-114.

SALMINEN, A. & KAARNIRANTA, K. 2011. Control of p53 and NF-kappaB signaling by WIP1 and MIF: role in cellular senescence and organismal aging. *Cell Signal,* 23**,** 747-52.

SANTIAGO, J., SILVA, J. V., ALVES, M. G., OLIVEIRA, P. F. & FARDILHA, M. 2019. Testicular Aging: An Overview of Ultrastructural, Cellular, and Molecular Alterations. *J Gerontol A Biol Sci Med Sci,* 74**,** 860-871.

SANTOS, J., LEITÃO-CORREIA, F., SOUSA, M. J. & LEÃO, C. 2016. Dietary Restriction and Nutrient Balance in Aging. *Oxidative Medicine and Cellular Longevity,* 2016**,** 4010357.

SCHELL, C., ALBRECHT, M., SPILLNER, S., MAYER, C., KUNZ, L., KOHN, F. M., SCHWARZER, U. & MAYERHOFER, A. 2010. 15-Deoxy-delta 12-14-prostaglandin-J2 induces hypertrophy and loss of contractility in human testicular peritubular cells: implications for human male fertility. *Endocrinology,* 151**,** 1257-68.

SCHEVZOV, G., KEE, A. J., WANG, B., SEQUEIRA, V. B., HOOK, J., COOMBES, J. D., LUCAS, C. A., STEHN, J. R., MUSGROVE, E. A., CRETU, A., ASSOIAN, R., FATH, T., HANOCH, T., SEGER, R., PLEINES, I., KILE, B. T., HARDEMAN, E. C. & GUNNING, P. W. 2015. Regulation of cell proliferation by ERK and signal-dependent nuclear translocation of ERK is dependent on Tm5NM1-containing actin filaments. *Molecular Biology of the Cell,* 26**,** 2475-2490.

SCHIEBER, M. & CHANDEL, NAVDEEP S. 2014. ROS Function in Redox Signaling and Oxidative Stress. *Current Biology,* 24**,** R453-R462.

SCHIEL, N. & SOUTO, A. 2017. The common marmoset: An overview of its natural history, ecology and behavior. *Dev Neurobiol,* 77**,** 244-262.

SCHLATT, S., WEINBAUER, G. F., ARSLAN, M. & NIESCHLAG, E. 1993. Appearance of alpha-smooth muscle actin in peritubular cells of monkey testes is induced by androgens, modulated by follicle-stimulating hormone, and maintained after hormonal withdrawal. *J Androl,* 14**,** 340-50.

SCHMID, N., FLENKENTHALER, F., STOCKL, J. B., DIETRICH, K. G., KOHN, F. M., SCHWARZER, J. U., KUNZ, L., LUCKNER, M., WANNER, G., ARNOLD, G. J., FROHLICH, T. & MAYERHOFER, A. 2019. Insights into replicative senescence of human testicular peritubular cells. *Sci Rep,* 9**,** 15052.

SCHMID, N., MISSEL, A., PETKOV, S., STOCKL, J. B., FLENKENTHALER, F., ARNOLD, G. J., FROHLICH, T., BEHR, R. & MAYERHOFER, A. 2020. A translational cellular model for the study of peritubular cells of the testis. *Reproduction,* 160**,** 259-268.

SCHMID, N., STOCKL, J. B., FLENKENTHALER, F., DIETRICH, K. G., SCHWARZER, J. U., KOHN, F. M., DRUMMER, C., FROHLICH, T., ARNOLD, G. J., BEHR, R. & MAYERHOFER, A. 2018. Characterization of a non-human primate model for the study of testicular peritubular cells-comparison with human testicular peritubular cells. *Mol Hum Reprod,* 24**,** 401-410.

SEN, P., SHAH, P. P., NATIVIO, R. & BERGER, S. L. 2016. Epigenetic Mechanisms of Longevity and Aging. *Cell,* 166**,** 822-839.

SHAH, P. P., DONAHUE, G., OTTE, G. L., CAPELL, B. C., NELSON, D. M., CAO, K., AGGARWALA, V., CRUICKSHANKS, H. A., RAI, T. S., MCBRYAN, T., GREGORY, B. D., ADAMS, P. D. & BERGER, S. L. 2013. Lamin B1 depletion in senescent cells triggers large-scale changes in gene expression and the chromatin landscape. *Genes Dev,* 27**,** 1787-99.

SHARMA, R., AGARWAL, A., ROHRA, V. K., ASSIDI, M., ABU-ELMAGD, M. & TURKI, R. F. 2015. Effects of increased paternal age on sperm quality, reproductive outcome and associated epigenetic risks to offspring. *Reprod Biol Endocrinol,* 13**,** 35.

SHARMA, S., WISTUBA, J., POCK, T., SCHLATT, S. & NEUHAUS, N. 2019. Spermatogonial stem cells: updates from specification to clinical relevance. *Human Reproduction Update,* 25**,** 275-297.

SHARPE, R., MCKINNELL, C., KIVLIN, C. & FISHER, J. 2003. Proliferation and functional maturation of Sertoli cells, and their relevance to disorders of testis function in adulthood. *Reproduction,* 125**,** 769-784.

SHARPLESS, N. E. & SHERR, C. J. 2015. Forging a signature of in vivo senescence. *Nature Reviews Cancer,* 15**,** 397-408.

SIERRA, F. 2016. The Emergence of Geroscience as an Interdisciplinary Approach to the Enhancement of Health Span and Life Span. *Cold Spring Harb Perspect Med,* 6**,** a025163.

SIES, H. & JONES, D. P. 2020. Reactive oxygen species (ROS) as pleiotropic physiological signalling agents. *Nature Reviews Molecular Cell Biology,* 21**,** 363-383.
SIMANSHU, D. K., NISSLEY, D. V. & MCCORMICK, F. 2017. RAS Proteins and Their Regulators in Human Disease. *Cell,* 170**,** 17-33.
SPINNLER, K., KOHN, F. M., SCHWARZER, U. & MAYERHOFER, A. 2010. Glial cell line-derived neurotrophic factor is constitutively produced by human testicular peritubular cells and may contribute to the spermatogonial stem cell niche in man. *Hum Reprod,* 25**,** 2181-7.
STEEN, H. & MANN, M. 2004. The ABC's (and XYZ's) of peptide sequencing. *Nat Rev Mol Cell Biol,* 5**,** 699-711.
STEFANATOS, R. & SANZ, A. 2018. The role of mitochondrial ROS in the aging brain. *FEBS Lett,* 592**,** 743-758.
STÖCKL, J. B., SCHMID, N., FLENKENTHALER, F., DRUMMER, C., BEHR, R., MAYERHOFER, A., ARNOLD, G. J. & FRÖHLICH, T. 2020. Proteomic Insights into Senescence of Testicular Peritubular Cells from a Nonhuman Primate Model. *Cells,* 9.
STÖCKL, J. B., SCHMID, N., FLENKENTHALER, F., DRUMMER, C., BEHR, R., MAYERHOFER, A., ARNOLD, G. J. & FRÖHLICH, T. 2021. Age-Related Alterations in the Testicular Proteome of a Non-Human Primate. *Cells,* 10**,** 1306.
STORER, M., MAS, A., ROBERT-MORENO, A., PECORARO, M., ORTELLS, M. C., DI GIACOMO, V., YOSEF, R., PILPEL, N., KRIZHANOVSKY, V., SHARPE, J. & KEYES, W. M. 2013. Senescence is a developmental mechanism that contributes to embryonic growth and patterning. *Cell,* 155**,** 1119-30.
SU, L., MRUK, D. D. & CHENG, C. Y. 2011. Drug transporters, the blood-testis barrier, and spermatogenesis. *J Endocrinol,* 208**,** 207-23.
SVENSSON, L., NÄRLID, I. & OLDBERG, A. 2000. Fibromodulin and lumican bind to the same region on collagen type I fibrils. *FEBS Lett,* 470**,** 178-82.
TAI, H., WANG, Z., GONG, H., HAN, X., ZHOU, J., WANG, X., WEI, X., DING, Y., HUANG, N., QIN, J., ZHANG, J., WANG, S., GAO, F., CHRZANOWSKA-LIGHTOWLERS, Z. M., XIANG, R. & XIAO, H. 2017. Autophagy impairment with lysosomal and mitochondrial dysfunction is an important characteristic of oxidative stress-induced senescence. *Autophagy,* 13**,** 99-113.
TAJAR, A., FORTI, G., O'NEILL, T. W., LEE, D. M., SILMAN, A. J., FINN, J. D., BARTFAI, G., BOONEN, S., CASANUEVA, F. F., GIWERCMAN, A., HAN, T. S., KULA, K., LABRIE, F., LEAN, M. E., PENDLETON, N., PUNAB, M., VANDERSCHUEREN, D., HUHTANIEMI, I. T. & WU, F. C. 2010. Characteristics of secondary, primary, and compensated hypogonadism in aging men: evidence from the European Male Ageing Study. *J Clin Endocrinol Metab,* 95**,** 1810-8.
TALENS, R. P., CHRISTENSEN, K., PUTTER, H., WILLEMSEN, G., CHRISTIANSEN, L., KREMER, D., SUCHIMAN, H. E. D., SLAGBOOM, P. E., BOOMSMA, D. I. & HEIJMANS, B. T. 2012. Epigenetic variation during the adult lifespan: cross-sectional and longitudinal data on monozygotic twin pairs. *Aging Cell,* 11**,** 694-703.
TAMURA, K., SHAN, W. S., HENDRICKSON, W. A., COLMAN, D. R. & SHAPIRO, L. 1998. Structure-function analysis of cell adhesion by neural (N-) cadherin. *Neuron,* 20**,** 1153-63.
TARDIF, S. D. 2019. Marmosets as a translational aging model—Introduction. *American Journal of Primatology,* 81**,** e22912.

TIWARI, V. & WILSON, D. M., III 2019. DNA Damage and Associated DNA Repair Defects in Disease and Premature Aging. *The American Journal of Human Genetics,* 105**,** 237-257.

TZEN, C. Y. & HUANG, Y. W. 2004. Cloning of murine early quiescence-1 gene: the murine counterpart of dermatopontin gene can induce and be induced by cell quiescence. *Exp Cell Res,* 294**,** 30-8.

UHLÉN, M., KARLSSON, M. J., HOBER, A., SVENSSON, A.-S., SCHEFFEL, J., KOTOL, D., ZHONG, W., TEBANI, A., STRANDBERG, L., EDFORS, F., SJÖSTEDT, E., MULDER, J., MARDINOGLU, A., BERLING, A., EKBLAD, S., DANNEMEYER, M., KANJE, S., ROCKBERG, J., LUNDQVIST, M., MALM, M., VOLK, A.-L., NILSSON, P., MÅNBERG, A., DODIG-CRNKOVIC, T., PIN, E., ZWAHLEN, M., OKSVOLD, P., VON FEILITZEN, K., HÄUSSLER, R. S., HONG, M.-G., LINDSKOG, C., PONTEN, F., KATONA, B., VUU, J., LINDSTRÖM, E., NIELSEN, J., ROBINSON, J., AYOGLU, B., MAHDESSIAN, D., SULLIVAN, D., THUL, P., DANIELSSON, F., STADLER, C., LUNDBERG, E., BERGSTRÖM, G., GUMMESSON, A., VOLDBORG, B. G., TEGEL, H., HOBER, S., FORSSTRÖM, B., SCHWENK, J. M., FAGERBERG, L. & SIVERTSSON, Å. 2019. The human secretome. *Science Signaling,* 12**,** eaaz0274.

VASTO, S., SCAPAGNINI, G., BULATI, M., CANDORE, G., CASTIGLIA, L., COLONNA-ROMANO, G., LIO, D., NUZZO, D., PELLICANO, M., RIZZO, C., FERRARA, N. & CARUSO, C. 2010. Biomarkes of aging. *Front Biosci (Schol Ed),* 2**,** 392-402.

WANG, J., TANG, C., YANG, C., ZHENG, Q. & HOU, Y. 2019. Tropomyosin-1 Functions as a Tumor Suppressor with Respect to Cell Proliferation, Angiogenesis and Metastasis in Renal Cell Carcinoma. *J Cancer,* 10**,** 2220-2228.

WANG, M., LI, W., CHANG, G.-Q., YE, C.-S., OU, J.-S., LI, X.-X., LIU, Y., CHEANG, T.-Y., HUANG, X.-L. & WANG, S.-M. 2011. MicroRNA-21 Regulates Vascular Smooth Muscle Cell Function via Targeting Tropomyosin 1 in Arteriosclerosis Obliterans of Lower Extremities. *Arteriosclerosis, Thrombosis, and Vascular Biology,* 31**,** 2044-2053.

WANG, X., SHEN, C. L., DYSON, M. T., EIMERL, S., ORLY, J., HUTSON, J. C. & STOCCO, D. M. 2005. Cyclooxygenase-2 regulation of the age-related decline in testosterone biosynthesis. *Endocrinology,* 146**,** 4202-8.

WANG, Y., CHEN, F., YE, L., ZIRKIN, B. & CHEN, H. 2017. Steroidogenesis in Leydig cells: effects of aging and environmental factors. *Reproduction,* 154**,** R111-r122.

WELTER, H., HERRMANN, C., DELLWEG, N., MISSEL, A., THANISCH, C., URBANSKI, H. F., KÖHN, F.-M., SCHWARZER, J. U., MÜLLER-TAUBENBERGER, A. & MAYERHOFER, A. 2020. The Glucocorticoid Receptor NR3C1 in Testicular Peritubular Cells is Developmentally Regulated and Linked to the Smooth Muscle-Like Cellular Phenotype. *Journal of Clinical Medicine,* 9**,** 961.

WELTER, H., KAMPFER, C., LAUF, S., FEIL, R., SCHWARZER, J. U., KOHN, F. M. & MAYERHOFER, A. 2013. Partial loss of contractile marker proteins in human testicular peritubular cells in infertility patients. *Andrology,* 1**,** 318-24.

WILEY, CHRISTOPHER D., VELARDE, MICHAEL C., LECOT, P., LIU, S., SARNOSKI, ETHAN A., FREUND, A., SHIRAKAWA, K., LIM, HYUNG W., DAVIS, SONNET S., RAMANATHAN, A., GERENCSER, AKOS A., VERDIN,

E. & CAMPISI, J. 2016. Mitochondrial Dysfunction Induces Senescence with a Distinct Secretory Phenotype. *Cell Metabolism,* 23**,** 303-314.
WINDSCHUTTL, S., KAMPFER, C., MAYER, C., FLENKENTHALER, F., FROHLICH, T., SCHWARZER, J. U., KOHN, F. M., URBANSKI, H., ARNOLD, G. J. & MAYERHOFER, A. 2015. Human testicular peritubular cells secrete pigment epithelium-derived factor (PEDF), which may be responsible for the avascularity of the seminiferous tubules. *Sci Rep,* 5**,** 12820.
WINTERS, S. J. & TROEN, P. 1982. Episodic luteinizing hormone (LH) secretion and the response of LH and follicle-stimulating hormone to LH-releasing hormone in aged men: evidence for coexistent primary testicular insufficiency and an impairment in gonadotropin secretion. *J Clin Endocrinol Metab,* 55**,** 560-5.
WU, F. C., TAJAR, A., PYE, S. R., SILMAN, A. J., FINN, J. D., O'NEILL, T. W., BARTFAI, G., CASANUEVA, F., FORTI, G., GIWERCMAN, A., HUHTANIEMI, I. T., KULA, K., PUNAB, M., BOONEN, S. & VANDERSCHUEREN, D. 2008. Hypothalamic-pituitary-testicular axis disruptions in older men are differentially linked to age and modifiable risk factors: the European Male Aging Study. *J Clin Endocrinol Metab,* 93**,** 2737-45.
XIA, S., ZHANG, X., ZHENG, S., KHANABDALI, R., KALIONIS, B., WU, J., WAN, W. & TAI, X. 2016. An Update on Inflamm-Aging: Mechanisms, Prevention, and Treatment. *Journal of Immunology Research,* 2016**,** 8426874.
YAMASHIRO, S., CHERN, H., YAMAKITA, Y. & MATSUMURA, F. 2001. Mutant Caldesmon lacking cdc2 phosphorylation sites delays M-phase entry and inhibits cytokinesis. *Mol Biol Cell,* 12**,** 239-50.
YANG, X. Z., LI, X. X., ZHANG, Y. J., RODRIGUEZ-RODRIGUEZ, L., XIANG, M. Q., WANG, H. Y. & ZHENG, X. F. 2016. Rab1 in cell signaling, cancer and other diseases. *Oncogene,* 35**,** 5699-5704.
YOKOUCHI, K., NUMAGUCHI, Y., KUBOTA, R., ISHII, M., IMAI, H., MURAKAMI, R., OGAWA, Y., KONDO, T., OKUMURA, K., INGBER, D. E. & MUROHARA, T. 2006. l-Caldesmon regulates proliferation and migration of vascular smooth muscle cells and inhibits neointimal formation after angioplasty. *Arterioscler Thromb Vasc Biol,* 26**,** 2231-7.
YU, M., HAZELTON, W. D., LUEBECK, G. E. & GRADY, W. M. 2020. Epigenetic Aging: More Than Just a Clock When It Comes to Cancer. *Cancer Research,* 80**,** 367-374.
ZHANG, H. J., WANG, J., LIU, H. F., ZHANG, X. N., ZHAN, M. & CHEN, F. L. 2015. Overexpression of mimecan in human aortic smooth muscle cells inhibits cell proliferation and enhances apoptosis and migration. *Exp Ther Med,* 10**,** 187-192.
ZHANG, Z. 2004. Prediction of Low-Energy Collision-Induced Dissociation Spectra of Peptides. *Analytical Chemistry,* 76**,** 3908-3922.
ZHOU, Y., SUN, M., TANG, Y., CHEN, Y., ZHU, C., YANG, Y., WANG, C., YU, G. & TANG, Z. 2020. Responses of the proteome in testis of mice exposed chronically to environmentally relevant concentrations of Microcystin-LR. *Ecotoxicol Environ Saf,* 187**,** 109824.
ZHU, Y., LIU, X., DING, X., WANG, F. & GENG, X. 2019. Telomere and its role in the aging pathways: telomere shortening, cell senescence and mitochondria dysfunction. *Biogerontology,* 20**,** 1-16.
ZIRKIN, B. R. & PAPADOPOULOS, V. 2018. Leydig cells: formation, function, and regulation. *Biol Reprod,* 99**,** 101-111.
ZUO, C., LI, X., HUANG, J., CHEN, D., JI, K., YANG, Y., XU, T., ZHU, D., YAN, C. & GAO, P. 2018. Osteoglycin attenuates cardiac fibrosis by suppressing cardiac

myofibroblast proliferation and migration through antagonizing lysophosphatidic acid 3/matrix metalloproteinase 2/epidermal growth factor receptor signalling. *Cardiovasc Res,* 114**,** 703-712.

7. Appendix

7.1. Abbreviations

BTB	Blood-testis barrier
cAMP	Cyclic adenosine monophosphate
DAVID	Database for Annotation, Visualization and Integrated Discovery
ECM	Extracellular matrix
FA	Formic acid
FDR	False discovery rate
FSH	Follicle stimulating hormone
GO	Gene ontology
GSEA	Gene set enrichment analysis
hp-MKTPC	High-passage-number MKTPC
HPT	Hypothalamus-pituitary-testicular
HTPC	Human testicular peritubular cells
IAA	Iodoacetamide
LC	Liquid chromatography
LC-MS/MS	Liquid chromatography-tandem mass spectrometry
LH	Luteinizing hormone
LHR	LH receptor
lp-MKTPC	Low-passage-number MKTPC
Lys-C	Endoproteinase Lys-C
MKTPC	Monkey testicular peritubular cell
MS	Mass spectrometry
PANTHER	Protein analysis through evolutionary relationships
PRIDE	Proteomics Identification Database
REVIGO	Reduce + Visualize Gene Ontology
ROS	Reactive oxygen species
RT-PCR	Reverse transcription polymerase chain reaction
SASP	Senescent-associated secretory phenotype
SILAC	Stable isotope labeling by amino acids in cell culture
SSC	Spermatogonial stem cell
STRING	Search Tool for the Retrieval of Interacting Genes/Proteins
TCA	Tricarboxylic acid cycle
TCEP	Tris-(2-carboxyethyl)-phosphine

7.2. List of Proteins and their Gene Symbols

Gene symbol	Protein name
ACBD5	Acyl-CoA-binding domain-containing protein 5
ACTA2	Smooth muscle actin
ALDH1L1	Cytosolic 10-formyltetrahydrofolate dehydrogenase
AR	Androgen receptor
ASAH1	Acid ceramidase
BGN	Biglycan
CALD1	Caldesmon
CALM1	Calmodulin-1
CALR	Calreticulin
CDH2	Cadherin-2
CDKN1A	Cyclin-dependent kinase inhibitor 1
CDKN2A	Cyclin-dependent kinase inhibitor 2A
CEBPB	CCAAT/enhancer-binding protein beta
CELF1	CUGBP Elav-like family member 1
CNN1	Calponin 1
CNN2	Calponin-2
CNN3	Calponin-3
COL12A1	Collagen al-pha-1(XII) chain
COL1A1	Collagen alpha-1(I) chain
COL6A1	Collagen alpha-1(VI) chain
COL6A2	Collagen alpha-2(VI) chain
CXCL12	Chemokine stromal cell-derived factor 1
CXCL8	Interleukin-8
CYP11A1	Cholesterol side-chain cleavage enzyme, mitochondrial
DAG1	Dystroglycan
DCN	Decorin
DDR	DNA damage response
DDX4	ATP-dependent RNA helicase DDX4

DES	Desmin
DPP4	Dipeptidyl peptidase 4
DPT	Dermatopontin
DTT	Dithiothreitol
EDIL3	EGF-like repeat and discoidin I-like domain-containing protein 3
EEF1A1	Elongation factor 1-alpha 1
FGB	Fibrinogen beta chain
FMOD	Fibromodulin
GDNF	Glial cell line-derived neurotrophic factor
GDP	Guanosine diphosphate
HNRNPD	Heterogeneous nuclear ribonucleoprotein D0
IL6	Interleukin-6
INSL3	Insulin-like 3
ITGA2	Transmembrane receptors integrin alpha-2
ITGB5	Integrin beta-5
LAMB1	Laminin subunit beta-1
LAMC1	Laminin subunit gamma-1
LUM	Lumican
MAGEA4	Melanoma-associated antigen 4
MIF	Macrophage migration inhibitory factor
MYH10	Myosin-10
MYH11	Myosin-11
MYL12B	Myosin regulatory light chain 12B
MYLK	Smooth muscle myosin light chain kinase
NADH	Nicotinamide-adenine dinucleotide
NFKB1	Nuclear factor NF-kappa-B
NONO	Non-POU domain-containing octamer-binding protein
OGN	Mimecan
p21	CDK-Inhibitor 1
PAK	p21 activated kinase
PCA	Principal component analysis
PRDX1	Peroxiredoxin-1
PRDX2	Peroxiredoxin-2
PRDX4	Peroxiredoxin-4
PRDX6	Peroxiredoxin-6
PRELP	Prolargin
PSPC1	Paraspeckle component 1

PTGS1	Prostaglandin G/H synthase 1
PTGS2	Prostaglandin G/H synthase 2
RAB1A	Ras-related protein Rab-1A
SERPINE1	Plasminogen activator inhibitor 1
SERPINF1	Pigment epithelium-derived factor
SFPQ	Splicing factor, proline- and glutamine-rich
SLRP	Small leucine-rich proteoglycan
SOD1	Cu-Zn superoxide dismutase
SOD2	Superoxide dismutase [Mn], mitochondrial
SOD3	Extracellular superoxide dismutase [Cu-Zn]
SRSF7	Serine/arginine-rich splicing factor 7
TAGLN	Transgelin
TPCs	Testicular peritubular cells
TPM1	Tropomyosin alpha-1 chain
TPM2	Tropomyosin beta chain
TPM4	Tropomyosin alpha-4 chain
TPP1	Tripeptidyl-peptidase 1
UBE2J2	Ubiquitin-conjugating enzyme E2 J2
VIM	Vimentin

7.3. Supporting Information

Additional information was uploaded alongside the original papers, which can be found at the following links:

Supplementary Info 1:
https://www.mdpi.com/2073-4409/9/11/2498#supplementary

Table S1: all proteins identified in the proteomes of lp- and hp-MKTPCs
Table S2: all proteins identified in the secretomes of lp- and hp-MKTPCs
Table S3: Proteins significantly different in abundance in hp-MKTPC proteomes (paired Welch *t*-test, q-value < 0.05) between low and high passages of MTPCs. Log_2 fold change is hp-MKTPC vs lp-MKTPC
Table S4: Proteins significantly different in abundance in hp-MKTPC secretomes versus lp-MKTPCs secretomes (paired Welch *t*-test, q-value < 0.05) between low and high passages of MTPCs. Log_2 fold change is hp-MKTPC vs lp-MKTPC
Table S5: all proteins identified in the proteomes of young and old MKTPCs
Table S6: all proteins identified in the secretomes of young and old MKTPCs
Table S7: GSEA results: gene sets enriched in older MKTPCs; ES: enrichment score, NES: normalized enrichment score
Table S8: GSEA results: gene sets enriched in younger MKTPCs; ES: enrichment score, NES: normalized enrichment score

Supplementary Info 2:
https://www.mdpi.com/2073-4409/10/6/1306#supplementary

Table S1: All identified proteins in the proteomes of old and young *Callithrix jacchus* donors
Table S2: Proteins significantly different in abundance in the proteomes of old individuals compared to young individuals. Log_2 fold change is old vs young

7.4. Publications and Conference Contributions

7.4.1. Original Articles

Characterization of a non-human primate model for the study of testicular peritubular cells-comparison with human testicular peritubular cells

Schmid N*, **Stöckl JB***, Flenkenthaler F, Dietrich KG, Schwarzer JU, Köhn FM, Drummer C, Fröhlich T, Arnold GJ, Behr R, Mayerhofer A.

Mol Hum Reprod. 2018 Aug, 1;24(8):401-410.

doi: 10.1093/molehr/gay025. PMID: 29846669.

*Contributed equally

Necroptosis in primate luteolysis: a role for ceramide

Bagnjuk K, **Stöckl JB**, Fröhlich T, Arnold GJ, Behr R, Berg U, Berg D, Kunz L, Bishop C, Xu J, Mayerhofer A.

Cell Death Discov. 2019 Feb, 11;5:67.

doi: 10.1038/s41420-019-0149-7. PMID: 30774995

Insights into replicative senescence of human testicular peritubular cells

Schmid N, Flenkenthaler F, **Stöckl JB**, Dietrich KG, Köhn FM, Schwarzer JU, Kunz L, Luckner M, Wanner G, Arnold GJ, Fröhlich T, Mayerhofer A.

Sci Rep. 2019 Oct, 21;9(1):15052.

doi: 10.1038/s41598-019-51380-w. PMID: 31636313

A translational cellular model for the study of peritubular cells of the testis

Schmid N, Missel A, Petkov S, **Stöckl JB**, Flenkenthaler F, Arnold GJ, Fröhlich T, Behr R, Mayerhofer A. Reproduction. 2020 Aug;160(2):259-268.

doi: 10.1530/REP-20-0100. PMID: 32449695.

Proteomic Insights into Senescence of Testicular Peritubular Cells from a Nonhuman Primate Model

Stöckl JB, Schmid N, Flenkenthaler F, Drummer C, Behr R, Mayerhofer A, Arnold GJ, Fröhlich T. Cells. 2020 Nov 17;9(11):2498.

doi: 10.3390/cells9112498. PMID: 33213088; PMCID: PMC7698562.

Age-Related Alterations in the Testicular Proteome of a Non-Human Primate

Stöckl, J.B.; Schmid, N.; Flenkenthaler, F.; Drummer, C.; Behr, R.; Mayerhofer, A.; Arnold, G.J.; Fröhlich, T. Cells 2021, 10, 1306.

doi: 10.3390/cells10061306. PMID: 34074003

7.4.2. Poster Presentation

HUPO 2019 - 18th Human Proteome Organization World Congress:

September 14 – 18, 2019, Adelaide, Australia

Aging in testis: proteome alterations in senescent testicular peritubular cells

Jan Bernd Stöckl, Thomas Fröhlich, Nina Schmid, Florian Flenkenthaler, Rüdiger Behr, Artur Mayerhofer, Georg J. Arnold

Supported by a travel grant of the DGPF

8. Acknowledgements

First, I would like to thank Dr. Georg J. Arnold and Dr. Thomas Fröhlich for giving me the opportunity to do my PhD in their group and entrusting me with this fascinating project. I am grateful for their constant support and scientific guidance. Special thanks to Dr. Thomas Fröhlich for teaching me so much about mass spectrometry and chromatography.

I would like to thank Prof. Dr. Eckhard Wolf for his support and for being my doctoral advisor at the Gene Center. I also want to thank Prof. Dr. Ernst Wagner for his help and willingness to be my doctoral advisor at the Department of Pharmacy. Additionally, I want to thank the other members of my doctoral committee: Prof. Dr. Artur Mayerhofer, PD Dr. Stefanie Fenske, Prof. Dr. Martin Biel, and Prof. Dr. Franz Paintner.

I am very grateful for the invaluable collaboration with the Mayerhofer group at the BMC Munich. In particular I want to thank Dr. Nina Schmid, Dr. Konstantin Bagnjuk and Prof. Dr. Artur Mayerhofer for their substantial support, fruitful discussions, and outstanding collaboration. Many thanks also to Prof. Dr. Rüdiger Behr and Dr. Charris Drummer for providing tissue samples and important input.

I want to thank all the current and former members of the AG Fröhlich and AG Wolf. Many thanks to Miwako for her constant help and to Flo, Klaus and Katrin, for giving me such a warm welcome. For the great and supportive working atmosphere and all the wonderful time spent together I would also like to thank Max, Sepp, Benni, Bachi, Youli, Karolina and Lena. A special thanks to Lena for the encouragement and all the memes exchanged, helping me through lockdown.

I want to thank my family, especially my parents for their immense support through my life. Finally, I am deeply grateful to Enrica for the wonderful years and for being my biggest supporter.